

UNIVERSITÄTSKLINIKUM HAMBURG-EPPENDORF

Center for Molecular Neurobiology Hamburg (ZMNH)

Prof. Dr. Matthias Kneussel

Functional role of the neural cell adhesion molecule NCAM and novel interaction partners

Dissertation

zur Erlangung des PhD

an der Medizinischen Fakultät der Universität Hamburg.

vorgelegt von:

Laura Amores-Bonet
from Parets del Vallès, Spain

Hamburg 2022

Angenommen von der

Medizinischen Fakultät der Universität Hamburg am: 11.05.2023

Veröffentlicht mit Genehmigung der

Medizinischen Fakultät der Universität Hamburg.

Prüfungsausschuss, der/die Vorsitzende: Prof. Dr. Hans-Jürgen Kreienkamp

Prüfungsausschuss, zweite/r Gutachter/in: PD Dr. Sabine Hoffmeister-Ullerich

Prüfungsausschuss, dritte/r Gutachter/in: _____

Table of Contents

1. Introduction	6
1.1 Neural cell adhesion molecule (NCAM).....	6
1.1.1. N-glycosylation of NCAM.....	7
1.1.2. Homo- and heterophilic interactions of NCAM-PSA.....	8
1.1.3. Functions of NCAM and NCAM-PSA in the central nervous system.....	10
1.2. Transient receptor potential canonical (TRPC) channels	11
1.2.1. Functions and binding partners of the TRPC1, -4, and -5 channels in the central nervous system.....	12
1.3. Indications for an interaction between NCAM and TRPC channels.....	15
1.4. Aims of the project	16
2. Materials & Methods	17
2.1. Buffers, solutions, and media	17
2.1.1. Agarose gel electrophoresis.....	17
2.1.2. Bacteria culture	17
2.1.3. Production of protein.....	18
2.1.4. SDS-PAGE and Western-Blot	19
2.1.5. ELISA	21
2.1.6. Cell culture	22
2.1.7. Immunostainings	25
2.2. Antibodies.....	26
2.2.1. Primary antibodies.....	26
2.2.2. Secondary antibodies.....	27
2.3. Oligonucleotides.....	28
2.4. Peptides and recombinant proteins.....	29
2.5. Plasmids.....	30
2.6. Inhibitors and other reagents	31
2.7. Cell lines.....	32
2.8. Bacteria.....	32
2.9. Animals.....	32
2.10. Suppliers of chemicals, reagents, and kits.....	32

2.11. Molecular biology and cloning strategy	33
2.11.1. Polymerase Chain Reaction (PCR) and cloning design.....	33
2.11.2. Agarose gel electrophoresis	34
2.11.3. PCR product clean-up from agarose gels	34
2.11.4. In-Fusion cloning ligation	34
2.11.5. Bacteria transformation and plasmid isolation	35
2.11.6. Plasmid DNA isolation and determination of DNA concentration	35
2.11.7. Production and expression of His-tag and GST-tag proteins in <i>E. coli</i>	35
2.11.8. Genotyping of NCAM mice	36
2.12. Biochemical methods	37
2.12.1. Preparation of brain extracts and cell lysates	37
2.12.2. Determination of protein concentration.....	38
2.12.3. SDS-PAGE gel electrophoresis	38
2.12.4. Coomassie blue staining.....	38
2.12.5. Western blot.....	39
2.12.6. Pull-down	39
2.12.7. Co-immunoprecipitation (Co-IP)	39
2.12.8. ELISA	40
2.13. Cell culture	41
2.13.1. Preparation of coverslips (PLL coating).....	41
2.13.2. Primary culture of mouse cortical and hippocampal neurons.....	41
2.13.3. Transfection of cortical cells	42
2.13.4. Primary culture of mouse cerebellar granule neurons	42
2.13.5. Primary culture of mouse astrocytes	42
2.13.6. CHO cell culture maintenance, passaging, and freezing	43
2.13.7. Transfection of CHO cells	43
2.13.8. Neurite outgrowth assay	43
2.14. Immunostainings	44
2.14.1. Fixation of cells.....	44
2.14.2. Immunofluorescence staining.....	44
2.14.3. Proximity Ligation Assay (PLA).....	44
2.14.4. Total Internal Reflection Fluorescence (TIRF) microscopy	45
2.15. Calcium live imaging experiments.....	45
2.15.1. Treatment with thapsigargin	45
2.15.2. Incubation with Fluo-4 AM dye	45
2.15.3. Treatment with TRPC inhibitors.....	45
2.15.4. Imaging of calcium flux	46
2.16. Statistical analysis	46

3. Results	47
3.1. NCAM associates with TRPC1, -4, and -5 in mouse brain.....	47
3.2. The intracellular domains of NCAM140 and NCAM180 directly bind to the N-terminal domain of TRPC1, -4, and -5	48
3.3. Colominic acid binds to the N-terminal domain of TRPC1, -4, and -5.....	49
3.4. NCAM co-localizes with TRPC1, -4, and -5 at the neuronal plasma membrane	52
3.4.1. NCAM-PSA co-localizes with TRPC1, -4, and -5 on cerebellar and hippocampal neurons	52
3.4.2. NCAM-PSA is in close proximity with TRPC1, -4, and -5 in neurons	56
3.4.3. NCAM associates with TRPC1, -4, and -5 in cortical cells at the plasma membrane.....	59
3.4.4. The association of NCAM with TRPC1, -4, and -5 at the neuronal plasma membrane is independent of PSA.....	62
3.5. NCAM regulates the Ca ²⁺ flux via TRPCs.....	64
3.5.1. Transfected CHO cells overexpress TRPC1/4 and TRPC1/5	64
3.5.2. The absence of PSA does not affect the co-immunoprecipitation of NCAM with TRPC1, -4, and -5.....	66
3.5.3. The overexpression of TRPC1/4 and TRPC1/5 in NCAM-PSA positive CHO cells leads to an increase of the NCAM-dependent Ca ²⁺ flux	67
3.5.4. The inhibition of TRPC channels reduces the NCAM-dependent Ca ²⁺ flux in NCAM-PSA-positive CHO cells	69
3.6. Wild-type and NCAM-deficient mouse brains express similar levels of TRPC1, -4, and -5	71
3.7. NCAM regulates the Ca ²⁺ influx via TRPC1, -4, and -5 in cortical neurons.....	73
3.7.1. The presence of NCAM-PSA is required for the NCAM-dependent function triggering	73
3.7.2. The inhibition of TRPC1, -4, and -5 with pico145 reduces the NCAM-dependent Ca ²⁺ flux.....	73
3.7.3. The treatment of cortical neurons with TRPC1 261-278 peptide increases the TRPC1-dependent Ca ²⁺ flux	76
3.8. The NCAM-dependent Ca ²⁺ signaling depends on the influx of extracellular calcium and, to a lower extent, on the influx from intracellular stores.....	77
3.9. The inhibition of TRPC1, -4, and -5 with pico145 reduces the NCAM-dependent Ca ²⁺ flux in astrocytes	79
3.10. The NCAM-dependent phosphorylation of Erk1/2 is modulated by TRPC1, -4, and -5.....	80
3.10.1. The NCAM antibody treatment leads to Erk1/2 and PKC phosphorylation	80
3.10.2. The NCAM-dependent Erk1/2 phosphorylation is affected by TRPC1, -4, and -5 inhibition.....	81

3.11. The NCAM-dependent promotion of neurite outgrowth depends on TRPC1, -4, and -5.....	84
4. Discussion.....	86
4.1. NCAM and colominic acid directly bind to TRPC1, -4, and -5.....	86
4.2. NCAM and TRPC1, -4, and -5 interact at the neuronal plasma membrane in a PSA-independent manner	88
4.3. NCAM-triggered Ca ²⁺ flux mediated by TRPC1, -4, and -5 requires the presence of PSA on NCAM.....	89
4.4. NCAM-dependent neurite outgrowth is affected by TRPC1, -4, and -5 inhibition ..	91
4.5. NCAM-PSA and TRPC1, -4, and -5 modulate fear memory formation and consolidation	92
4.6. Conclusions	95
5. Summary	97
5.1. Summary	97
5.2. Zusammenfassung	98
6. Abbreviations.....	100
7. Bibliography	103
8. Acknowledgements.....	126
9. Curriculum Vitae	127
10. Appendix: Table of chemicals.....	128
11. Eidesstattliche Erklärung	131

1. Introduction

The most abundant cells of the central nervous system (CNS) are neurons and glia. Neuronal, glial, and neuronal-glial interactions are required to form neuronal networks, which are necessary to control neuronal cognition, behavior, and sensory and motor functions. The cell interactions occur together with the extracellular matrix (ECM) molecules, which confer structural and biochemical support. The ECM is formed by glycoproteins, such as laminin, collagen, and fibronectin. Essential players in the formation of cell-cell and cell-ECM interactions are the cell adhesion molecules (CAMs) (Aplin et al., 1998; Benson et al., 2001; Shapiro et al., 2007).

CAMs are the most abundant type of surface proteins in the cell. They mainly include 4 different superfamilies: integrins, cadherins, and selectins, which promote calcium-dependent interactions, and immunoglobulin-like proteins, which promote calcium-independent interactions. CAMs play essential roles in the regulation of cellular dynamics and surface receptors, in the modulation of cell signaling from the cell surface into the intracellular space, and in the adhesion and communication between cells (Aplin et al., 1998; Benson et al., 2001; Maness & Schachner, 2007; Shapiro et al., 2007).

1.1 Neural cell adhesion molecule (NCAM)

The NCAM family includes three different isoforms generated by alternative splicing: NCAM120, NCAM140, and NCAM180, which differ in their molecular structure and molecular weight (Figure 1). All three isoforms contain an extracellular N-terminal domain formed by two fibronectin type III (FNIII) homologous repeats and five immunoglobulin (Ig) domains. NCAM140 and NCAM180 contain transmembrane and C-terminal intracellular domains that differ in their structure due to an extra sequence called exon 18, which is only found in NCAM180 (Cunningham et al., 1987; Schachner, 1997). NCAM120 does not contain transmembrane and intracellular domains and is attached to the plasma membrane by a glycosylphosphatidylinositol (GPI) anchor (He et al., 1986).

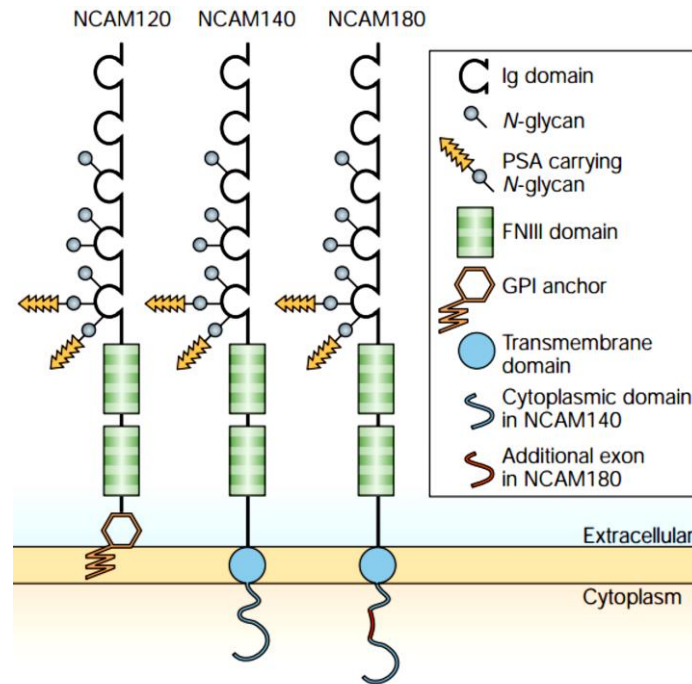


Figure 1. Representation of the different isoforms of NCAM. All NCAM isoforms contain an extracellular domain formed by five immunoglobulin-like and two fibronectin-type III-like domains. NCAM120 isoform is anchored to the plasma membrane by a GPI anchor, and NCAM140 and NCAM180 isoforms contain transmembrane and cytoplasmic domains. NCAM180 includes an extra sequence encoded by exon 18 in its intracellular domain (Kleene & Schachner, 2004).

NCAM is widely expressed in the CNS. NCAM120 is predominantly present in glial cells (Jucker et al., 1995; Keilhauer et al., 1985), NCAM140 is present in both presynaptic and postsynaptic neuronal membranes and glial cells, and NCAM180 is predominantly present in the postsynaptic neuronal membrane (Persohn et al., 1989; Schachner, 1997). Moreover, NCAM140 and NCAM180 accumulate in growth cones (Cunningham et al., 1987). Finally, apart from the neural tissue, NCAM expression was also found in other regions, such as muscle, kidney, and liver (Kolkova, 2010).

1.1.1. N-glycosylation of NCAM

There are different posttranslational modifications of the NCAM protein, which include phosphorylation, sulfation (Sorkin et al., 1984), palmitoylation (Niethammer et al., 2002), glycosylation (Albach et al., 2004), and ubiquitinylation (Diestel et al., 2007).

The three isoforms of NCAM undergo N-glycosylation in the endoplasmic reticulum (ER) and the Golgi apparatus. Six potential glycosylation sites are found in the third, fourth, and fifth IgG domains (Albach et al., 2004; Finne et al., 1983; Mühlenhoff et al., 2013).

Two of the most relevant N-linked glycans of NCAM are the human natural killer cell glycan 1 (HNK-1) (Kruse et al., 1984) and polysialic acid (PSA). PSA is a homopolymer of up to 100 α -2,8-linked N-acetyl-neuraminic acids attached to the N-glycans at the fifth and sixth glycosylation sites located in the fifth IgG domain of NCAM by the action of the polysialyltransferases ST8SiaII (STX) and ST8SiaIV (PST) (Figure 1) (Liedtke et al., 2001; Mühlenhoff et al., 1998; Nelson et al., 1995; Ohe et al., 2002). It is noteworthy to mention that other molecules, such as synaptic cell adhesion molecule (SynCAM) or neuropilin, can also be polysialylated (Curreli et al., 2007; Werneburg et al., 2015).

PSA, due to its carboxyl groups, is a highly negatively charged glycan that reduces the homophilic NCAM interactions and modulates the interaction of NCAM to heterophilic binding partners. Thus, the polysialylation of NCAM is known to modulate its adhesive properties (Johnson et al., 2005; Muller et al., 1996).

NCAM expression starts when the neural tube closes and increases during the maturation of the nervous system. The polysialylated NCAM (NCAM-PSA) level is high during embryonic development and at early postnatal stages and is strongly reduced during the maturation of the CNS (Finne et al., 1983; Kurosawa et al., 1997; Oltmann-Norden et al., 2008). The localization of NCAM-PSA in adulthood is restricted to areas associated with neuronal regeneration and neural plasticity (Chuong & Edelman, 1984; Gascon et al., 2007; Oltmann-Norden et al., 2008).

1.1.2. Homo- and heterophilic interactions of NCAM-PSA

NCAM is known to perform homo- and heterophilic interactions. The homophilic binding of two NCAM molecules in different adjacent cells activates multiple intracellular signaling pathways that lead to neurite extension (Doherty et al., 1991; Jessen et al., 2001; Kolkova et al., 2000; Schmidt et al., 1999).

Heterophilic interactions of NCAM with other molecules have become a subject of interest due to the diversity of intracellular cascades that are triggered after their association. NCAM activation in growth cones leads to the induction of the Pak1 signaling pathway and regulation of neurite outgrowth (Li et al., 2013). This NCAM-dependent neurite outgrowth also requires the activation of the non-receptor tyrosine kinases fyn and fak, the binding of NCAM to calmodulin (Beggs et al., 1994; Beggs et al., 1997; Kleene, Mzoughi, et al., 2010) and the induction of Ca^{2+} influx and Ca^{2+} /calmodulin-dependent protein kinase II (CaMKII) activation (Sheng et al., 2015). Moreover, the tropomyosin receptor kinase B (TrkB) mediates the phosphorylation of NCAM, and the interaction between the intracellular domains of NCAM and TrkB mediates the NCAM-dependent neurite outgrowth. The binding complex of NCAM and TrkB also includes the K^+ channel Kir3.3, and the overexpression of this channel is known to decrease the NCAM-dependent neurite outgrowth, suggesting that the interplay between ion channels and recognition molecules regulate neurite outgrowth (Cassens et al., 2010; Kleene & Cassens, et al., 2010).

Other molecules that participate in the triggering of NCAM-derived intracellular cascades are the fibroblast growth factor (FGF) receptor (FGFR) that activates NCAM signaling through the phospholipase C (PLC) pathway, the glial cell-derived neurotrophic factor (GDNF), and the brain-derived neurotrophic factor (BDNF) (Kiselyov, 2010; Muller et al., 2000; Paratcha et al., 2003). Furthermore, an NCAM deficiency reduces the phosphorylation state of FGF, CaMKII, and the cAMP response element-binding protein (CREB) (Aonurm-Helm et al., 2008; Aonurm-Helm et al., 2010).

Finally, NCAM is known to regulate the phosphorylation of the protein kinase C (PKC) and the extracellular signal-regulated kinase 1/2 (Erk1/2) (Ditlevsen et al., 2008; Niethammer et al., 2002). The phosphorylation of PKC, more specifically of PKC α , - β I, - β II, and - ϵ , is involved in NCAM-mediated neurite outgrowth and extension (Kolkova et al., 2005; Leshchyns'ka et al., 2003).

The NCAM-associated glycan PSA binds directly to the effector domain of myristoylated alanine-rich C-kinase substrate (MARCKS) in the cell membrane of hippocampal neurons to modulate the neuritogenesis in these cells (Theis et al., 2013). Other PSA extracellular binding partners involved in neuritogenesis and cell growth processes include FGF-2 (Ono et al., 2012), BDNF (Muller et al., 2000), and histone H1 (Mishra et al., 2010).

1.1.3. Functions of NCAM and NCAM-PSA in the central nervous system

NCAM is involved in the recognition between cells, neuronal differentiation and migration, regulation of neurite outgrowth, neuronal migration, and axonal guidance, as well as synaptogenesis, synaptic plasticity, and regulation of learning and memory (Cunningham et al., 1987; Kolkova et al., 2005; Maness & Schachner, 2007; Rønn et al., 2000).

NCAM has been widely studied in regions associated with learning and memory, like the amygdala, the hippocampus, or the piriform cortex (Brenneman et al., 2011; Rutishauser, 2008). Moreover, NCAM-PSA has essential roles in the regulation of behavior and the circadian rhythm (Bonfanti & Theodosis, 2009; Johnson et al., 2005; Mühlhoff et al., 1998; Westphal et al., 2016).

It is noteworthy to mention that NCAM-deficient mice show abnormalities in long-term potentiation (LTP) and long-term depression (LTD) processes and morphological alterations in the hippocampus and dentate gyrus (Bukalo et al., 2004; Muller et al., 1996; Muller et al., 2000). Focusing on behavioral studies, NCAM-deficient mice show anxiety-like behaviors and impairments in innate and learned avoidance behaviors (Brandewiede et al., 2014; Stork et al., 1999; Stork et al., 2000) and age-related working memory deficits (Bisaz et al., 2013). Furthermore, recent studies by Shiwaku et al. (2022) show that the autoantibodies against NCAM are increased in humans with schizophrenia, leading to reduced spine and synapse numbers in the frontal cortex.

Regarding PSA dysregulation, the degradation of PSA alters the circadian rhythmicity, spatial learning, and memory consolidation (Becker et al., 1996; Fedorkova et al., 2002) and reduces the behavioral responses to contextual fear conditioning (Lopez-Fernandez et al., 2007). Mice with a deficiency in the polysialyltransferase ST8SiaII show reduced behavioral responses to fear conditioning (Angata et al., 2004), and impaired spatial and reversal learning was observed in mice lacking ST8SiaIV (Markram et al., 2007). Finally, the overexpression of PSA in the substantia nigra has been related to Parkinson's disease (Sato et al., 2016).

All these studies show a possible implication of NCAM-PSA in the development of psychiatric disorders, such as schizophrenia or bipolar disorders (Arai et al., 2004; Arai et al., 2006; Atz et al., 2007; Vawter, 2000).

1.2. Transient receptor potential canonical (TRPC) channels

It has been suggested that the interplay between ion channels and recognition molecules is essential for neurite outgrowth. Preliminary studies in our and other groups suggest an interaction between NCAM and the transient receptor potential canonical (TRPC) channels (Kiryushko et al., 2006; Kleene & Cassens, et al., 2010; Theis, 2011). The TRPC channels belong to the TRP family, which is classified into six subfamilies based on sequence homology: TRPC (canonical), TRPM (melastatin), TRPV (vanilloid), TRPP (polycystic), TRPA (ankyrin) and TRPML (mucolipin) (Clapham, 2003).

The TRPC subfamily comprises 7 members, from TRPC1 to TRPC7, although TRPC2 is a pseudogene in humans. These channels are non-selective cation channels permeable for Ca^{2+} , K^{+} , and Na^{+} and are classified into 3 subgroups based on their sequence homology: TRPC1; TRPC3, -6, and -7; and TRPC4 and -5 (Harteneck et al., 2000; Vannier et al., 1999; Zheng, 2013).

Under physiological conditions, the TRPC channels are found as homo- or heteromers formed by members of the subgroups mentioned above. However, TRPC1 is mainly known to work only as a heteromeric channel and to associate with TRPC4 and -5 or with TRPC3, -6, and -7 (Liu et al., 2005; Phelan et al., 2012; Storch et al., 2012; Strübing et al., 2001). Other studies also showed that TRPC1 could interact with members of other TRP families, such as TRPV4 or TRPP2 (Du et al., 2014).

The structure of the TRPC channels consists of an N-terminal intracellular domain containing four ankyrin-like repeat domains (ARD) and a coiled-coil domain, six transmembrane segments (S1-S6) with three extracellular and two intracellular loops, and an intracellular C terminal domain containing a highly conserved TRP box, a coiled-coil domain, and a calmodulin and inositol trisphosphate receptor (IP_3R) binding site (CIRB motif). The loop region between the S5 and S6 domains forms the channel's pore and is characterized by having a conserved LWF motif essential for pore formation (Figure 2). The ARD domains have been identified as responsible for the tetramerization of the TRPC units. The TRP box is responsible for the binding and formation of TRPC complexes with other molecules, while the binding sites of calmodulin and IP_3R regulate the activation and inhibition of the channel (Schindl et al., 2008; Wang et al., 2020).

A specific characteristic of the C-terminal domain of TRPC4 and -5 is that it contains a PDZ-binding motif that is not present in other TRPC channels. This motif allows the binding of TRPC4 and -5 to the scaffolding proteins Na⁺/H⁺ exchanger regulatory factor (NHERF) 1 and 2, which is vital for regulating the channel sensitivity to diacylglycerol (DAG) (Storch et al., 2017).

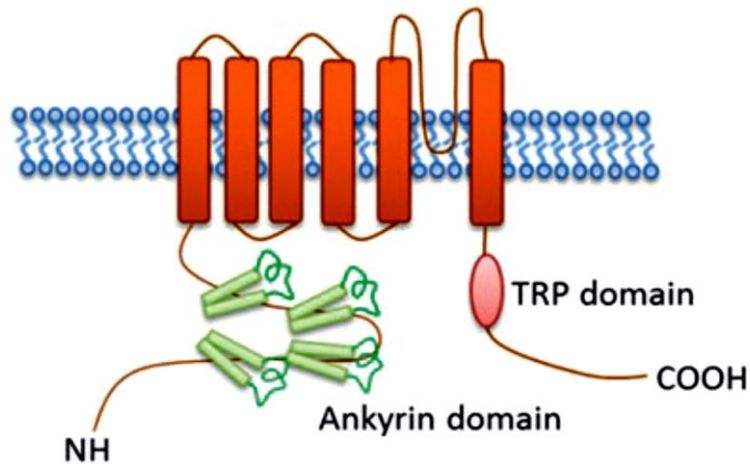


Figure 2. Representation of the general structure of the TRPC channels. An intracellular N-terminal domain (NH) with four ankyrin repeats, six transmembrane domains (orange boxes), and an intracellular C-terminal domain (COOH) with a TRP box are represented. Scheme adapted from (Wang, 2017).

While TRPC1 and TRPC3 are ubiquitously expressed in the CNS, TRPC4 is restrictive to the cortex, hippocampus, nucleus accumbens, and amygdala. Like TRPC4, TRPC5 is mainly found in the amygdala, hippocampus, and cortex. The expression of TRPC6 and TRPC7 localizes to the hippocampus, substantia nigra, and cerebellum (Fowler et al., 2007; Riccio et al., 2002; Wang et al., 2020).

Finally, TRPC channel expression is not exclusive to the CNS. These channels are found in peripheral tissues, such as the heart, the endothelium, the pituitary gland, and the kidney (Abramowitz & Birnbaumer, 2009).

1.2.1. Functions and binding partners of the TRPC1, -4, and -5 channels in the central nervous system

TRPC channels are involved in many functions in the CNS, including cell proliferation, neuronal development, growth and survival, axonal guidance, synaptic plasticity, modulation of the cellular excitability, and maintenance of cytosolic, endoplasmic reticulum and mitochondrial Ca²⁺ levels (Selvaraj et al., 2010; Vangeel & Voets, 2019).

These channels can function as receptor-operated or store-operated Ca^{2+} channels. The activation of the G protein-coupled receptors (GPCRs) or the tyrosine kinase receptors by their ligand can activate the PKC and PLC pathway. PLC hydrolyzes phosphatidylinositol-4,5-bisphosphate (PIP_2), producing DAG and inositol trisphosphate (IP_3). The receptor-operated Ca^{2+} entry is modulated by the binding of DAG to the TRPC channels or by the stimulation mediated by PLC. In contrast, the store-operated Ca^{2+} entry is triggered after the binding of IP_3 to its receptor in the ER and the release of Ca^{2+} from the intracellular stores into the cytoplasm (Figure 3) (Kim et al., 2012; Salido et al., 2009; Selvaraj et al., 2010; Vangeel & Voets, 2019). A specific modulatory role of PKC leading to the opening of TRPC3 and TRPC5 channels has been described by Venkatachalam et al. (2004). Moreover, recent studies by Myeong et al. (2018) suggested that the action of the GPCRs could directly open TRPC1/4 and TRPC1/5 heteromers.

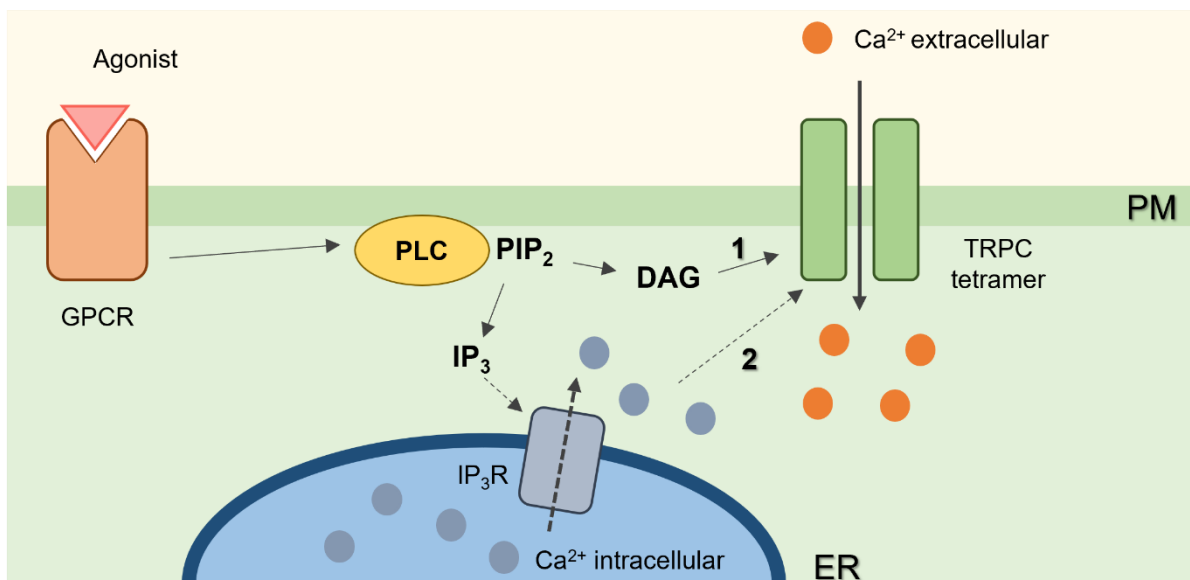


Figure 3. Schematic representation of TRPC channels opening. A G-protein-coupled receptor (GPCR) in the plasma membrane (PM) is stimulated by the binding of its agonist, which in turn activates phospholipase C (PLC). Then, PLC hydrolyzes the phosphatidylinositol-4,5-bisphosphate (PIP_2) into diacylglycerol (DAG), which modulates the receptor-operated Ca^{2+} entry together with PLC (1), and inositol trisphosphate (IP_3) that binds to its receptors (IP_3R) in the endoplasmic reticulum (ER). Intracellular Ca^{2+} is released from the stores, leading to the store-operated entry of extracellular Ca^{2+} (2, dashed line).

TRPC1 modulates axonal growth cones' detection of extracellular guidance factors mediated by netrin-1 and BDNF (Wang & Poo, 2005). It plays a role in the Ca²⁺-mediated proliferation of neural stem cells (NSC) (Fiorio Pla et al., 2005) as well as in the differentiation of cultured hippocampal cells (Wu et al., 2004) and neuroprotection (Bollimuntha et al., 2005).

The level of TRPC4 is increased in rat dorsal root ganglion neurons after a nerve injury, and reduced TRPC levels decrease neurite length (Wu et al., 2008). Therefore, TRPC4 is postulated to be an essential modulator of axonal regeneration after nerve injury. Moreover, TRPC4 is also involved in the neurotransmitter release from thalamic interneurons (Freichel et al., 2004).

TRPC5 channels interact with CaMKII β and induce its phosphorylation, modulating the dendrite morphogenesis in neurons (Davare et al., 2009; Puram et al., 2011). Moreover, the TRPC5 interaction with the growth-cone enriched protein stathmin 2 (STMN2) regulates neurite extension and growth cone morphology (Greka et al., 2003).

The silencing of TRPC5 and -6 reduce the proline-rich tyrosine kinase 2 (Pyk2)-Erk-CREB activation mediated by platelet-derived growth factor-BB (PDGF) in neurons (Yao et al., 2009), suggesting a possible role of TRPC5 and TRPC6 in the PDGF-mediated neuroprotection.

Behavioral studies show that the intraperitoneal administration of M084, a TRPC4 and -5 inhibitor, increases the BDNF expression in the prefrontal cortex of mice and induces the phosphorylation of Akt and Erk1/2, exerting rapid antidepressant and anxiolytic-like effects (Yang et al., 2015). Similar anxiolytic and antidepressant effects are also observed when administrating the TRPC4 and -5 inhibitor HC-070 to mice (Just et al., 2018). Finally, mice lacking the TRPC4 or TRPC5 subunits in a heteromeric complex with TRPC1 show decreased innate fear responses and levels (Riccio et al., 2009; Riccio et al., 2014). Considering all these findings, TRPC1, -4, and -5 have been postulated as important players in anxiety- and fear-related behaviors.

1.3. Indications for an interaction between NCAM and TRPC channels

NCAM homophilic and heterophilic bindings increase intracellular Ca^{2+} levels by triggering the PLC γ pathway that produces DAG and IP₃ (Kolkova et al., 2000; Schmidt et al., 1999). It is known that the PLC γ pathway is involved in the activation of the non-selective cation channels (NSCCs), which include the TRPC channels (Vangeel & Voets, 2019). Moreover, studies performed by Kiryushko et al. (2006) and Rønn et al. (2002) showed that the NSCCs and the voltage-dependent calcium channels (VDDCs) are involved in NCAM-dependent neuritogenesis.

The treatment of hippocampal neurons with an NCAM-triggering peptide leads to a Ca^{2+} influx in these cells. Moreover, the application of L- and N-type VDDCs inhibitors do not completely block the NCAM-dependent Ca^{2+} flux, suggesting that other VDDCs or NSCCs channels could be involved. In this same study, the administration of a general NSCCs inhibitor, known as SKF-96562, completely blocks the NCAM-dependent elevation of cytoplasmic Ca^{2+} and subsequent neuritogenesis (Kiryushko et al., 2006). These results indicate that the TRPC channels could regulate the NCAM-dependent Ca^{2+} influx.

Finally, based on previous studies, NCAM and TRPC share similar binding partners, such as the dopamine D2 receptor (Hannan et al., 2008; Xiao et al., 2009), the receptor tyrosine kinase TrkB (Cassens et al., 2010; Li et al., 1999; McGurk et al., 2011), calmodulin (Dionisio et al., 2011; Kleene & Mzoughi, et al., 2010; Tang et al., 2001) and the FGFR (Fiorio Pla et al., 2005; Kiselyov, 2010).

1.4. Aims of the project

Considering that NCAM and TRPC share similar binding partners and signaling pathways, that the inhibition of NSCCs, which include the TRPC channels, affects the NCAM-dependent Ca^{2+} influx, and that previous data from our group support the idea of direct interaction between NCAM and TRPC (Theis, 2011); it is reasonable to speculate that NCAM and TRPC channels work in conjunction in the regulation of the NCAM-dependent Ca^{2+} influx and neurite outgrowth. Thus, the aims of this thesis are the following:

- To verify a direct interaction of NCAM and TRPC1, -4, and -5.
- To characterize the interaction between NCAM and TRPC1, -4, and -5.
- To analyze the implications of NCAM-TRPC interactions in the NCAM-dependent Ca^{2+} flux.
- To investigate the consequences of the interaction between NCAM and TRPCs in the NCAM-mediated signaling and neurite outgrowth.

2. Materials & Methods

2.1. Buffers, solutions, and media

All the solutions are prepared in ddH₂O unless specified. Detailed information about chemicals, solutions, and reagents can be found in Table A1 (see 10. Appendix: Table of chemicals).

2.1.1. Agarose gel electrophoresis

TAE 50x (pH 8.0)

2 M Tris

1 M acetic acid

50 mM EDTA

Agarose gel solution

0.8 – 3% (w/v) Agarose

TAE 1x

0.1 µl/ml Roti-Safe GelStain

DNA Ladders

1 kb Plus DNA Ladder

100 bp Plus DNA Ladder

2.1.2. Bacteria culture

LB medium

10 g/l bacto-tryptone pH 7.4

10 g/l NaCl

5 g/l yeast extract

LB medium with ampicillin

100 mg/l ampicillin

LB medium

Agar plates with ampicillin

20 g/l agar

100 mg/l ampicillin

LB medium

LB medium with kanamycin

50 mg/l kanamycin

LB medium

Agar plates with kanamycin

20 g/l agar

50 mg/l kanamycin

LB medium

2.1.3. Production of protein**Lysis buffer His-Tag**

Washing buffer His-Tag

Protease inhibitors solution

Protease inhibitors solution

Stock (in ddH₂O) in lysis buffer prepared according to manufacturer's protocol (cOmplete EDTA-Free Protease Inhibitor Cocktail)

Washing buffer His-Tag (pH 8.0)50 mM NaHPO₄

300 mM NaCl

30 mM Imidazole

Elution buffer His-Tag (pH 8.0)

50 mM Tris

250 mM Imidazole

Lysis buffer GST-Tag (pH 8.0)

Washing buffer GST-Tag

Protease inhibitors solution

Washing buffer GST-Tag (pH 8.0)

1x PBS

1% (v/v) Triton X-100

Elution buffer GST-Tag (pH 8.0)

20 mM Reduced glutathione

50 mM Tris-HCl

2.1.4. SDS-PAGE and Western-Blot

Separating gel (8% gel)

1.7 ml ddH₂O

2 ml 30% acrylamide-bisacrylamide

2.3 ml 1 M Tris-HCl pH 8.8

60 µl 10% SDS

15 µl 10% APS

6 µl TEMED

Stacking gel

1.05 ml ddH₂O

250 µl 30% acrylamide-bisacrylamide

200 µl 1 M Tris-HCl pH 6.8

20 µl 10% SDS

10 µl 10% APS

4 µl TEMED

RIPA buffer (pH 7.4)

50 mM Tris

180 mM NaCl

1 mM Na₄P₂O₇

1% (v/v) NP-40

Phosphatase and protease inhibitors solutions

Phosphatase inhibitors solution

Stock (in ddH₂O) in RIPA buffer prepared according to manufacturer's protocol (PhosSTOP EASYpack)

Protease inhibitors solution

Stock (in ddH₂O) in RIPA buffer prepared according to manufacturer's protocol (cOmplete EDTA-Free Protease Inhibitor Cocktail)

Sample buffer 4x

31 ml ddH₂O
24 ml 1 M Tris-HCl pH 6.8
8 g SDS
0.04 g Bromophenol blue
40 ml Glycerol 100%
5 ml β-mercaptoethanol

TBS 10x (pH 7.5)

100 mM Tris
1.5 M NaCl

TBS-T

100 μl Tween 20 in 1 l TBS 1x

SDS 10%

10 g SDS
100 ml ddH₂O

Running buffer 10x

1.9 M Glycine
250 mM Tris
1% (w/v) SDS

Blotting buffer 10x

250 mM Tris
1.9 M Glycine

Blotting buffer 1x	70% ddH ₂ O 10% (v/v) Blotting buffer 10x 20% (v/v) Methanol
WB blocking solution	5% (w/v) nonfat milk powder TBS-T
Coomassie staining solution	60 ml ddH ₂ O 20 ml Methanol 20 ml Roti-Blue
Coomassie washing solution	75 ml ddH ₂ O 25 ml Methanol
Protein Ladder	PageRuler™ Plus Prestained Protein Ladder
iMAC buffer (pH 7.2)	20 mM HEPES 100 mM Potassium acetate 40 mM KCl 5 mM EGTA 5 mM MgCl ₂ Phosphatase and protease inhibitors solutions 1% (v/v) Triton X-100
<u>2.1.5. ELISA</u>	
ELISA blocking solution	2% (w/v) BSA fatty acids-free PBS without calcium and magnesium ions

ELISA washing solution	0.05% (v/v) Tween 20 PBS without calcium and magnesium ions
OPD solution	0.5 mg/ml OPD substrate Stable peroxidase buffer (10x)
Stopping solution	2.4 M H ₂ SO ₄
<u>2.1.6. Cell culture</u>	
Dissection medium	PBS 10 mM Glucose
Maintenance medium granule cells	Neurobasal A medium 1x Pen/Strep 0.1% (w/v) BSA 10 µg/ml Insulin 4 nM L-Thyroxine 100 µg/ml Transferrin, holo 30 nM Na-Selenite 1 mM Na-Pyruvate 2 mM L-Glutamine B27 supplement With or without 5% (v/v) Fetal Horse Serum (FHS)
Dissociation solution	10 mg DNase I 50 mg Glucose 20 ml Neurobasal A medium

Trypsin/DNase solution	0.2 g Trypsin 20 mg DNase I 80 mM MgCl ₂ 20 ml HBSS
Maintenance medium hippocampal cells	BrainPhys Neuronal medium 1% (v/v) L-Glutamine 1% (v/v) Pen/Strep 2% (v/v) NeuroCult SMI Neuronal Supplement
Maintenance medium cortical cells	Neurobasal medium 2 mM L-Glutamine 1% (v/v) Pen/Strep B27 supplement
Digestion solution cortical/hippocampal cells	0.05% Trypsin + 0.02% EDTA
Stopping solution cortical/hippocampal cells	HBSS 10% (v/v) FBS
Maintenance medium astrocytes	DMEM 10% (v/v) FBS 2% (v/v) Pen/Strep

Maintenance medium CHO C6 / 2A10 cells	DMEM/F12 (1:1) 2 mM L-Glutamine 1% (v/v) Pen/Strep 5% (v/v) FBS 1 mM Na-Pyruvate
Maintenance medium CHO WT	GMEM/F12 (1:1) 2mM L-Glutamine 2% (v/v) Pen/Strep 25 ml CHO Master Mix 10% (v/v) FBS
CHO Master Mix	50 ml non-essential amino acids (100x) 50 ml Na-pyruvate (100 mM) 50 ml glutamate + aspartate solution (100x) 100 ml nucleosides solution (50x)
Glutamate + aspartate solution (100x)	300 mg Na-glutamate 300 mg aspartate
Nucleosides solution (50x)	35 mg adenosine 35 mg guanosine 35 mg cytidine 35 mg uridine 12 mg thymidine
Freezing medium CHO cells	DMEM with L-glutamine 20% (v/v) FBS 10% (v/v) DMSO

HEPES buffer (pH 7.5)

10 mM HEPES
135 mM NaCl
5 mM KCl
2 mM CaCl₂ (if necessary)
2 mM MgCl₂ (if necessary)
15 mM Glucose

Coating solution

PBS
5% (w/v) PLL

2.1.7. Immunostainings**PBS 10x (pH 7.4)**

137 mM NaCl
2.7 mM KCl
8 mM Na₂HPO₄
15 mM KH₂PO₄

Fixing solution (pH 7.5 with NaOH)

8% (w/v) paraformaldehyde
PBS 1x

Permeabilizing blocking buffer

0.25% (v/v) Triton X-100
5% (v/v) normal donkey serum
PBS 1x

Non-permeabilizing blocking buffer

5% (v/v) normal donkey serum
PBS 1x

Neurite outgrowth staining solution

1% (w/v) Toluidine blue O
1% (w/v) Methylene blue
in 1% (w/v) Borax solution

2.2. Antibodies

2.2.1. Primary antibodies

The primary antibodies used for the experiments are listed in Table 1.

Table 1. Primary antibodies.

Antibody	Source	Species	Dilution
α -Tubulin (TU-02)	Santa Cruz (sc-8035)	Mouse	WB 1:200
CHL 1 (C-18)	Santa Cruz (sc-34986)	Goat	ELISA 1:1000
Chondroitin Sulfate (CS-56)	C8035 Sigma-Aldrich	Mouse	ELISA 1:150
phospho-p44/42 MAPK (Erk1/2)	Cell signaling (#4370)	Rabbit	WB 1:2000
p44/42 MAPK (Erk1/2) (L34F12)	Cell signaling (#4696)	Mouse	WB 1:2000
γ -adaptn	BD Biosciences (610386)	Mouse	WB 1:10000
Mouse IgG	Dianova (MAA544Ra22)	Mouse	IP 3 μ g
NCAM Chicken	Pineda (Biocompare)	Chicken	Stim 1:100 WB 1:3000
NCAM GTX	GeneTex (GTX133217)	Rabbit	ELISA 1:300 IF 1:200 IP 3 μ g WB 1:800
NCAM Guinea pig	Pineda (Biocompare)	Guinea pig	Stim 1:100
NCAM P61	(Gennarini et al., 1984)	Rat	ELISA 1:300
phospho-PKC (pan) (β II Ser660)	Cell signaling (#9371)	Rabbit	WB 1:1000
phospho-PKC α / β II (Thr638/641)	Cell signaling (#9375)	Rabbit	WB 1:1000
PKC (A-3)	Santa Cruz (sc-17769)	Mouse	WB 1:400
PSA (735)	(Frosch et al., 1985)	Mouse	ELISA 1:400 IF 1:400 WB 1:3000
Rabbit IgG	Dianova (011-000-003)	Rabbit	IP 3 μ g
TRPC1	GeneTex (GTX54876)	Rabbit	IF 1:100

TRPC1 (ACC-010)	Alomone labs	Rabbit	IF 1:200 IP 4 µg WB 1:400
TRPC1 (E-6)	Santa Cruz (sc-133076)	Mouse	IF 1:30 WB 1:800
TRPC4 (ACC-018)	Alomone labs	Rabbit	IF 1:150 IP 5 µg WB 1:400
TRPC4 (ACC-119)	Alomone labs	Rabbit	IF 1:60
TRPC4 (N77/15)	NeuroMab 75-119	Mouse	IF 1:150 IP 5 µg
TRPC5 (1C8)	Santa Cruz (sc-293259)	Mouse	WB 1:150
TRPC5 (ACC-020)	Alomone labs	Rabbit	IP 3 µg
TRPC5 (N67/15)	NeuroMab 75-104	Mouse	IF 1:150

2.2.2. Secondary antibodies

The secondary antibodies used for the experiments are listed in Table 2.

Table 2. Secondary antibodies.

Antibody	Source	Dilution
Cy3-conjugated donkey anti-mouse	Jackson ImmunoResearch (715-165-150)	IF 1:200
Cy5-conjugated donkey anti-rabbit	Jackson ImmunoResearch (711-175-152)	IF 1:200
HRP-conjugated donkey anti-chicken IgY	Jackson ImmunoResearch (703-035-155)	WB 1:10000
HRP-conjugated donkey anti-goat IgG	Jackson ImmunoResearch (705-035-147)	ELISA 1:1000 WB 1:10000
HRP-conjugated donkey anti-mouse IgM	Jackson ImmunoResearch (715-036-020)	ELISA 1:1000 WB 1:10000
HRP-conjugated goat anti-mouse IgG	LI-COR (926-80010)	ELISA 1:1000 WB 1:10000
HRP-conjugated goat anti-rabbit IgG	LI-COR (926-80011)	ELISA 1:1000 WB 1:10000

HRP-Monoclonal goat anti-mouse IgG, light chain specific	Jackson ImmunoResearch (115-035-174)	WB 1:10000
HRP-Monoclonal mouse anti-rabbit IgG, light chain specific	Jackson ImmunoResearch (211-032-171)	WB 1:10000

2.3. Oligonucleotides

All the oligonucleotides were obtained from Metabion International.

NCAM Genotyping

NCAM up

5'-CTGCCTCAGATAGTGACCCAGTGC-3'

NCAM KO

5'-CGGAGAACCTGCGTGCAATCCATC-3'

NCAM WT

5'-TTGGAGGCAGGGAGCTGACCACAT-3'

Sequencing NCAM 140ICD and NT-TRPC bacteria producing protein

pQE30 6xHis Forward

5'-GGATCGCATCACCATCACCATCAC-3'

pQE30 stop codons Re

5'-CAGGAGTCCAAGCTCAGCTAATTAAGC-3'

GST-tag Rev

5'-AAGGAAGATTGGGAAACTCCAAACCC-3'

TRPC1

5'-ATGATGGCGGCCCTGTAC-3'

TRPC4 Rev

5'-CTCTGATGGTGAGAGCTCAGATTCTG-3'

TRPC5 Rev

5'-GCCTGCTTCACTGTGGCATA-3'

Cloning for CHO cells

pCAGIG_A

5'-GCCGGCCGCCAGCACAGTG-3'

pCAGIG_B

5'-TAACGCGGTCAGTCAGAGCC-3'

TRPC1_B

5'-ACTGAGCCATATTTCTTGGATAAAACATAGC-3'

TRPC1_C

5'-GCTGGGCCATATTTCTTGGATAAAACATAG-3'

TRPC1_D

5'-GGCTCTGACTGACCGCGTTAATGATGGCGGCCCTGTACC-3'

TRPC4_A

5'-TCCAAGAAATATGGCTCAGTTCTATTACAAAAGAA-3'

TRPC4_C

5'-CTGTGCTGGCGGCCGGCTCACAATCTTGTGGTCACATAATCT-3'

TRPC5_A

5'-TCCAAGAAATATGGCCCAGCTGTACTACAAG-3'

TRPC5_C

5'-CCACTGTGCTGGCGGCCGGCTTAGAGCCGAGTTGTAAGTTGTTTC-3'

2.4. Peptides and recombinant proteins

The following peptides were produced by Daniel Novak and published in his dissertation (Novak, 2009):

NCAM140 ΔN ICD

SKEPIVEVRTEEERTPNHDGGKHTEPNETTPLTEPEKGPVETKSEPPPESEAKPAPTEVKTVPN
DATQTKENESKA

NCAM140 ΔM ICD

MDITCYFLNKCGLLMCIAVNLCGKAGPGAKGKDMEEGKGPVETKSEPPPESEAKPAPTEVKT
VPNDATQTKENESKA

NCAM140 Δ C ICD

MDITCYFLNKCGLLMCIAVNLCGKAGPGAKGKDMEEGKAAFSKDESKEPIVEVRTEEERTP
NHDGGKHTEPNETTP

The following peptides were obtained from Schafer-N:

MARCKS-ED

H-KKKKKRFSFKKSFKLSGFSFKKNKK-OH

TRPC1 peptide

Biotin – RNDYEELARQCKMFAKDLLAQARNSRELE-OH

TRPC1 peptide + TAT

H-YGRKKRRQRRRNDYEELARQCKMFAKDLLAQARNSRELE-OH

TRPC1 mutated peptide + TAT

H-YGRKKRRQRRRQNDYEELAQQCQMFFAQDLLAQANSQELE-OH

2.5. Plasmids

pcDNA-TRPC1	Kind gift from Dr. Markus Delling, Boston, USA
pcDNA-TRPC4	Kind gift from Dr. Markus Delling, Boston, USA
pcDNA-TRPC5	Kind gift from Dr. Markus Delling, Boston, USA
pGEX-4T-2 TRPC1 N-terminus	Thomas Theis Dissertation, Hamburg, Germany
pGEX-4T-2 TRPC4 N-terminus	Thomas Theis Dissertation, Hamburg, Germany
pGEX-4T-2 TRPC5 N-terminus	Thomas Theis Dissertation, Hamburg, Germany
pQE30 NCAM140 ICD	Thomas Theis Dissertation, Hamburg, Germany
pQE30 NCAM180 ICD	Thomas Theis Dissertation, Hamburg, Germany
pQE30 NCAM140 ICD Δ N	Daniel Novak Dissertation, Hamburg, Germany
pQE30 NCAM140 ICD Δ M	Daniel Novak Dissertation, Hamburg, Germany
pQE30 NCAM140 ICD Δ C	Daniel Novak Dissertation, Hamburg, Germany

pCAGIG	Gift from Connie Cepko (Addgene plasmid #11159; http://n2t.net/addgene:11159 ; RRID: Addgene_11159)
pCAGIG_TRPC14	Cloned in this thesis (see Results 3.5.1.)
pCAGIG_TRPC15	Cloned in this thesis (see Results 3.5.1.)
pTagBFP-N vector	Evrogen BioCat FP172
pMH4-SYN-EGFP-ER	Gift from Thomas Oertner (Addgene plasmid #22285; http://n2t.net/addgene:22285 ; RRID: Addgene_22285)
tagBFP2-CAAX	Gift from Gerry Hammond (Addgene plasmid #116856; http://n2t.net/addgene:116856 ; RID: Addgene_116856)

2.6. Inhibitors and other reagents

Endo N (Endoneuraminidase N)	Endoneuraminidase cleaving α -2, 8-linked polysialic acid. Kind gift from Rita Gerardy-Schahn, Medizinische Hochschule (Hannover, Germany)
HC-070	Antagonist of TRPC4- and -5-containing channels
M084 hydrochloride	Antagonist of TRPC4- and -5-containing channels. Weakly blocks TRPC3
Pico145	Inhibitor of TRPC1, -4, and -5 channels. Inhibitor englerin-A-activated TRPC4 and -5 channels
GSK-417651A	Inhibitor of TRPC3 and -6 channels
SKF96365 hydrochloride	Inhibitor of the receptor-mediated influx of Ca^{2+} via voltage-gated calcium channels
Thapsigargin	Inhibitor of the sarco/endoplasmic reticulum Ca^{2+} -ATPases (SERCA)

2.7. Cell lines

Chinese Hamster Ovary cells (CHO) WT

CHO C6 cells (express NCAM and PSA) Kind gift from Martina Mühlenhoff (Hannover, Germany)

CHO 2A10 cells (express NCAM) Kind gift from Martina Mühlenhoff (Hannover, Germany)

2.8. Bacteria

Stellar competent *Escherichia coli* (*E. coli*) InFusion Clontech PT5055-2

One Shot DH5 α Chemically Competent *E.coli* Thermo Fisher Scientific 18265017

One Shot BL21 (DE3) Competent cells *E.coli* Thermo Fisher Scientific C601003

2.9. Animals

NCAM $-/-$ (NCAM KO) mice (Cremer et al., 1994) were generated by crossing heterozygous mutant mice with a C57BL/6J background. The animals were maintained at the animal facility of the University Hamburg-Eppendorf and housed on a light-dark cycle of 12 hours under standard conditions with food and water *ad libitum*. All animal experiments were approved by the University and State of Hamburg authorities accordingly to the guidelines set by the European Union and the ARRIVE guidelines for animal research.

2.10. Suppliers of chemicals, reagents, and kits

All chemicals, reagents and kits were purchased from the following companies: Addgene (Massachusetts, USA), Alomone labs (Jerusalem, Israel), Amersham Pharmacia Biotech (Amersham, UK), BD biosciences (New Jersey, USA), Bio-Rad Laboratories (Munich, Germany), Biocompare (California, USA), BioTek Instruments (Vermont, USA), BIOZOL (Eching, Germany), Carl-Roth (Karlsruhe, Germany), Carl Zeiss (Jena, Germany), Cayman Chemical (Tallinn, Estonia), Cell Signaling technology (Massachusetts, USA), Clontech-Takara Bio (California, USA), Corning (New York, USA), Dianova (Hamburg, Germany), Evrogen BioCat (Heidelberg, Germany), GE Healthcare (Illinois, USA), GeneTex (California, USA), Greiner (Kremsmünster, Austria), Herolab (Wiesloch, Germany), Jackson ImmunoResearch (Pennsylvania, USA), LI-COR Biosciences (Nebraska, USA), Life technologies (California, USA), Macherey-Nagel (Düren, Germany), MedChemExpress

(New Jersey, USA), MERCK (Darmstadt, Germany), Meridian Bioscience (Ohio, USA), Metabion International (Planegg, Germany), NeuroMab (California, USA), Nikon (Tokyo, Japan), Olympus (Tokyo, Japan), PAN Biotech (Aidenbach, Germany), QIAGEN (Hilden, Germany), Roche (Darmstadt, Germany), Santa Cruz Biotechnology (Texas, USA), Sartorius (Göttingen, Germany), Schafer-N (Copenhagen, Denmark), SERVA (Heidelberg, Germany), Sigma-Aldrich (Darmstadt, Germany), STEMCELL technologies (Cologne, Germany), TECAN (Männedorf, Switzerland), Th. Geyer (Hamburg, Germany), Thermo Fisher Scientific (Massachusetts, USA), TOCRIS Bioscience (Bristol, UK), VWR (Pennsylvania, USA).

2.11. Molecular biology and cloning strategy

2.11.1. Polymerase Chain Reaction (PCR) and cloning design

DNA fragments were amplified for PCR with the SimpliAmp Thermal Cycler (Life Technologies). pcDNA-TRPC1, pcDNA-TRPC4, and pcDNA-TRPC5 were used as templates with the primers: TRPC1_B or TRPC1_C with TRPC1_D, TRPC4_A with TRPC4_C and TRPC5_A with TRPC5_C (Table 3). For every PCR, 10 ng of cDNA template, 6.67 pM of each primer, and 12.5 µl of CloneAmp HiFi PCR™ premix were combined. Nuclease-free water was used to adjust the final volume to 25 µl.

Table 3. Templates and primers used for each cloning reaction.

Template	Forward primer	Reverse primer	Final product name
pcDNA-TRPC1 for TRPC4	TRPC1_D	TRPC1_B	TRPC1 D + B
pcDNA-TRPC1 for TRPC5	TRPC1_D	TRPC1_C	TRPC1 D + C
pcDNA-TRPC4	TRPC4_A	TRPC4_C	TRPC4 A + C
pcDNA-TRPC5	TRPC5_A	TRPC5_C	TRPC5 A + C

The linearization of the cloning vector (pCAGIG) was also performed by PCR technique. In that case, the primers pCAGIG_A and pCAGIG_B were used. A general protocol of the cycling conditions is shown in Table 4.

Table 4. General PCR protocol.

Number of cycles	Step	Temperature	Time
35	Denaturation	98 °C	10 seconds
	Primer annealing	62 °C	15 seconds
	Extension	72 °C	5 seconds / 1 kb of template

All the primers used for cloning were chosen according to the standards of the In-Fusion®HD Cloning Kit User Manual (Clontech-Takara Bio, 638920) and with the support of the Takara Bio Cloning Design Tool.

2.11.2. Agarose gel electrophoresis

0.8 – 3% agarose gels were prepared dissolving by heating the agarose powder in 1x TAE buffer. Afterwards, Roti-Safe GelStain was added to the solution (10 µl / 100 ml solution) to visualize the DNA, and the mixture was poured into a horizontal gel form with combs. After solidification, the gel was transferred into an electrophoresis chamber (Bio-Rad) and filled with 1x TAE buffer. If necessary, the PCR product was mixed with DNA Loading Dye (6x) and loaded on the gel. A constant voltage of 80 V or 170 V was applied to separate the DNA, and the bands were visualized using the EASY UV-light documentation system (Herolab).

2.11.3. PCR product clean-up from agarose gels

Desired DNA bands were cut out from the agarose gels and extracted with a NucleoSpin Gel and PCR Clean-up Kit (Macherey-Nagel, 740609) following the manufacturer's protocol. Pure DNA was stored at -20 °C until use.

2.11.4. In-Fusion cloning ligation

After purification, the desired inserts and the linearized vector were prepared in a ligation reaction following the manufacturer's protocol (In-Fusion®HD Cloning Kit User Manual), as shown in Table 5.

Table 5. Ligation reactions.

Insert 1	Insert 2	Linearized vector
TRPC1 B + D	TRPC4 A + C	pCAGIG
TRPC1 C + D	TRPC5 A + C	pCAGIG

5 µl of the ligation reaction was used to transform Stellar Competent *E. coli*. Bacteria were then plated into an LB plate with an appropriate antibiotic. The different colonies were inoculated in 4 ml liquid cultures, DNA was isolated, and the plasmids were sequenced to screen for the expression of the correct construct.

2.11.5. Bacteria transformation and plasmid isolation

One Shot DH5α (for plasmid DNA isolation) or BL21 (DE3) (for protein production) Chemically Competent *E. coli* were incubated on ice with 100 ng of DNA for 30 min. The cells were heat-shocked in a pre-warmed water bath for 30 seconds at 42 °C following incubation on ice for 2 minutes. Pre-warmed super optimal catabolite (SOC) medium was added to the bacteria and incubated for 1 hour at 37 °C on a shaker set at 220 rpm.

2.11.6. Plasmid DNA isolation and determination of DNA concentration

A single bacteria colony was inoculated into LB medium with an appropriate antibiotic and was grown at 37 °C under agitation (180 rpm) overnight. 200 µl of each type of bacteria were mixed with 200 µl of 50% glycerol and stored at -80 °C.

Small-scale culture (Miniprep): The colony was inoculated into 6 ml LB medium with an appropriate antibiotic. The plasmid was isolated using the NucleoSpin Plasmid kit (Macherey-Nagel, 740588) following the manufacturer's protocol.

Large-scale culture (Midiprep): The colony was inoculated into 100 ml LB medium with an appropriate antibiotic. The plasmid was isolated using the NucleoBond Xtra Midi kit (Macherey-Nagel, 740410) following the manufacturer's protocol. Plasmid DNA was resuspended with nuclease-free water.

The plasmid DNA concentration was measured using the microplate reader Infinite® 200 PRO NanoQuant (TECAN), and purity was obtained by dividing the absorbance of light at 260 nm with the absorbance of light at 280 nm. A 260/280 ratio between 1.8 and 1.9 was accepted. DNA was stored at -20 °C.

500 ng of the plasmid DNA was sequenced in the ZMNH Core Facility Bioanalytics.

2.11.7. Production and expression of His-tag and GST-tag proteins in *E. coli*

A single bacteria colony was inoculated into 8 ml of LB medium with an appropriate antibiotic and was grown at 37 °C under agitation (180 rpm) overnight.

The next day, the liquid culture was transferred into 300 ml of LB medium with appropriate antibiotic and grown at room temperature (RT) under agitation (180 rpm). Every hour the optical density 600 (OD₆₀₀) was determined to monitor the growth of the bacteria using a μ QuantTM Spectrophotometer (BioTek Instruments). Once the OD₆₀₀ value was 0.5-0.7, the bacteria were stimulated with isopropyl β -D-1-thiogalactopyranoside (IPTG) to a final concentration of 1 mM to induce protein expression and were grown for an additional 5-6 hours. Every two hours, 1 ml of the culture was sampled as a control.

The liquid culture was harvested by centrifugation at 6000 g for 12 minutes and stored at -20 °C until further use.

The cell pellet was resuspended with 5 ml of appropriate lysis buffer and kept on ice for 10 minutes. The resuspended cells were sonicated 6 times (~10 seconds) at 200-300 W, and the lysate was centrifuged at 10000 g at 4 °C for 30 minutes. Finally, the supernatant was incubated with 3 ml of appropriate beads, Ni-NTA agarose beads for His-tagged proteins, and glutathione-agarose beads for GST-tagged proteins overnight at 4 °C with an upside-down movement.

The beads were washed with appropriate washing buffer 3 times for 10 minutes and centrifuged at 1000 g for 4 min at 4 °C. The beads were incubated with 1 ml of proper elution buffer for 1 hour at RT or 4 hours to ON at 4 °C with an upside-down movement to elute the proteins. Samples from the different washing steps were kept as controls.

The eluate with the purified protein was dialyzed and concentrated in PBS 1x using Vivaspin 20 columns (Sartorius, VS2021) with a cut-off of 5 kDa centrifuged at 5000 g. Appropriate protein expression was determined by SDS-PAGE and Coomassie blue staining.

2.11.8. Genotyping of NCAM mice

The Phire Animal Tissue Direct PCR kit was used to extract the DNA. Mice tail cuts from the NCAM line were incubated with dilution buffer and DNA release for 10 minutes at RT and then for 5 minutes at 98 °C to be finally frozen at -20 °C for at least one hour.

1 μ l of each sample was mixed with 12.5 μ l of 2x MyTaqTM Red Mix buffer and the primers NCAM up, NCAM WT, and NCAM KO to a final concentration of 20 pM. Nuclease-free water was used to adjust the final volume to 24 μ l. Then, all samples were incubated in the SimpliAmp Thermal Cycler following the protocol shown in Table 6.

Table 6. General PCR protocol for NCAM genotyping.

Number of cycles	Step	Temperature	Time
1	Initial denaturation	95 °C	5 min
40	Denaturation	98 °C	10 sec
	Annealing	68 °C	90 sec
	Extension	72 °C	60 sec
1	Final extension	72 °C	5 min
1	Cooling	4 °C	∞

The PCR product was analyzed in a 3% agarose gel, and NCAM genotyping was determined, as described in the following image (Figure 4).

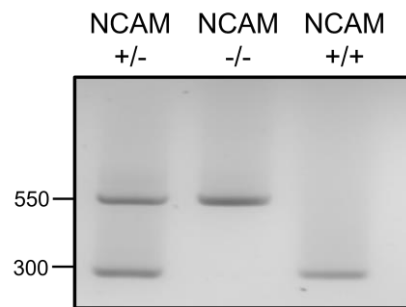


Figure 4. Representation of the different NCAM genotypes in a 3% agarose gel. Heterozygous mouse (NCAM +/-), NCAM-deficient mouse (NCAM -/-), and wild-type mouse (NCAM +/+).

2.12. Biochemical methods

2.12.1. Preparation of brain extracts and cell lysates

Brain extracts: Mice brains were homogenized with 1 ml ice-cold RIPA buffer containing protease inhibitors using an Elvehjem potter to disrupt the tissue. The homogenates were centrifuged at 10000 g for 15 minutes at 4 °C, and the supernatant was kept at - 20 °C.

Cell lysates: If necessary, cells were treated with HC-070 or pico145 to a final concentration of 200 nM, M084 to a final concentration of 50 µM, or colominic acid to a final concentration of 10 µg/ml for 35 minutes at 37 °C and 90% of relative humidity. During the last 15 minutes of incubation, NCAM-antibody was added to the medium.

After incubation, the plates were placed on ice, and the medium was removed. Two washings with cold PBS were performed, and RIPA was added. The plate was then incubated for 15 minutes with gentle shaking, and cells were removed from the well using a cell scraper. Finally, the lysates were centrifuged at 8000 g for 10 minutes at 4 °C. The supernatant was collected and stored at - 20 °C.

2.12.2. Determination of protein concentration

Pierce™ BCA Protein Assay Kit (Thermo Fisher Scientific, 23227) was used following the manufacturer's protocol to determine the protein concentration of each sample. Different solutions of BSA in 2000, 1000, 500, 250, 125, and 62.5 µg/ml were used as standards and analyzed together with the samples in a 96-well plate.

The plate with the samples and the reagents was incubated for 30 minutes at 37 °C, and the absorbance was measured at 562 nm using the µQuant™ Spectrophotometer (BioTek Instruments). Desired protein concentration was achieved by diluting the samples in 4x sample buffer. Finally, samples were boiled at 95 °C for 5 minutes to denature the protein and stored at -20 °C.

2.12.3. SDS-PAGE gel electrophoresis

Protein was separated using SDS-PAGE mini-PROTEAN TGX™ pre-cast 4-20%, 4-15% gels, or homemade acrylamide gels. The gels were run using Power Pac 200 (Bio-Rad) at 80 V for 20 min and 120 V until the bromophenol blue from the sample buffer reached the bottom of the gel. Once the running was finished, the gel was used for either Coomassie blue staining or Western blot. PageRuler™ Plus Prestained Protein Ladder was used as the molecular weight standard.

2.12.4. Coomassie blue staining

To visualize proteins from an acrylamide gel, the Coomassie blue staining was used. The gels were stained with Coomassie staining solution overnight with gentle shaking and then washed with Coomassie washing solution until the clear visualization of the bands. The gel was visualized using light and scanned to obtain an image.

2.12.5. Western blot

To identify the specific proteins separated in the SDS-PAGE, the proteins were transferred into a nitrocellulose membrane (Amersham) with a pore diameter of 0.45 μm . The blotting sandwich was assembled according to the manufacturer's protocol, and Power Pac 200 (Bio-Rad) was used at 90 V for 90 min.

After the transference of the protein, the membranes were placed in a glass container and incubated for 1h at RT with 5% skim milk powder in TBS-T. Then, the membranes were incubated with the desired dilution of the primary antibody in 5% skim milk powder in TBS-T overnight at 4 °C.

Afterwards, membranes were washed three times for 10 minutes with TBS-T while shaking and incubated for 1 hour with the appropriate HRP-coupled secondary antibody. Finally, membranes were rewashed three times with TBS-T for 10 minutes and visualized using ECL select or ECL prime reagents and the LAS4000 Mini (GE Healthcare).

2.12.6. Pull-down

Mice brains were homogenized with iMAC buffer and centrifuged at 1000 g and 4 °C for 10 minutes. The supernatant was kept and centrifuged at 10000 g and 4 °C for 10 minutes. Then, the resulting pellet was resuspended with iMAC-Triton buffer.

NCAM140-ICD His-tagged protein or NT-TRPC1, -4, and -5 GST-tagged proteins were incubated with Ni-NTA agarose beads or glutathione-agarose beads, respectively, for 1 hour and gentle shaking at 4 °C. Then, beads were washed twice with PBS-Triton buffer for 10 minutes and gentle shaking, and the resuspended brain homogenate was added for 2 hours and gentle shaking at 4 °C. Finally, beads were washed two times with iMAC-Triton buffer for 10 minutes and an extra washing was performed for 10 minutes with iMAC buffer. Beads were boiled with 4x sample buffer at 95 °C for 5 minutes to denature the protein and stored at -20 °C.

2.12.7. Co-immunoprecipitation (Co-IP)

3 to 5 μg of the primary antibody was incubated with pre-washed DynabeadsTM, protein G for mouse antibodies, and protein A for rabbit antibodies, for 1 hour at 4 °C and with gentle shaking. Meanwhile, brain homogenate resuspension and CHO cell lysate were obtained:

Brain homogenate resuspension: Brain homogenate resuspension was obtained as in 2.12.6. Pull-down.

CHO cell lysate: CHO cells were washed twice with cold PBS and incubated for 15 minutes and gentle shaking with cold iMAC buffer. Cells were removed from the well using a cell scraper, and cell resuspension was centrifuged at 1000 g and 4 °C for 10 minutes. The supernatant was kept and centrifuged at 10000 g and 4 °C for 10 minutes. Finally, the resulting pellet was resuspended with iMAC-Triton buffer.

If necessary, both samples were pre-cleared with the appropriate beads for 30 minutes at 4 °C and gentle shaking before incubation with the antibody.

Then, Ab-linked beads were washed twice with PBS-Triton and once with iMAC-Triton buffers, and cell/brain lysate was added and incubated for 2 hours and gentle shaking at 4 °C. Finally, beads were washed twice with iMAC-Triton buffer and twice with iMAC buffer. Samples were boiled with 4x sample buffer at 95 °C for 5 minutes to denature the protein and stored at -20 °C.

2.12.8. ELISA

To perform the ELISA experiments, 10 µg/ml of the recombinant protein was added to each well with a final volume of 25 µl in PBS. The coating solution (recombinant protein and PBS) was incubated overnight at 4 °C with gentle shaking.

The coating solution was discarded the next day, and three washes were performed with ELISA washing solution. 50 µl of the ELISA blocking solution was added to each well and incubated for 1 h 30 min at room temperature with shaking. In the last 30 minutes of incubation, the ligand was added to the positive control wells. Then, three washings were performed, and the ligand solution (desired protein in PBS) was added and incubated for 1 h 30 min at room temperature.

The plate was washed three times and incubated for 1 hour at room temperature with the desired primary antibody diluted in PBS. Then, three washes were performed, and the wells were incubated for 1 hour more at room temperature with the proper HRP secondary antibody diluted in PBS.

Finally, the plate was washed three times and incubated with OPD solution at room temperature for 3 – 5 minutes. After that, a stopping solution was added to stop the OPD reaction. The absorbance was measured at 492 nm using the µQuant™ Spectrophotometer (BioTek Instruments).

2.13. Cell culture

2.13.1. Preparation of coverslips (PLL coating)

Glass coverslips were incubated for 30 minutes with 3 M HCl at room temperature under shaking. Then, the coverslips were washed twice for 10 minutes with ddH₂O and incubated with acetone for 4 hours at room temperature. Later, five short washings with ddH₂O and two washings of 10 minutes with EtOH were performed.

The EtOH of the second washing was stored for future coverslips preparation, and the glass coverslips were heated for at least 2 hours at 160 °C to sterilize them.

On the previous day of the culture, the desired number of coverslips was added to the culture plates and coated with 0.01% PLL in PBS. The plates were incubated overnight at 37 °C and washed twice with ddH₂O.

2.13.2. Primary culture of mouse cortical and hippocampal neurons

For the primary culture of cortical neurons, mice embryos at the embryonic day 16 to 18 were used, and for the primary culture of hippocampal neurons, mice embryos at embryonic day 15.5 were used.

The pregnant female was sacrificed with CO₂, and the embryos were removed using sterile dissection tools. The head of the embryos was transferred into a dish with ice-cold PBS-G, the skull and meninges were removed, and the cortex or hippocampi were dissected and cut into small pieces. All the pieces were then collected and transferred into a 15 ml tube containing 1 ml of HBSS.

The HBSS was removed, and the cortexes or hippocampi were incubated for 5 min at 37 °C with 1 ml of trypsin-EDTA. Then, the trypsin was removed, and 2 ml of HBSS + 10% FBS was added to stop the trypsin reaction. HBSS + FBS was removed, and 1 ml of HBSS was used to resuspend and triturate the brain pieces using a fire-polished Pasteur pipette to get single cells.

Finally, cell number was counted using trypan blue solution 0.4% 1:1. The cells were seeded at the desired concentration and cultured for 5 to 7 days at 37 °C, in 5% CO₂, and at 90% relative humidity.

2.13.3. Transfection of cortical cells

Transfection of cortical cells was performed after 5 days in culture. 2 – 3 μg of the desired plasmid was added to the cells together with LipofectamineTM 2000 following the manufacturer's protocol. After one hour of incubation with lipofectamine, the cells were washed twice with pre-warmed HEPES buffer, and maintenance medium was again added. Finally, cells were kept in culture for two extra days.

2.13.4. Primary culture of mouse cerebellar granule neurons

For the primary culture of cerebellar granule neurons, mice at the postnatal day 6 to 8 were used. The mice were sacrificed with CO_2 , and the skull was removed using sterile dissection tools. The brain was transferred into a dish with ice-cold HBSS, and the cerebellum was dissected and cut into small pieces. All the pieces were then collected and transferred into a 15 ml tube containing 5 ml of HBSS.

The supernatant was removed, and cerebella were washed three times with HBSS and incubated for 15 min at 37 °C with trypsin/DNase solution. Then, the supernatant was removed, the dissociation solution was added, and the tissue was homogenized with three different diameters of fire-polished Pasteur pipettes. After homogenization, ice-cold HBSS was added to the cerebella and centrifuged for 15 min at 0.8 rpm and 4 °C.

Finally, the cell pellet was resuspended with maintenance medium, and the cell number was counted using trypan blue solution 0.4% 1:1. The cells were seeded at the desired concentration and cultured for 1 to 7 days at 37 °C in 5% CO_2 and 90% relative humidity.

2.13.5. Primary culture of mouse astrocytes

For the primary culture of astrocytes, mice at postnatal days 1 to 2 were used.

The mice were sacrificed with CO_2 , and the skull was removed using sterile dissection tools. The brain was transferred into a dish with ice-cold HBSS, and the cortex was dissected and cut into small pieces. All the pieces were then collected and transferred into a 15 ml tube containing 1 ml of HBSS.

The HBSS was removed, and cortexes were washed three times with ice-cold HBSS. The tissue was homogenized with pre-warmed medium and squeezed through 200 μm and 30 μm filter meshes. Then, the cell suspension was transferred into a 50 ml tube, and cells were counted and plated at the desired concentration.

Finally, astrocytes were cultured for 3 to 5 days at 37 °C, in 5% CO₂ and 90% relative humidity, and the medium was changed entirely after 24 hours.

2.13.6. CHO cell culture maintenance, passaging, and freezing

CHO cells were maintained in CHO maintenance medium at 37 °C, in 5% CO₂ and 90% relative humidity, in a flat-bottom cell culture flask.

The passaging or freezing was done when the cells reached 80% confluence. CHO cells were washed with HBSS without calcium and magnesium ions and incubated with Trypsin-EDTA for 2 minutes. The trypsinized cells were collected with HBSS and centrifuged at 1000 g for 5 minutes.

Passaging: The resulting pellet was resuspended with maintenance medium, and cells were seeded at the desired concentration in new flasks or plates.

Freezing: The resulting pellet was resuspended with freezing medium, and cells were transferred into cryotubes. Then, the tubes were frozen at -80 °C in an isopropanol box and transferred into a liquid nitrogen tank two days after.

2.13.7. Transfection of CHO cells

CHO cells were kept for 1 day in culture in a 6-well plate before transfection. 3 µg of the desired plasmid was added to the cells together with 3 µl of PlusTM Reagent and 9 µl of LipofectamineTM LTX following the manufacturer's protocol. After six hours of incubation with lipofectamine, the cells were washed twice with pre-warmed HEPES buffer, and maintenance medium was added. Finally, cells were kept in culture for one extra day.

2.13.8. Neurite outgrowth assay

Cortical cells were seeded on PLL-coated 48-well plates. After 30 minutes, the cells were treated with TRPC inhibitors and NCAM-antibody, as explained in 2.15.3. Treatment with TRPC inhibitors. The cells were grown at 37 °C, in 5% CO₂ and 90% relative humidity, and fixed with a final concentration of 2.5% glutaraldehyde after 30 hours. Cells were fixed for 30 - 60 minutes at 37 °C and washed three times with ddH₂O. Finally, neurite outgrowth staining solution was added to the wells for 30 - 60 minutes at room temperature, and three extra washings with ddH₂O were performed. 48-well plates were dried at room temperature.

Neurite length was measured from all the neurites of each neuron using an Axiovert 135 microscope (Carl Zeiss) with Axiovision 4.6. imaging software.

2.14. Immunostainings

2.14.1. Fixation of cells

The cells grown in glass coverslips were fixed with a final solution of 4% formaldehyde for 15 minutes at room temperature. Then, cells were washed three times with PBS 1x for 5 minutes with gentle shaking and kept in PBS 1x at 4 °C until their use.

2.14.2. Immunofluorescence staining

Fixed cells were blocked for 1 hour with blocking serum and permeabilized if necessary. The primary antibody was diluted in PBS 1x at the desired concentration and incubated overnight at 4 °C. The following day, cells were washed three times for 5 minutes with PBS 1x and incubated for 1 hour at room temperature with the secondary antibody and 4',6-diamidino-2-phenylindole (DAPI, final concentration of 5 µg/ml) diluted in PBS 1x. Next, cells were rewashed three times for 5 minutes with PBS 1x, and coverslips were mounted using mounting medium (Shandon Immu-Mount™). Finally, pictures of the cells were taken at a confocal microscope (Olympus FV1000) using a 60x objective. Images were analyzed using ImageJ and the Coloc2 plugin for colocalization.

2.14.3. Proximity Ligation Assay (PLA)

PLA was performed using the Duolink® Proximity Ligation Assay according to the manufacturer's protocol. Cells were permeabilized, if necessary, for 5 minutes before starting the blocking incubation. The primary antibody was diluted in Duolink AB Diluent at the desired concentration and incubated overnight at 4 °C.

Confocal microscope: After finishing the PLA protocol, coverslips were incubated with DAPI for 5 minutes and washed twice with PBS 1x for 10 minutes. Then, the coverslips were mounted with mounting medium, and pictures were taken the next day at a confocal microscope (Olympus FV1000) using a 60x objective.

Spinning disk – confocal microscope: After finishing the PLA protocol, cells were kept in HEPES buffer at 4 °C until their use the same day. No incubation with DAPI was performed. Images were taken at a spinning disk–confocal microscope (Nikon Eclipse Ti), as explained in 2.14.4. Total Internal Reflection Fluorescence (TIRF) microscopy.

2.14.4. Total Internal Reflection Fluorescence (TIRF) microscopy

For TIRF microscopy, a Nikon Eclipse Ti spinning disk microscope equipped with a Nikon CFI Apo TIRF 100x 1.49 NA oil objective was used. Cortical cells were transfected with tagBFP2-CAAX and pMH4-SYN-EGFP-ER, which label the plasma membrane and the endoplasmic reticulum. 405nm, 488nm, and 561nm lasers were used, and images were recorded using Visitron Systems software; the quantification of the PLA dots was performed in ImageJ.

2.15. Calcium live imaging experiments

Mouse cortical neurons were cultured and kept for 4 to 5 days at 37 °C, in 5% CO₂ and 90% relative humidity. If necessary, cortical cells were pre-treated with Endo N at a final concentration of 5 µg/ml for 1 hour at 37 °C before starting the experiment.

2.15.1. Treatment with thapsigargin

Cortical neurons were washed once and incubated with pre-warmed HEPES buffer without Ca₂Cl for 3 hours and thapsigargin to a final concentration of 1 µM at 37 °C.

2.15.2. Incubation with Fluo-4 AM dye

Cortical neurons or CHO cells were maintained in pre-warmed HEPES buffer with 2.5 µM and 5 µM Fluo-4 AM, respectively, and 0.02% Pluronic F-127 for 30 minutes. Cells were washed twice with HBSS and incubated, if necessary, for 20 minutes with the proper TRPC inhibitors (see 2.15.3. Treatment with TRPC inhibitors).

2.15.3. Treatment with TRPC inhibitors

Cortical neurons: Cortical cells were treated with HC-070, pico145, or GSK-417651A to a final concentration of 200 nM, M084 to a final concentration of 50 µM, or colominic acid to a final concentration of 10 µg/ml for 20 minutes at 37 °C in pre-warmed HEPES buffer.

CHO cells: CHO cells were treated with SKF-96365 to a final concentration of 10 µM for 20 minutes at 37 °C pre-warmed HEPES buffer.

2.15.4. Imaging of calcium flux

Imaging of the cortical and CHO cells' calcium flux was performed in a spinning disk-confocal microscope (Nikon Eclipse Ti) using a 20x objective and Visitron Systems software. Images were taken every second, and cells were triggered with NCAM-antibody after a 1-minute recording. The total video time was 5 minutes for both types of cells. Finally, the intensity of the Fluo-4 AM signal was analyzed using ImageJ software.

2.16. Statistical analysis

All statistical analyses were performed using the software GraphPad Prism 8. First, outliers were excluded, then normality distribution and equality of variances were analyzed using D'Agostino - Pearson test and F test, respectively.

Normally distributed and equal variances: Unpaired t-test to compare two groups and one-way ANOVA followed by Holm-Sidak post hoc for more than two groups.

Normally distributed but non-equal variances: Unpaired t-test with Welch's correction.

Non-normally distributed: Mann-Whitney test to compare two groups and one-way ANOVA followed by Kruskal-Wallis post hoc for more than two groups.

The specific type of test used in each experiment is indicated in the graph legend. P-values of < 0.05 , < 0.01 , < 0.001 , and < 0.0001 were accepted as an indication of a significant difference.

3. Results

3.1. NCAM associates with TRPC1, -4, and -5 in mouse brain

Previous studies showed that NCAM cytoplasmic Ca²⁺ signaling could be inhibited by SKF96562, a general NSCC inhibitor. Moreover, the NSCCs, which include the TRPC channels, are involved in NCAM-dependent neuritogenesis (Kiryushko et al., 2006; Vangeel & Voets, 2019). In addition, initial immunoprecipitation (IP) experiments suggested a possible interaction between NCAM and TRPC (Theis, 2011).

To further determine if there is an association between NCAM and TRPC1, -4, and -5, immunoprecipitation experiments were performed using membrane-enriched fractions of young adult mouse brains and TRPC1, -4, and -5 antibodies. Western blot analysis using NCAM antibodies against its C-terminal or extracellular domains showed an NCAM-positive band at 250 kDa corresponding to the NCAM-carrying PSA (NCAM-PSA) that was not present in the non-immune control (Figure 5a). These results indicate that NCAM interacts with TRPC1, -4, and -5 in the mouse brain.

To study the exact binding sites of the interaction between NCAM and TRPC1, -4, and -5, membrane-enriched brain fractions from young adult mice were used for pull-down experiments with the GST-tagged N-terminal domain of TRPC1, -4, and -5. NCAM was pulled down as seen by an NCAM-positive band at 250 kDa detected using an NCAM antibody against the C-terminal domain in Western blot analysis. The band was not present when using beads alone (Figure 5b). Also, the reverse experiment using membrane-enriched brain fractions of young adult mice and the His-tagged ICD of NCAM140 for pull-down showed TRPC1- and TRPC4-positive bands at ~90 kDa that were not present in the beads control (Figure 5c). These results indicate that NCAM associates with TRPC1, -4, and -5 via their N-terminal domains in the mouse brain.

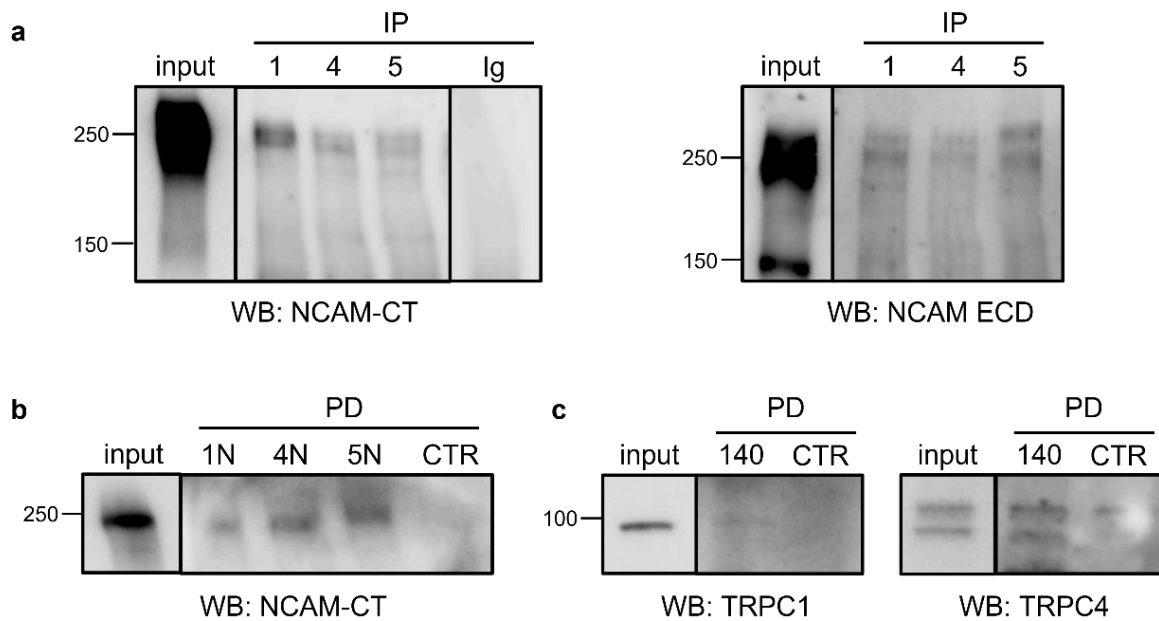


Figure 5. NCAM is present in a complex with TRPC1, -4, and -5. **(a)** Membrane-enriched brain fractions were used for immunoprecipitation (IP) with TRPC1 ACC-010 (1), TRPC4 ACC-018 (4), and TRPC5 ACC-020 (5) antibodies and a non-immune control antibody (Ig). The membrane-enriched brain fraction (input) and the immunoprecipitates were subjected to Western blot (WB) analysis with NCAM antibody GTX133217 against a C-terminal epitope (NCAM-CT) (left) and a chicken antibody against the extracellular NCAM domain (NCAM ECD) (right). **(b, c)** A membrane-enriched brain fraction was used for pull-down (PD) without (CTR) or with GST-tagged NT-TRPC1 (1N), -4 (4N), or -5 (5N) and glutathione beads **(b)** or with His-tagged NCAM140 ICD (140) and Ni-NTA beads **(c)**. **(b)** NCAM-CT and **(c)** TRPC1 ACC-010 (TRPC1) or TRPC4 ACC-018 (TRPC4) antibodies were used for Western blot analysis of the immunoprecipitates.

3.2. The intracellular domains of NCAM140 and NCAM180 directly bind to the N-terminal domain of TRPC1, -4, and -5

To further characterize the NCAM-TRPC interaction and test if the intracellular domains of NCAM140 and NCAM180 bind directly to TRPC1, -4, and -5, ELISA experiments were performed using recombinant NCAM140- and NCAM180-ICD, NT-TRPC1, -4, and -5, and the ICD of the cell adhesion molecule L1 like (CHL1) as control. The ELISA showed a concentration-dependent binding of NCAM140- and NCAM180-ICD, but not of CHL1-ICD, to NT-TRPC1, -4, and -5. Furthermore, the NCAM140- and NCAM180-ICD bound with a higher affinity to TRPC1 than TRPC4 or -5, while the binding of NCAM140- and NCAM180-ICD to TRPC4 and -5 was similar (Figure 6a-c). Interestingly, ELISA experiments using NT-TRPC1, -4, and -5 with NCAM140-ICD lacking the N-terminal,

middle, or C-terminal region showed a concentration-dependent binding only for the NCAM140-ICD lacking the middle part (Figure 6d-f), suggesting that the N- and C-terminal regions are essential for the binding of NCAM140 to NT-TRPC1, -4, and -5.

3.3. Colominic acid binds to the N-terminal domain of TRPC1, -4, and -5

PSA is a posttranslational modification of NCAM (Finne et al., 1983) that is known to bind to MARCKS within the plasma membrane plane (Theis et al., 2013). Furthermore, PSA plays an important role in modulating the interaction of NCAM with its binding partners, thereby modulating NCAM functions (Johnson et al., 2005; Muller et al., 1996). Thus, a possible binding of PSA to TRPC1, -4, and -5 was analyzed. Since PSA is not commercially available and difficult to isolate from mammalian cells, ELISA experiments were performed using colominic acid, the bacterial homolog of PSA. The ELISA using the N-terminal domain of TRPC1, -4, and -5 showed a concentration-dependent binding of colominic acid to these N-terminal TRPC domains, while no binding was observed for chondroitin sulfate, which is another negatively charged glycan used as control (Figure 7a-c). Moreover, increasing concentrations of soluble colominic acid reduced the binding of NCAM140-ICD to NT-TRPC1, -4, and -5 (Figure 7d), suggesting that NCAM140 and PSA share the same binding site in the N-terminal domain of TRPC1, -4, and -5.

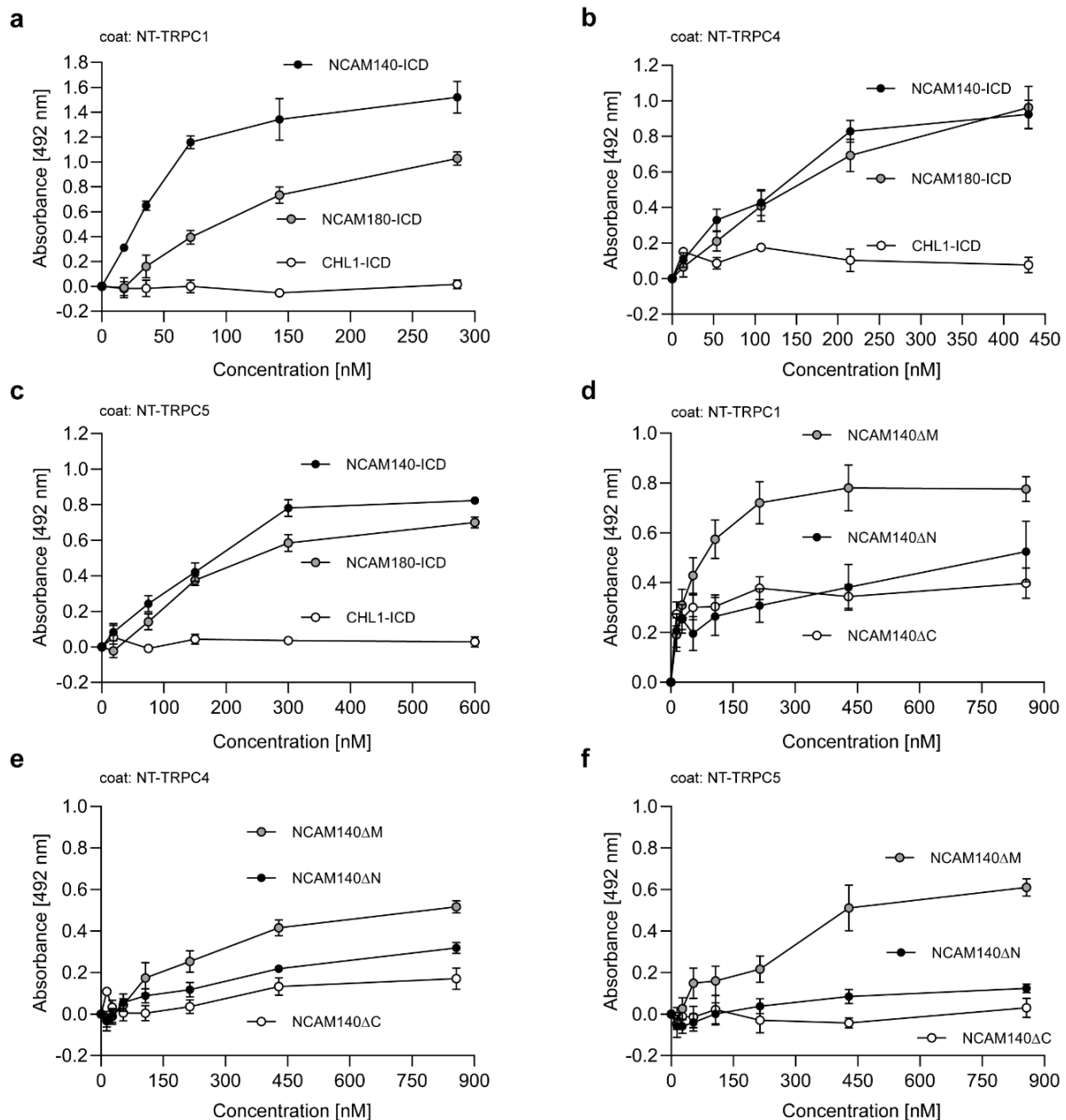


Figure 6. NCAM140- and NCAM180-ICDs bind to NT-TRPC1, -4, and -5. Recombinant N-terminal fragments of TRPC1 (NT-TRPC1) (**a**, **d**), TRPC4 (NT-TRPC4) (**b**, **e**), and TRPC5 (NT-TRPC5) (**c**, **f**) were substrate-coated and incubated with increasing concentrations of NCAM140-ICD, NCAM180-ICD, and CHL1-ICD (**a-c**) or NCAM140-ICD with a deletion in the N-terminal region (NCAM140 Δ N), the middle region (NCAM140 Δ M) or the C-terminal region (NCAM140 Δ C) (**d-f**). Binding was determined using the NCAM P61 and the CHL1 C-18 antibodies (**a-c**) or the NCAM antibody GTX133217 (**d-f**). Mean values \pm SEM are plotted from three independent experiments carried out in triplicates.

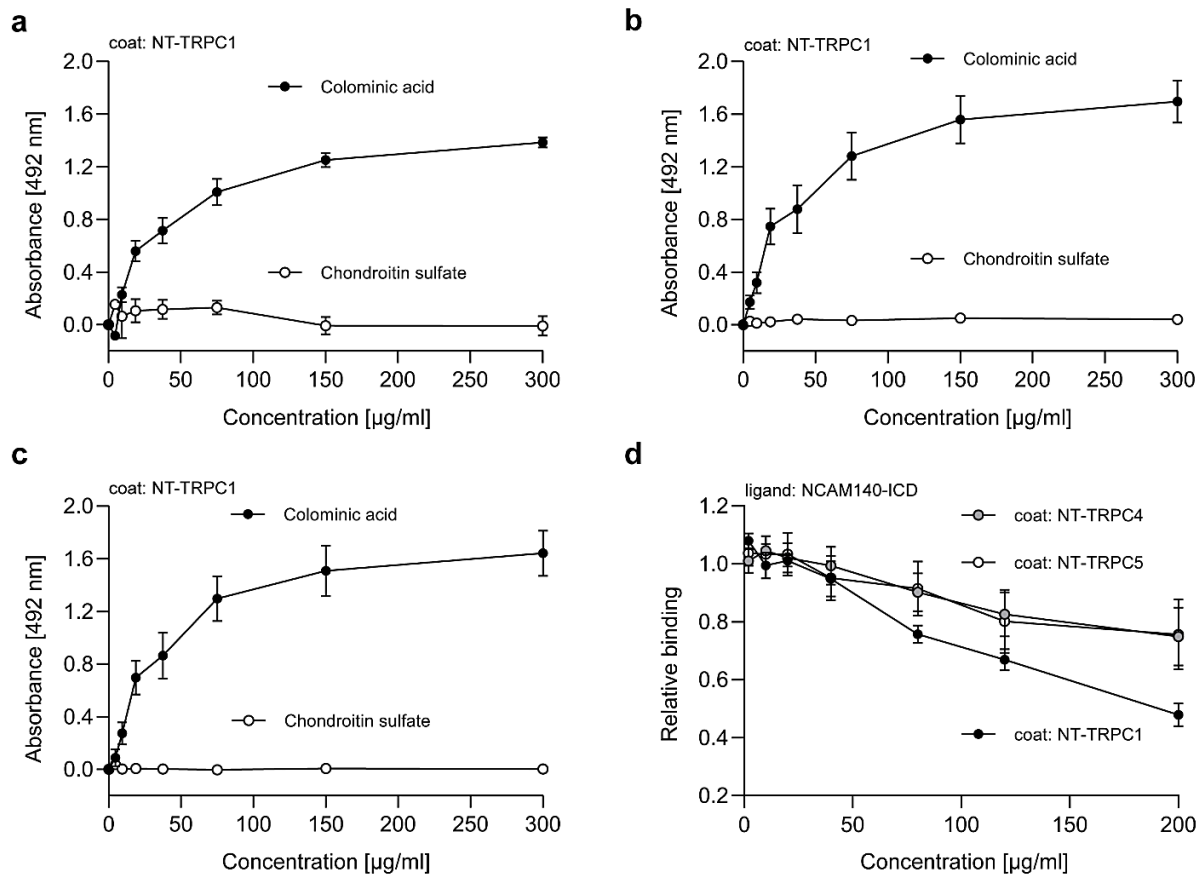


Figure 7. Colominic acid binds to NT-TRPC1, -4, and -5 in the same region as NCAM140-ICD. Recombinant N-terminal fragments of TRPC1 (NT-TRPC1) (**a**, **d**), TRPC4 (NT-TRPC4) (**b**, **d**), and TRPC5 (NT-TRPC5) (**c**, **d**) were substrate-coated and incubated with increasing concentrations of colominic acid and chondroitin sulfate (**a-c**) or with a constant concentration of NCAM140-ICD and increasing concentrations of colominic acid (**d**). Binding was determined using the PSA735 and the chondroitin sulfate CS-56 antibodies (**a-c**) or the NCAM P61 antibody (**d**). Mean values \pm SEM are plotted from three independent experiments carried out in triplicates.

It is known that the effector domain of MARCKS contains an amphipathic structure where PSA binds (Theis et al., 2013). The search for an amphipathic helical structure in the N-terminal domain of murine TRPC1 revealed a putative structure for the sequence LARQCKMFAKDLLAQARN at position 261-278 (Figure 8a) that could be responsible for the binding of PSA to TRPC1, -4, and -5. This sequence is conserved in the N-terminal domains of TRPC1, -4, and -5 from all mammalian species.

To test if PSA binds to the predicted helical structure of NT-TRPC1, a TRPC1 peptide containing the putative amphipathic sequence LARQCKMFAKDLLAQARN (TRPC1 peptide) and colominic acid were used for ELISA experiments together with chondroitin sulfate used as control. The ELISA showed a concentration-dependent binding of colominic acid, but not of chondroitin sulfate, to the substrate-coated TRPC1 peptide (Figure 8b). Interestingly, NCAM140-ICD, but not CHL1-ICD, bound to the TRPC1 peptide (Figure 8c). Moreover, the binding of NCAM140-ICD to NT-TRPC1 was reduced when NCAM140-ICD was preincubated with the TRPC1 peptide (Figure 8d). Finally, the TRPC1 peptide was mutated by substituting the positively charged amino acids (arginines and lysines) for neutral-charged amino acids (glutamines) to disrupt the predicted amphipathic structure. The mutated peptide showed a slightly reduced binding to NCAM140-ICD compared to the TRPC1 peptide, but the difference was not significant (Figure 8e). These results indicate that the binding sites for NCAM140-ICD and PSA in the NT-TRPC1 overlap, that the binding of PSA to the TRPC1 peptide interferes with the binding of NCAM140-ICD, and that the positively charged amino acids in the TRPC1 peptide are not crucial for binding to NCAM140-ICD.

3.4. NCAM co-localizes with TRPC1, -4, and -5 at the neuronal plasma membrane

3.4.1. NCAM-PSA co-localizes with TRPC1, -4, and -5 on cerebellar and hippocampal neurons

To investigate whether NCAM or PSA are associated with TRPC1, -4, and -5 in a cellular context, double immunostainings were performed with murine cerebellar granule and hippocampal neurons and antibodies labeling NCAM or PSA and TRPC1, -4, or -5. Pearson correlation coefficient indicated a strong correlation between NCAM and TRPC1, -4, and -5 staining and a moderate correlation between PSA and TRPC1 and -4 staining in both cultured cerebellar neurons (Figure 9a, b) and hippocampal neurons (Figure 10a, b). Of note, the immunofluorescence experiments to analyze the interaction between PSA and TRPC5 could not be performed because no suitable antibodies against the extracellular domain of TRPC5 were available.

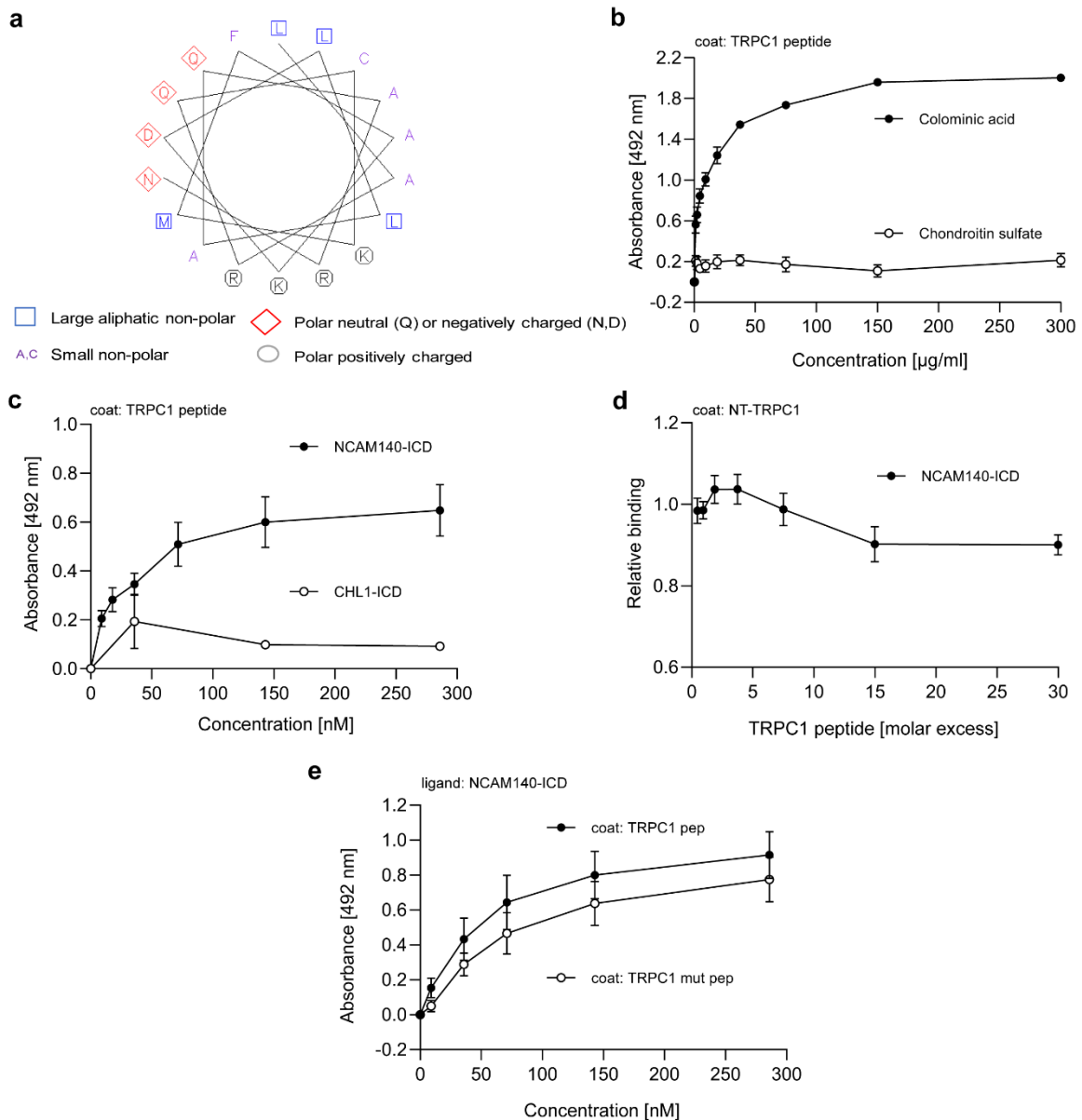


Figure 8. NCAM140-ICD and colominic acid bind to a peptide containing the amphipathic sequence located in the N-terminal domain of TRPC1. **(a)** Helical wheel representation of amino acids 261-278 in the N-terminal domain of murine TRPC1. TRPC1 peptide (TRPC1 pep) **(b, c, e)**, mutated TRPC1 peptide (TRPC1 mut pep) **(e)**, and the recombinant N-terminal domain of TRPC1 (NT-TRPC1) **(d)** were substrate-coated and incubated with increasing concentrations of colominic acid and chondroitin sulfate **(b)**, NCAM140-ICD **(c, e)**, CHL1-ICD **(c)** or a constant concentration of NCAM140-ICD and increasing concentrations of TRPC1 peptide **(d)**. Binding was determined using the PSA735 and the chondroitin sulfate CS-56 antibodies **(b)**, the CHL1 C-18 antibody **(c)**, or the NCAM P61 antibody **(c-e)**. Mean values \pm SEM are plotted from three independent experiments carried out in triplicates.

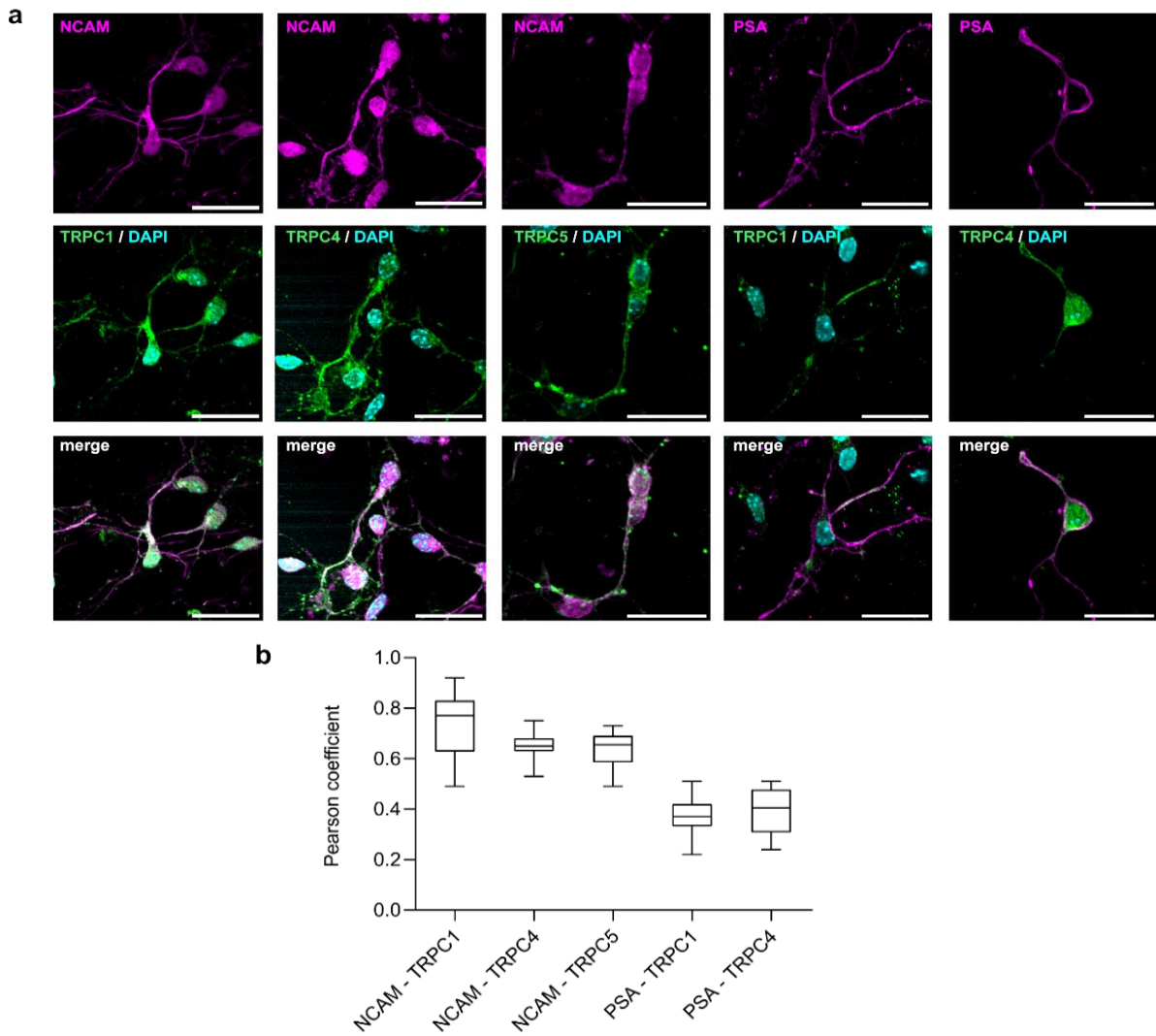


Figure 9. NCAM and PSA co-localize with TRPC1, -4, and -5 in cerebellar neurons. Double immunostainings of cultured murine cerebellar neurons were performed with rabbit NCAM GTX133217 and mouse TRPC1 E6, TRPC4 N77/15, or TRPC5 N67/15 antibodies or mouse PSA735 and rabbit TRPC1 GTX54876 or TRPC4 ACC-119 antibodies. Nuclei were stained using DAPI. **(a)** Representative images of each immunostaining showing NCAM or PSA (magenta), TRPCs (green), and DAPI (cyan), and a superimposition image (merge) that shows co-localization in white. Scale bars: 20 μ m. **(b)** Box plots showing Pearson coefficients from 10 immunostained neurons per group and two independent cultures indicate an overlap between NCAM or PSA and TRPCs signals.

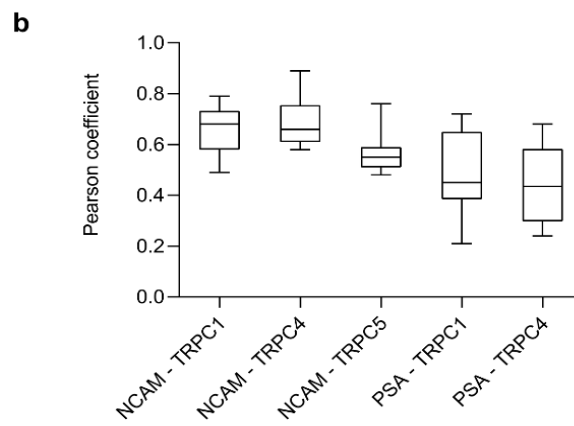
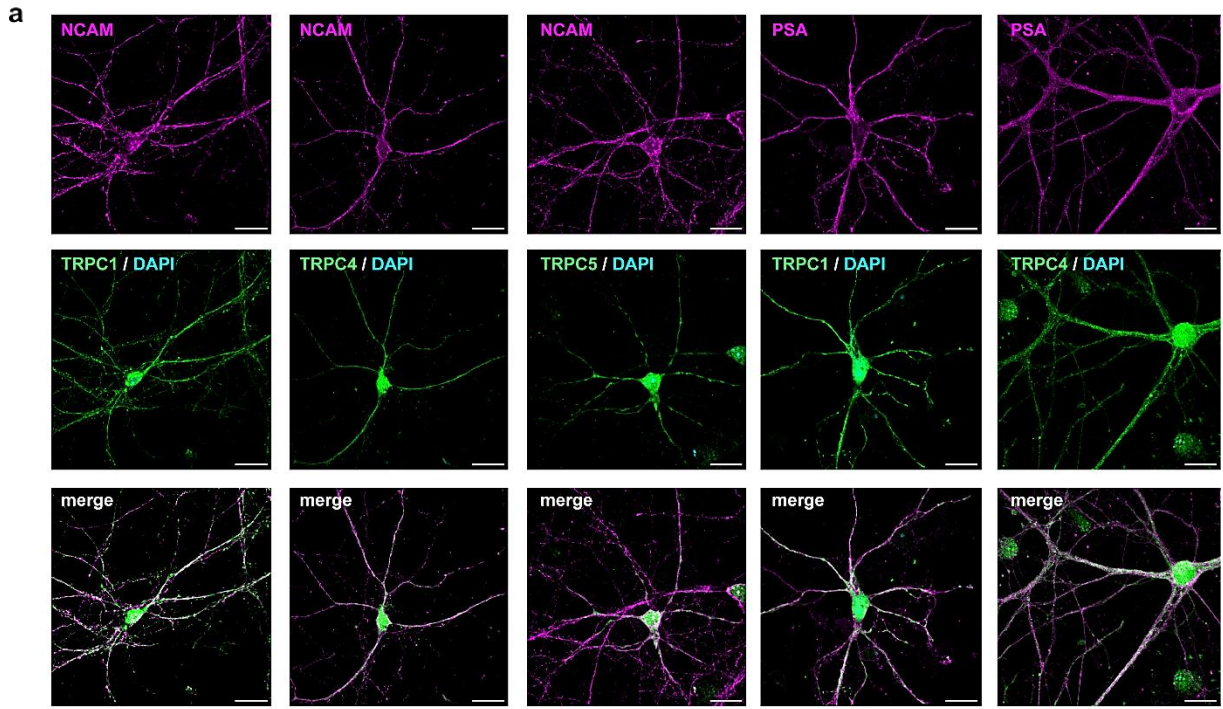


Figure 10. NCAM and PSA co-localize with TRPC1, -4, and -5 in hippocampal neurons. Double immunostainings of cultured murine hippocampal neurons were performed with rabbit NCAM GTX133217 and mouse TRPC1 E6, TRPC4 N77/15, or TRPC5 N67/15 antibodies or mouse PSA735 and rabbit TRPC1 GTX54876 or TRPC4 ACC-119 antibodies. Nuclei were stained using DAPI. **(a)** Representative images of each immunostaining showing NCAM or PSA (magenta), TRPCs (green), and DAPI (cyan), and a superimposition image (merge) that shows co-localization in white. Scale bars: 20 μ m. **(b)** Box plots showing Pearson coefficients from 10 immunostained neurons per group and two independent cultures indicate an overlap between NCAM or PSA and TRPCs signals.

3.4.2. NCAM-PSA is in close proximity with TRPC1, -4, and -5 in neurons

The proximity ligation assay (PLA) allows the detection of proteins at less than 40 nm of distance. The appearance of fluorescent dots indicates co-localization between the molecules. NCAM-TRPC1-, NCAM-TRPC4-, NCAM-TRPC5-, PSA-TRPC1-, and PSA-TRPC4-positive dots were observed in cultured wild-type cerebellar and hippocampal neurons using antibodies against NCAM-TRPC1, NCAM-TRPC4, NCAM-TRPC5, PSA-TRPC1, and PSA-TRPC4 but not in neurons from NCAM-deficient mice (Figures 11a-f and 12a-f).

It is known that PSA regulates clock-related gene expression and that its levels fluctuate during the day (Westphal et al., 2016), so it was conceivable to test whether the amount of PSA-TRPC1- or PSA-TRPC4-positive dots changed depending on the time of the day the neurons were fixed. The comparison of the number of PSA-TRPC1- and PSA-TRPC4-positive dots between cerebellar granule neurons fixed either in the morning or in the afternoon showed no differences for PSA-TRPC1 and PSA-TRPC4 interactions (Figure 13a, b). Finally, a proximity ligation assay in wild-type cortical neurons showed high numbers of NCAM-TRPC1-, NCAM-TRPC4-, NCAM-TRPC5, PSA-TRPC1-, and PSA-TRPC4-positive dots that were not observed in cortical neurons from NCAM-deficient mice (Figure 14a-f). Positive-PLA dots were mainly observed along the processes of neurons but also found at the cell somata (Figures 11a, 12a, and 14a). All these results indicate a close association between NCAM or PSA with TRPC1, -4, or -5 in cultured cerebellar granule, hippocampal and cortical neurons and that these interactions are not affected by the circadian rhythm.

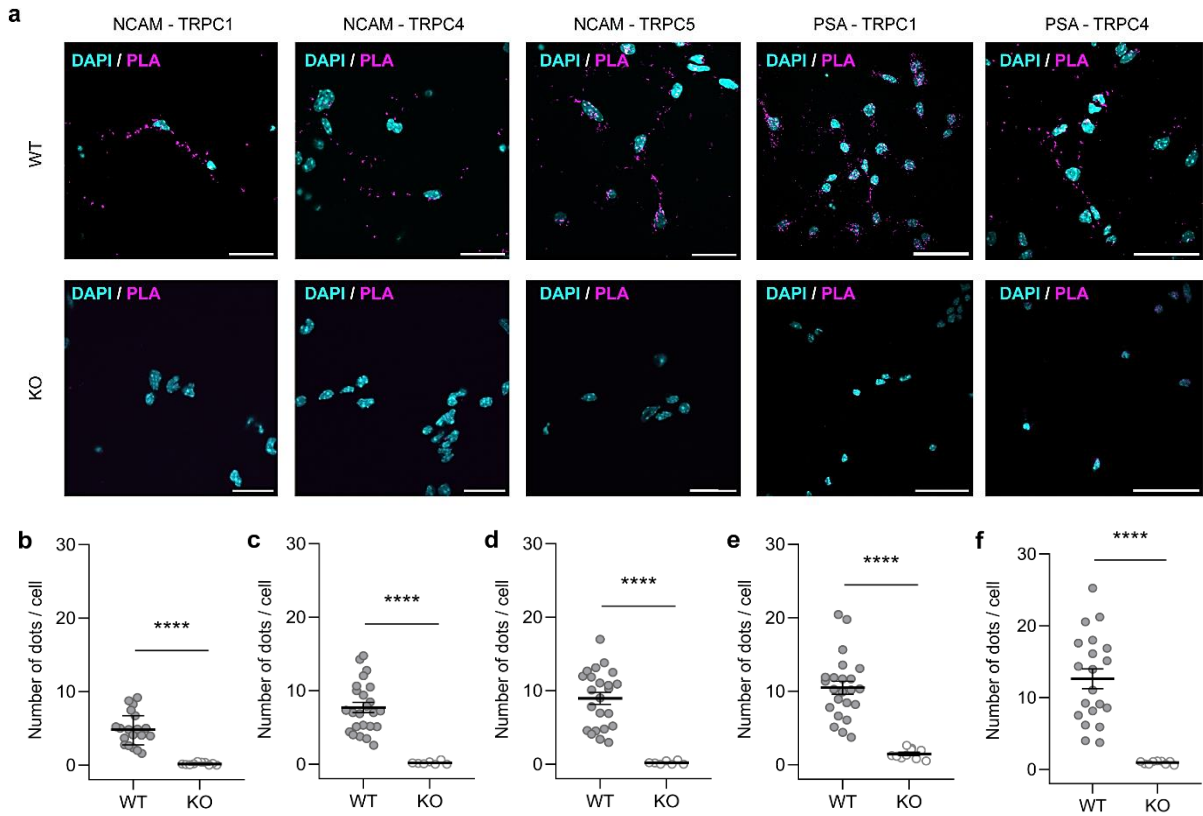


Figure 11. NCAM and PSA localize in close proximity with TRPC1, -4, and -5 in cultured murine cerebellar neurons. NCAM $+/+$ neurons (WT) and NCAM $-/-$ neurons (KO) were subjected to PLA with rabbit NCAM GTX133217 and mouse TRPC1 E6, TRPC4 N77/15, or TRPC5 N67/15 antibodies or mouse PSA735 and rabbit TRPC1 GTX54876 or TRPC4 ACC-119 antibodies. Nuclei were stained using DAPI. **(a)** Representative images of each immunostaining showing NCAM-TRPC1-, NCAM-TRPC4-, NCAM-TRPC5-, PSA-TRPC1-, and PSA-TRPC4-positive dots (magenta) and DAPI (cyan) for NCAM WT and NCAM KO neurons. Scale bars: 20 μm . **(b-f)** Quantification of the number of dots per cell for the NCAM-TRPC1 **(b)**, NCAM-TRPC4 **(c)**, NCAM-TRPC5 **(d)**, PSA-TRPC1 **(e)**, and PSA-TRPC4 **(f)** interactions. Each circle indicates the number of positive dots in one cell. The number of dots was determined from 10 neurons per condition from two independent cultures. Scatter plots show mean values \pm SEM. **** $p < 0.0001$ for an unpaired t-test with Welch's correction.

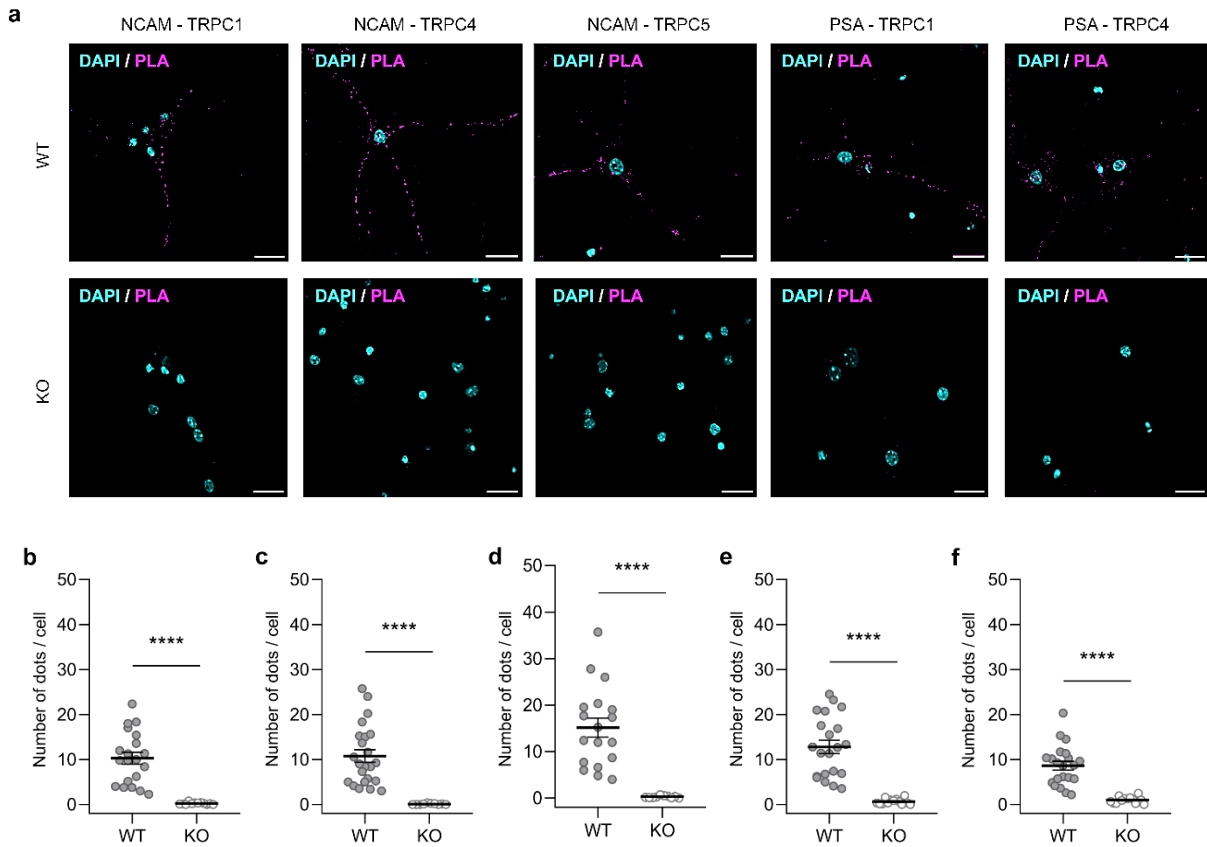


Figure 12. NCAM and PSA localize in close proximity with TRPC1, -4, and -5 in cultured murine hippocampal neurons. NCAM $+/+$ neurons (WT) and NCAM $-/-$ neurons (KO) were subjected to PLA with rabbit NCAM GTX133217 and mouse TRPC1 E6, TRPC4 N77/15, or TRPC5 N67/15 antibodies or mouse PSA735 and rabbit TRPC1 GTX54876 or TRPC4 ACC-119 antibodies. Nuclei were stained using DAPI. (a) Representative images of each immunostaining showing NCAM-TRPC1-, NCAM-TRPC4-, NCAM-TRPC5-, PSA-TRPC1-, and PSA-TRPC4-positive dots (magenta) and DAPI (cyan) for NCAM WT and NCAM KO neurons. Scale bars: 20 μ m. (b-f) Quantification of the number of dots per cell for the NCAM-TRPC1 (b), NCAM-TRPC4 (c), NCAM-TRPC5 (d), PSA-TRPC1 (e), and PSA-TRPC4 (f) interactions. Each circle indicates the number of positive dots in one cell. The number of dots was determined from 10 neurons per condition from two independent cultures. Scatter plots show mean values \pm SEM. **** $p < 0.0001$ for an unpaired t-test with Welch's correction.

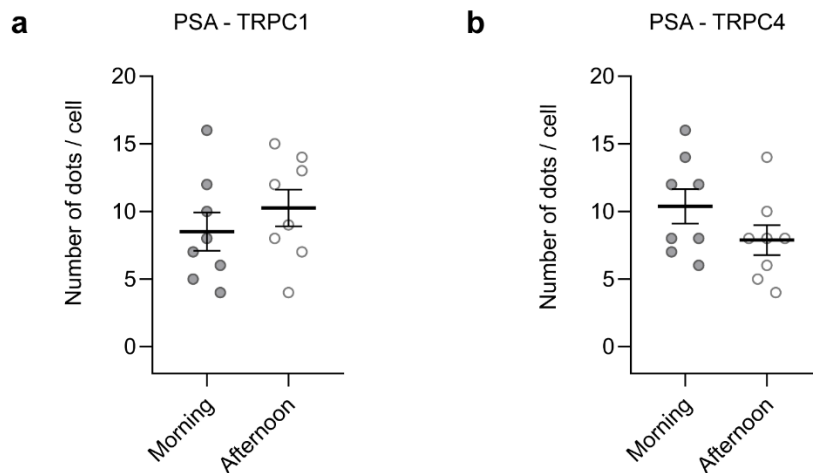


Figure 13. The association of PSA and TRPC1 and -4 is not affected by circadian rhythm. Cultured murine cerebellar neurons fixed in the morning or afternoon were subjected to PLA with mouse PSA735 and rabbit TRPC1 GTX54876 (**a**) or TRPC4 ACC-119 antibodies (**b**). (**a, b**) Graphs show the quantification of the number of dots per cell. Each circle indicates the number of positive dots in one cell. The number of dots was determined from 4 neurons per condition from two independent cultures. Scatter plots show mean values \pm SEM. Non significant differences in an unpaired t-test with Welch's correction.

3.3.3. NCAM associates with TRPC1, -4, and -5 in cortical cells at the plasma membrane

After I determined the co-localization between NCAM and PSA with TRPC1, -4, and -5, I wanted to investigate whether these associations take place at the neuronal plasma membrane (PM) or in the endoplasmic reticulum (ER) by TIRF microscopy. This type of microscopy allows the detection of proteins at a maximum of 100 nm distance from the PM, thus allowing the distinction of the specific compartment where a protein is localized (Figure 15a). For this aim, cultured cortical neurons were transfected with plasmids encoding plasma membrane (Goulden et al., 2019) or endoplasmic reticulum (Holbro et al., 2009) proteins, fixed, and subjected to PLA assay using antibodies labeling NCAM or PSA and TRPC1, -4, or -5. High numbers of NCAM-TRPC1-, NCAM-TRPC4-, NCAM-TRPC5-, PSA-TRPC1-, and PSA-TRPC4-positive dots were observed near or at the plasma membrane but not near the endoplasmic reticulum (Figure 15b-h). Moreover, the localization of the NCAM-TRPC1-positive dots was not altered after stimulating the cells with a function-triggering NCAM antibody neither in the plasma membrane, the plasma membrane and the endoplasmic reticulum, and the endoplasmic reticulum (Figure 16). These results indicate that NCAM-PSA co-localizes with TRPC1, -4, and -5 at the plane of the plasma membrane and that this association is not affected after NCAM triggering.

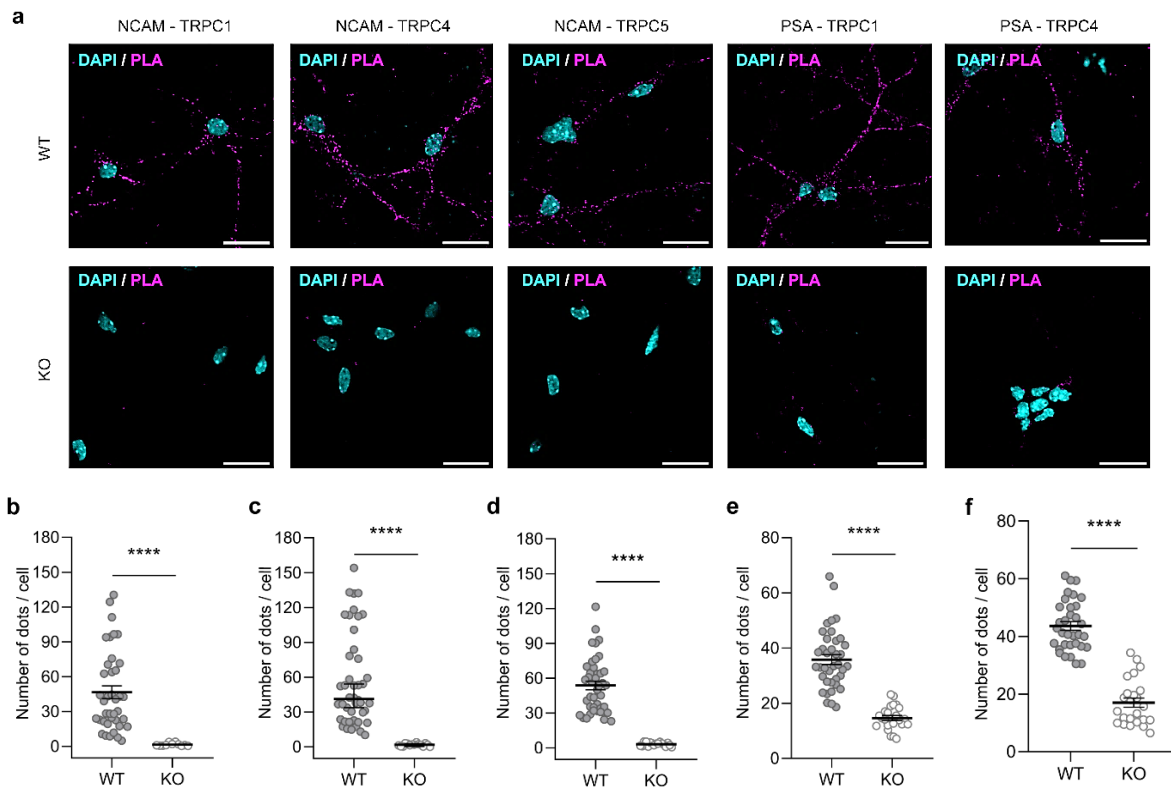


Figure 14. NCAM and PSA localize in close proximity with TRPC1, -4, and -5 in cultured murine cortical neurons. NCAM $+/+$ neurons (WT) and NCAM $-/-$ neurons (KO) were subjected to PLA with rabbit NCAM GTX133217 and mouse TRPC1 E6, TRPC4 N77/15, or TRPC5 N67/15 antibodies or mouse PSA735 and rabbit TRPC1 GTX54876 or TRPC4 ACC-119 antibodies. Nuclei were stained using DAPI. (a) Representative images of each immunostaining showing NCAM-TRPC1-, NCAM-TRPC4-, NCAM-TRPC5-, PSA-TRPC1-, and PSA-TRPC4-positive dots (magenta) and DAPI (cyan) for NCAM WT and NCAM KO neurons. Scale bars: 20 μm . (b-f) Quantification of the number of dots per cell for the NCAM-TRPC1 (b), NCAM-TRPC4 (c), NCAM-TRPC5 (d), PSA-TRPC1 (e), and PSA-TRPC4 (f) interactions. Each circle indicates the number of positive dots in one cell. The number of dots was determined from 10 neurons per condition from three independent cultures. Scatter plots show mean values \pm SEM. **** $p < 0.0001$ for an unpaired t-test with Welch's correction.

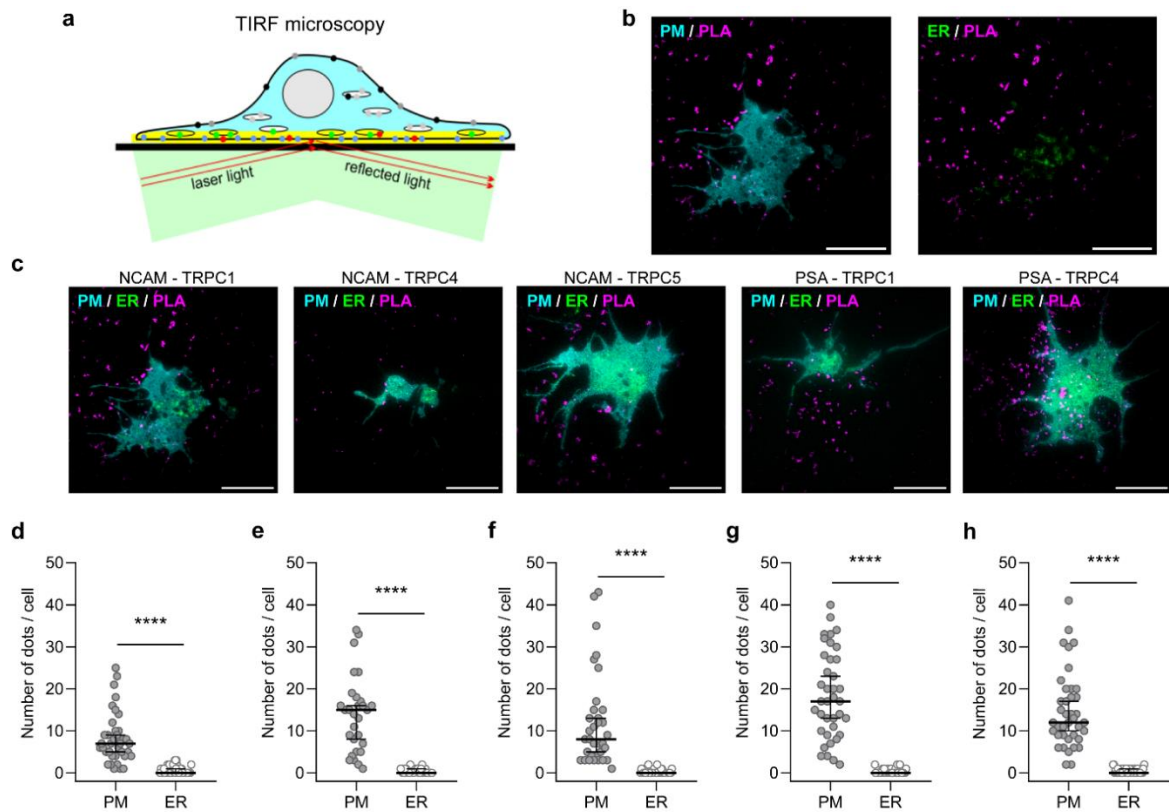


Figure 15. NCAM-PSA localizes with TRPC1, -4, and -5 at the neuronal plasma membrane. **(a)** Schematic representation of TIRF microscopy. A neuron (light blue) attached to a glass coverslip (black bar) with nucleus and ER as ovals are shown. The application of a laser light (green light, red arrows) with a specific angle leads to total refraction of the light, allowing us to stimulate particles only around 60-100 nm deep (yellow background, evanescent field). The fluorophores close to the glass coverslip are the only ones that can be excited. The evanescent field includes fluorophores for the plasma membrane (blue circles), the endoplasmic reticulum (green circles), and the PLA-positive dots (red circles). The non-excited fluorophores are indicated outside the field (black and grey circles). Scheme from (Amores-Bonet et al., 2022). **(b-h)** Cultured cortical neurons transfected with tagBFP2-CAAX (PM) and pMH4-SYN-EGFP-ER (ER) and subjected to PLA with rabbit NCAM GTX133217 and mouse TRPC1 E6, TRPC4 N77/15 or TRPC5 N67/15 antibodies or mouse PSA735 and rabbit TRPC1 ACC-010 or TRPC4 ACC-018 antibodies. **(b)** Representative images showing NCAM-TRPC1 interaction (magenta dots) predominantly near the plasma membrane (PM/PLA) but rarely in the endoplasmic reticulum (ER/PLA). Scale bars: 20 μm . **(c)** Representative images of each immunostaining showing NCAM-TRPC1-, NCAM-TRPC4-, NCAM-TRPC5-, PSA-TRPC1-, and PSA-TRPC4-positive dots (magenta), PM marker (cyan), and ER marker (green). Scale bars: 20 μm . **(d-h)** Quantification of the number of dots per cell. Each circle indicates the number of positive dots per cell. The number of dots was determined separately from the PM and the ER (overlapping dots were not considered) from 10 neurons per condition from three independent cultures. Scatter plots show median values with a 95% confidence interval. **** $p < 0.0001$ for a Mann-Whitney test.

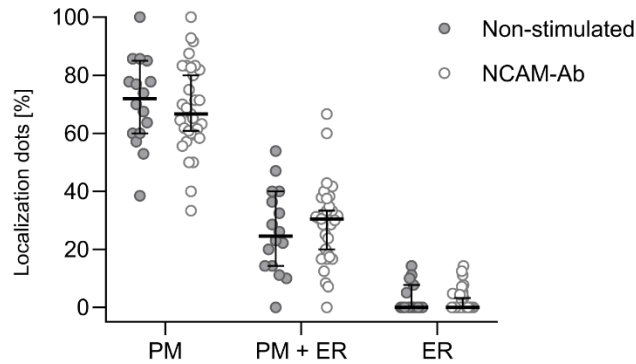


Figure 16. The association of NCAM-TRPC1 at the neuronal plasma membrane is not affected after NCAM triggering. Cultured cortical neurons transfected with tagBFP2-CAAX and pMH4-SYN-EGFP-ER and subjected to PLA with rabbit NCAM GTX133217 and mouse TRPC1 E6 antibodies in the absence (non-stimulated) or presence of NCAM antibody treatment. The graph shows the quantification of the number of positive dots per cell. Each circle indicates the percentage of positive dots localized close to or at the plasma membrane (PM), overlapping dots from the plasma membrane and the endoplasmic reticulum (PM + ER), or in the endoplasmic reticulum (ER) from cultured cortical neurons non-stimulated or stimulated with a function-triggering NCAM antibody (NCAM-Ab). The number of dots was determined from 10 neurons per condition from three independent cultures. Scatter plots show median values with a 95% confidence interval. Mann-Whitney test between non-stimulated and NCAM-Ab stimulated cells from each condition showed no differences.

3.4.4. The association of NCAM with TRPC1, -4, and -5 at the neuronal plasma membrane is independent of PSA

Considering that NCAM-TRPC1-, NCAM-TRPC4-, NCAM-TRPC5-, PSA-TRPC1-, and PSA-TRPC4-positive dots indicated a close association of NCAM-TRPC1, NCAM-TRPC4, NCAM-TRPC5, PSA-TRPC1, and PSA-TRPC4, it was important to clarify whether PSA was relevant for the localization of the association between NCAM and TRPC. For that purpose, TIRF microscopy was performed with cultured cortical neurons transfected with plasmids encoding plasma membrane or endoplasmic reticulum proteins, treated with endoneuraminidase N (Endo N) to degrade PSA (Gerardy-Schahn et al., 1995), fixed, and subjected to PLA assay using antibodies labeling NCAM and TRPC1, -4, or -5. After quantification, no differences were found in the localization of the NCAM-TRPC1-, NCAM-TRPC4-, and NCAM-TRPC5-positive dots with or without Endo N treatment; neither in the plasma membrane, the plasma membrane and the endoplasmic reticulum, and the endoplasmic reticulum (Figure 17a-c). These results indicate that the absence of PSA is not

affecting the association between NCAM and TRPC1, -4, and -5 at the neuronal plasma membrane.

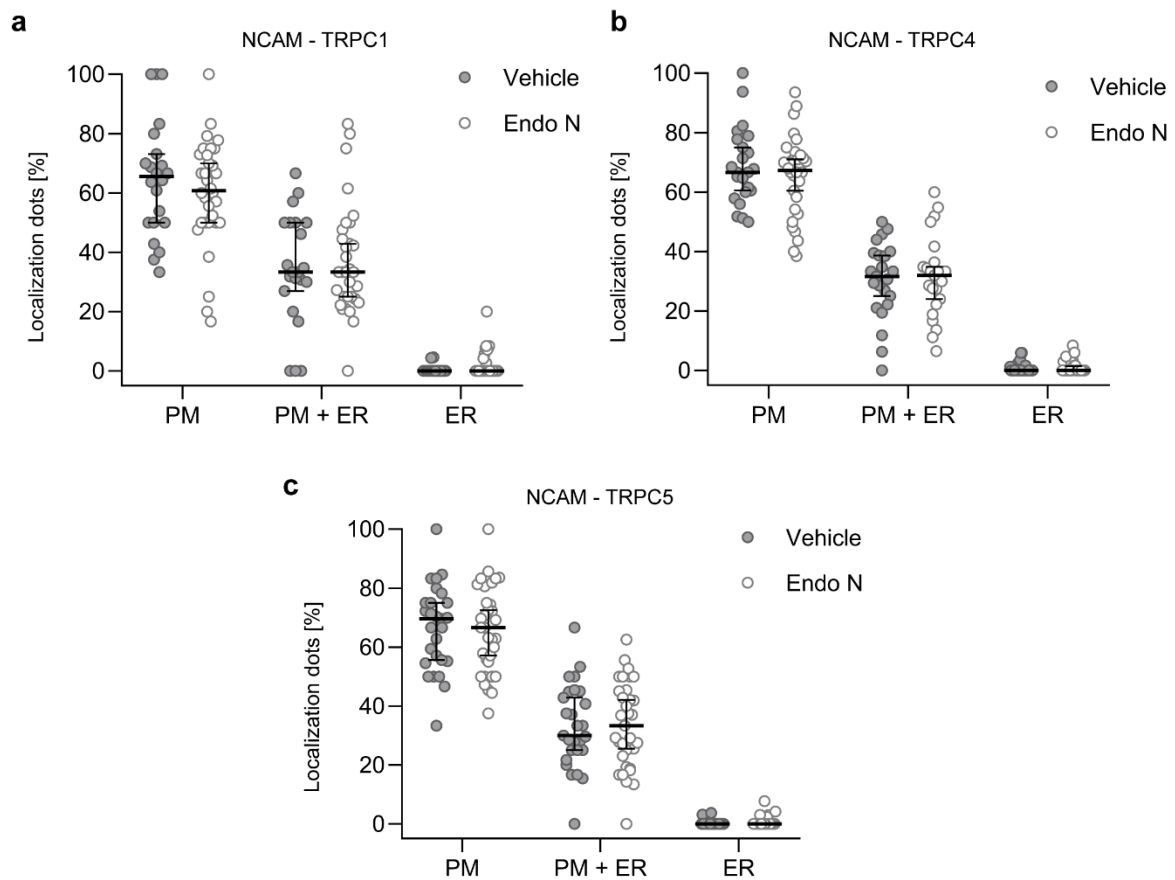


Figure 17. The association of NCAM with TRPC1, -4, and -5 at the neuronal plasma membrane is independent of PSA. Cultured cortical neurons transfected with tagBFP2-CAAX and pMH4-SYN-EGFP-ER and subjected to PLA with rabbit NCAM GTX133217 (**a-c**) and mouse TRPC1 E6 (**a**), TRPC4 N77/15 (**b**), or TRPC5 N67/15 (**c**) antibodies in the absence (vehicle) or presence of Endo N treatment. (**a-c**) The graphs show the quantification of the number of positive dots per cell. Each circle indicates the percentage of positive dots localized at the plasma membrane (PM), overlapping dots from the plasma membrane and the endoplasmic reticulum (PM + ER) or in the endoplasmic reticulum (ER) from vehicle- and Endo N-treated cultured cortical neurons. The number of dots was determined from 10 neurons per condition from three independent cultures. Scatter plots show median values with a 95% confidence interval. Mann-Whitney test between vehicle and Endo N from each condition showed no differences.

3.5. NCAM regulates the Ca²⁺ flux via TRPCs

TRPC channels are regulators of the Ca²⁺ flux, and it is also known that NCAM stimulation elevates cytoplasmic Ca²⁺ levels (Kiryushko et al., 2006; Vangeel & Voets, 2019). Once I established that these proteins interact in neurons from mouse brains, the next step was to determine if NCAM and TRPC1, -4, and -5 work together in regulating calcium signaling. For that purpose, CHO C6 cells constitutively expressing NCAM-PSA, CHO 2A10 cells expressing NCAM alone but not NCAM-PSA, and NCAM^{neg} CHO cells not expressing NCAM or NCAM-PSA were used after transfection with the TRPC1/4 plasmid coding for TRPC1 and TRPC4 or the TRPC1/5 plasmid coding for TRPC1 and TRPC5. Moreover, SKF-96365, a general inhibitor for TRPC channels, was used together with a function-triggering NCAM antibody for calcium imaging experiments.

3.5.1. Transfected CHO cells overexpress TRPC1/4 and TRPC1/5

TRPC1/4 and TRPC1/5 plasmids were produced by inserting TRPC1- and TRPC4- or TRPC1- and TRPC5-encoding cDNA in a pCAGIG vector (Matsuda & Cepko, 2004). The analysis of the cells transfected with these plasmids by Western blot revealed TRPC1-, TRPC4-, and TRPC5-positive bands at around 250 kDa after 24 hours of transfection. The intensity of the bands decreased after 48 hours, and they were not present in the mock-transfected cells (Figure 18a-c). Moreover, immunoprecipitation experiments revealed bands for TRPC1, TRPC4, and TRPC5 at 250 kDa in TRPC1 precipitates from transfected CHO C6 and CHO 2A10 cells. The TRPC1-, TRPC4-, and TRPC5-positive bands were not present in the non-immune controls (Figure 19). These results indicate that transfected CHO cells express TRPC1/4 and TRPC1/5.

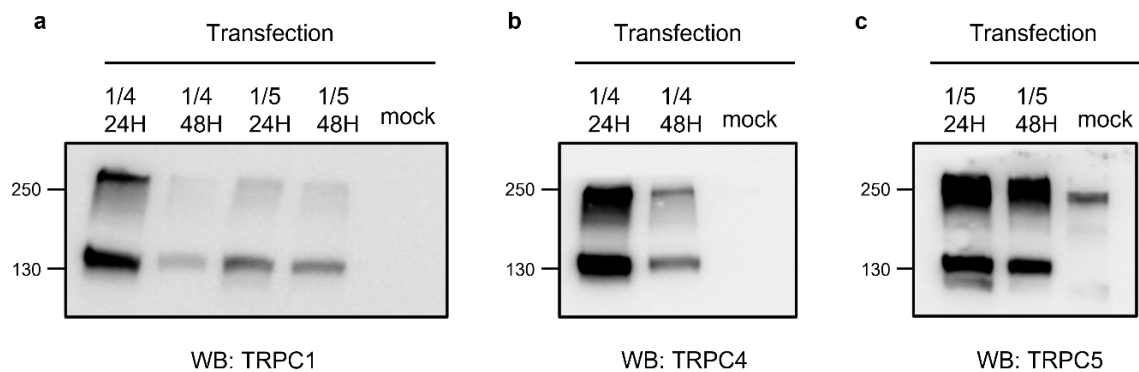


Figure 18. Expression of TRPC1, -4, and -5 in CHO C6 cells after transfection. (a-c) CHO cells transfected with TRPC1/4 plasmid (1/4), TRPC1/5 plasmid (1/5), or mock transfected (mock) were lysed, and the lysates were subjected to Western blot (WB) analysis with TRPC1 E6 (TRPC1) (a), TRPC4 ACC-018 (TRPC4) (b) and TRPC5 1C8 (TRPC5) (c) antibodies after 24 (24H) or 48 (48H) hours transfection time (a-c).

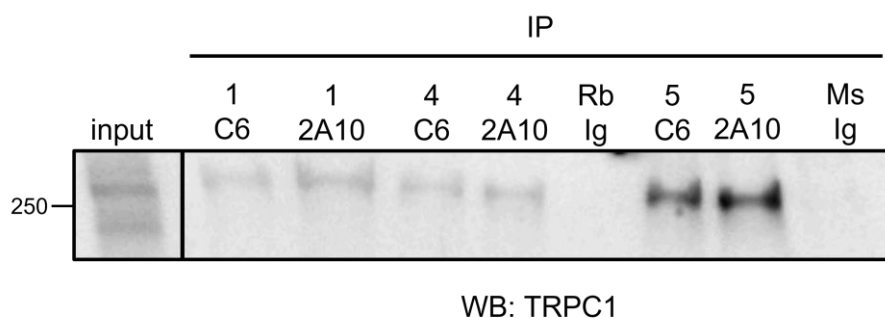


Figure 19. Expression of TRPC1, -4, and -5 in CHO cells after transfection. CHO C6 (C6) and CHO 2A10 (2A10) cells were transfected with TRPC1/4 or TRPC1/5 plasmids. Lysed cells were used for immunoprecipitation (IP) with TRPC1 ACC-010 (1), TRPC4 ACC-018 (4), and TRPC5 1C8 (5) antibodies and non-immune rabbit (Rb) or mouse (Ms) control antibodies (Ig). The cell lysate (input) and the immunoprecipitates were subjected to Western blot (WB) analysis with TRPC1 E6 (TRPC1) antibody.

Next, CHO C6 and CHO 2A10 cells were analyzed to determine the expression of NCAM and NCAM-PSA. Western blot analysis using antibodies against NCAM, PSA, and γ -adaptin revealed an NCAM-positive band at 250 kDa for CHO C6 and CHO 2A10 cells, while the PSA-positive band at 250 kDa was only found in CHO C6 cells. γ -adaptin was used as a loading control (Figure 20a, b). After quantification of the relative levels of NCAM in CHO C6 and CHO 2A10 cells, no differences were found for the total levels of the protein between both cell types (Figure 20c). These results indicate that CHO C6 and CHO 2A10 cells express NCAM similarly and that only CHO C6 cells express PSA.

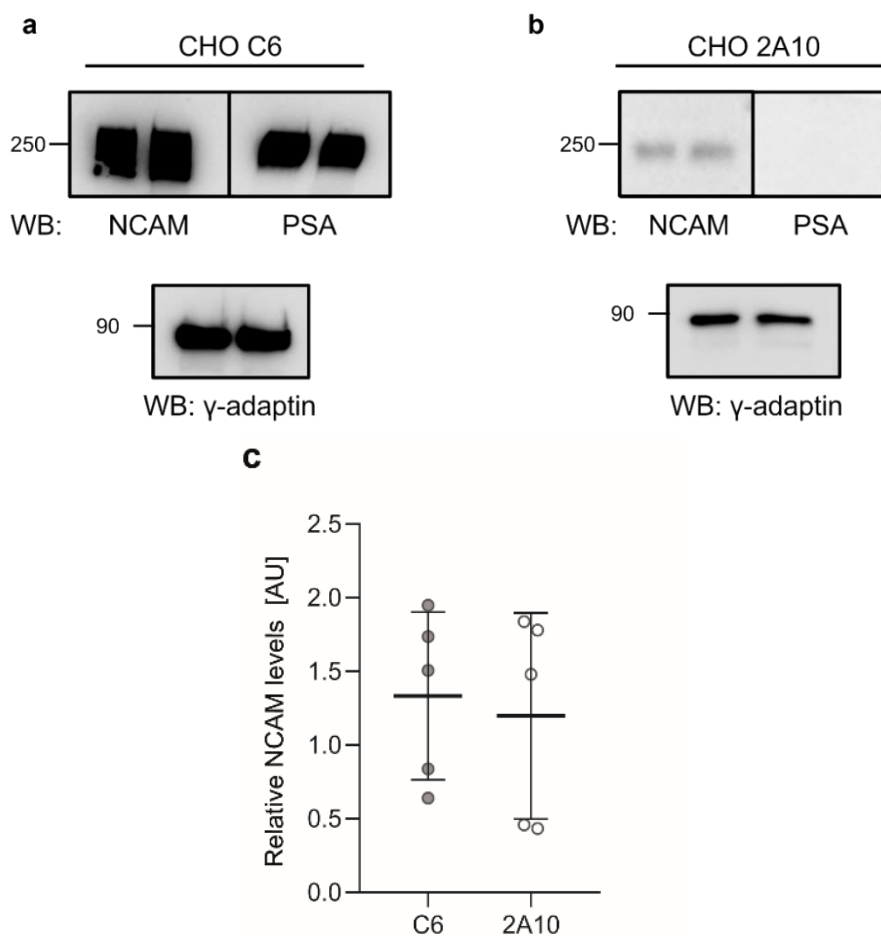


Figure 20. Expression of NCAM and NCAM-PSA in CHO C6 and CHO 2A10 cells. CHO C6 (**a**) and CHO 2A10 (**b**) cells were lysed and subjected to Western blot (WB) analysis with NCAM GTX133217 (NCAM), PSA735 (PSA), and γ -adaplin (γ -adaplin) antibodies. (**c**) Levels of NCAM and γ -adaplin were determined by densitometry. Each dot indicates the relative NCAM level in one culture. Scatter plots show median values with a 95% confidence interval. Mann-Whitney test showed no differences.

3.5.2. The absence of PSA does not affect the co-immunoprecipitation of NCAM with TRPC1, -4, and -5

To further characterize if PSA is relevant for the protein-protein interaction of NCAM with TRPC, immunoprecipitation experiments were performed with CHO C6 and CHO 2A10 cells using TRPC1, -4, and -5 antibodies. Western blot analysis using an antibody against the C-terminal NCAM domain in CHO C6 and CHO 2A10 cells revealed an NCAM-positive band at 250 kDa that was not present in the non-immune control (Figure 21a, b). The opposite experiment using an antibody against the C-terminal domain of NCAM for immunoprecipitation and a TRPC4 antibody for Western blot analysis in CHO C6 and CHO

2A10 cells revealed a TRPC4-positive band at ~230 kDa that was not present in the non-immune control (Figure 21c). These results suggest that the presence or absence of PSA does not affect the NCAM-TRPC association.

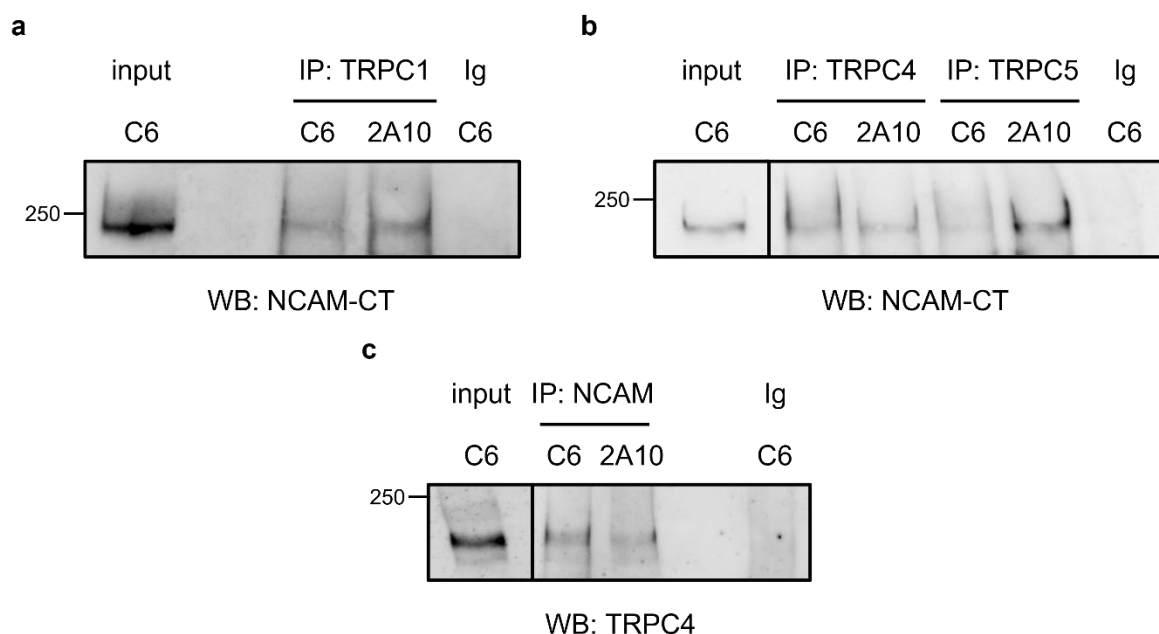


Figure 21. NCAM is associated with TRPC1, -4, and -5. **(a-c)** CHO C6 (C6) and CHO 2A10 (2A10) cells were transfected with TRPC1/4 or TRPC1/5 plasmids. Lysed cells were used for immunoprecipitation (IP) with TRPC1 ACC-010 (TRPC1) **(a)**, TRPC4 ACC-018 (TRPC4), TRPC5 ACC-020 (TRPC5) **(b)**, and NCAM GTX133217 (NCAM) antibodies **(c)**, and a non-immune control antibody (Ig) **(a-c)**. The CHO lysates (input) and the immunoprecipitates were subjected to Western blot (WB) analysis with NCAM GTX133217 (NCAM-CT) **(a, b)** or TRPC4 ACC-018 (TRPC4) **(c)** antibodies.

3.5.3. The overexpression of TRPC1/4 and TRPC1/5 in NCAM-PSA positive CHO cells leads to an increase of the NCAM-dependent Ca²⁺ flux

To perform the calcium imaging experiments, NCAM-negative CHO cells (NCAM^{neg} CHO) or NCAM-positive (NCAM^{pos} CHO) CHO C6 cells were treated with a function-triggering NCAM antibody and incubated with Fluo-4 AM (Fluo4) to monitor calcium flux. The addition of an NCAM antibody to the imaging medium of NCAM^{pos} CHO cells induced an increase of the Fluo4 signal after four seconds, which was not observed in NCAM^{neg} CHO cells (Figure 22a). Moreover, the Fluo4 signal was increased in CHO C6 and CHO 2A10 after treatment with an NCAM antibody (Figure 22b), suggesting that NCAM, but not PSA, is required for the CHO cell response to the NCAM antibody treatment.

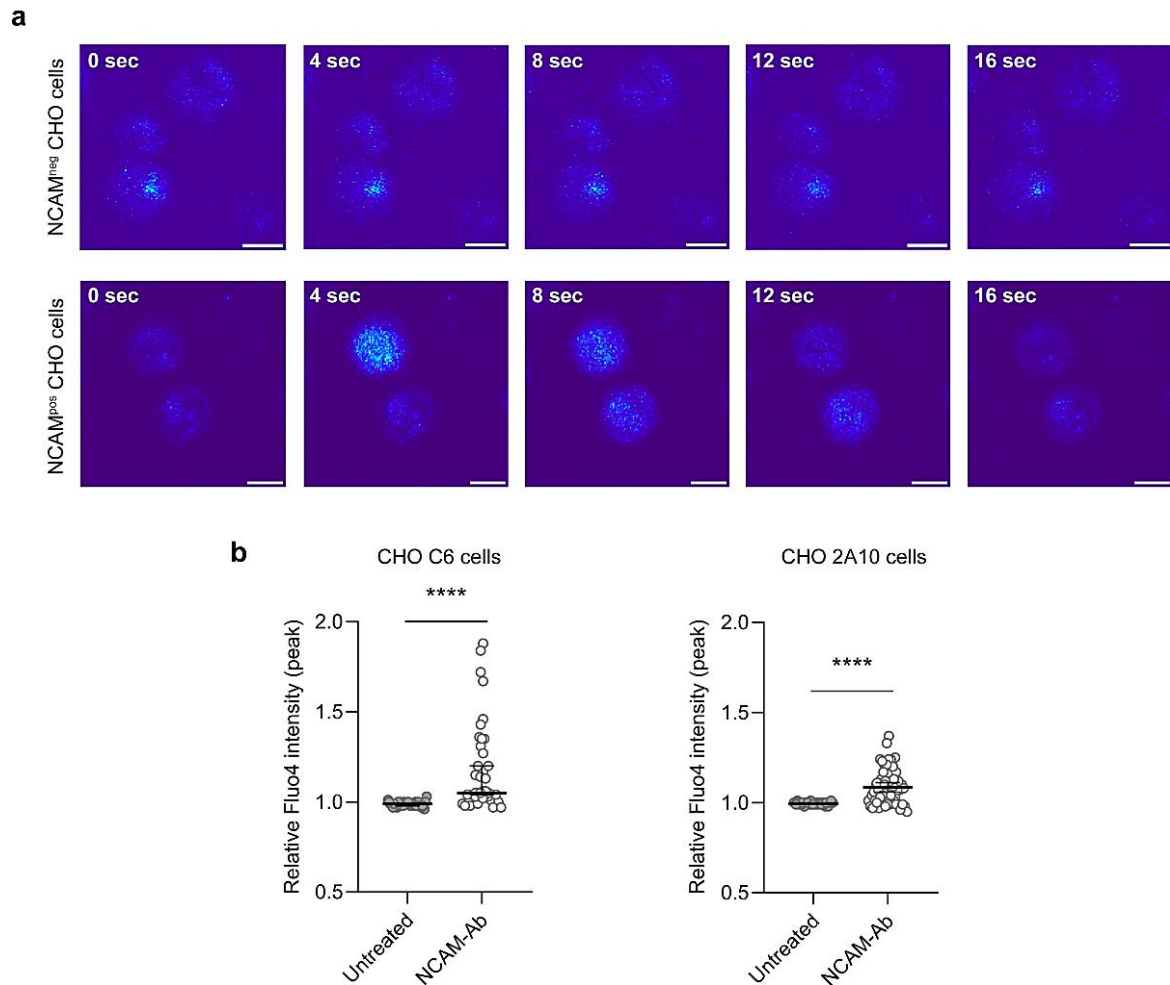


Figure 22. NCAM, but not PSA, is necessary to induce NCAM-dependent Ca^{2+} flux. Cultured CHO cells were treated with an NCAM antibody and incubated with Fluo4 to monitor calcium flux. **(a)** Representative images from a live imaging recording of NCAM^{pos} or NCAM^{neg} CHO cells after adding NCAM antibody at the time point 0. Scale bars: 10 μm . **(b)** Quantification of CHO C6 and CHO 2A10 signal intensity before (Untreated) and after NCAM antibody treatment (NCAM-Ab). The Fluo4 peak values were determined from 10 cells per condition from three independent cultures. Individual cells are plotted. Scatter plots show median values with a 95% confidence interval. **** $p < 0.0001$ for Mann-Whitney test.

To investigate whether NCAM or PSA regulate the NCAM-dependent Ca^{2+} flux via TRPC1/4 or TRPC1/5 heteromers, CHO C6, CHO 2A10, and NCAM^{neg} CHO cells were transfected with plasmids encoding TRPC1/4 or TRPC1/5 fusion proteins and subjected to NCAM antibody treatment. Fluo4 was used to monitor the intracellular calcium changes. After NCAM antibody addition, a lag phase of 10-40 seconds was observed before the channels could open. Afterwards, the signal intensities decreased to background levels in 10-20 seconds in CHO C6 and CHO 2A10 cells, while the increase in Fluo4 intensity was not observed in NCAM^{neg} CHO cells (Figure 23a, c, e). The treatment of CHO C6 cells transfected with TRPC1/4 or TRPC1/5 plasmids with an NCAM antibody resulted in an increase in the Fluo4 signal compared to the mock-transfected CHO C6 cells. The differences between transfections were not observed in CHO 2A10 and NCAM^{neg} CHO cells (Figure 23b, d, f). These results suggest that the modulation of the NCAM-dependent Ca^{2+} flux is mediated by TRPC1/4 or TRPC1/5 and requires PSA attached to NCAM.

3.5.4. The inhibition of TRPC channels reduces the NCAM-dependent Ca^{2+} flux in NCAM-PSA-positive CHO cells

The pre-treatment of CHO C6 and CHO 2A10 cells with the general TRPC inhibitor SKF-96365 showed a decrease in the Fluo4 intensities in CHO C6 cells transfected with TRPC1/4 and TRPC1/5 plasmids but not in mock-transfected cells (Figure 24a). The differences between SKF-96365-treated and vehicle-treated cells were not detectable in TRPC1/4- and TRPC1/5-transfected CHO 2A10 cells (Figure 24b), strengthening the notion that the presence of NCAM-PSA is necessary for the NCAM-dependent Ca^{2+} flux mediated by TRPC, -4, and -5.

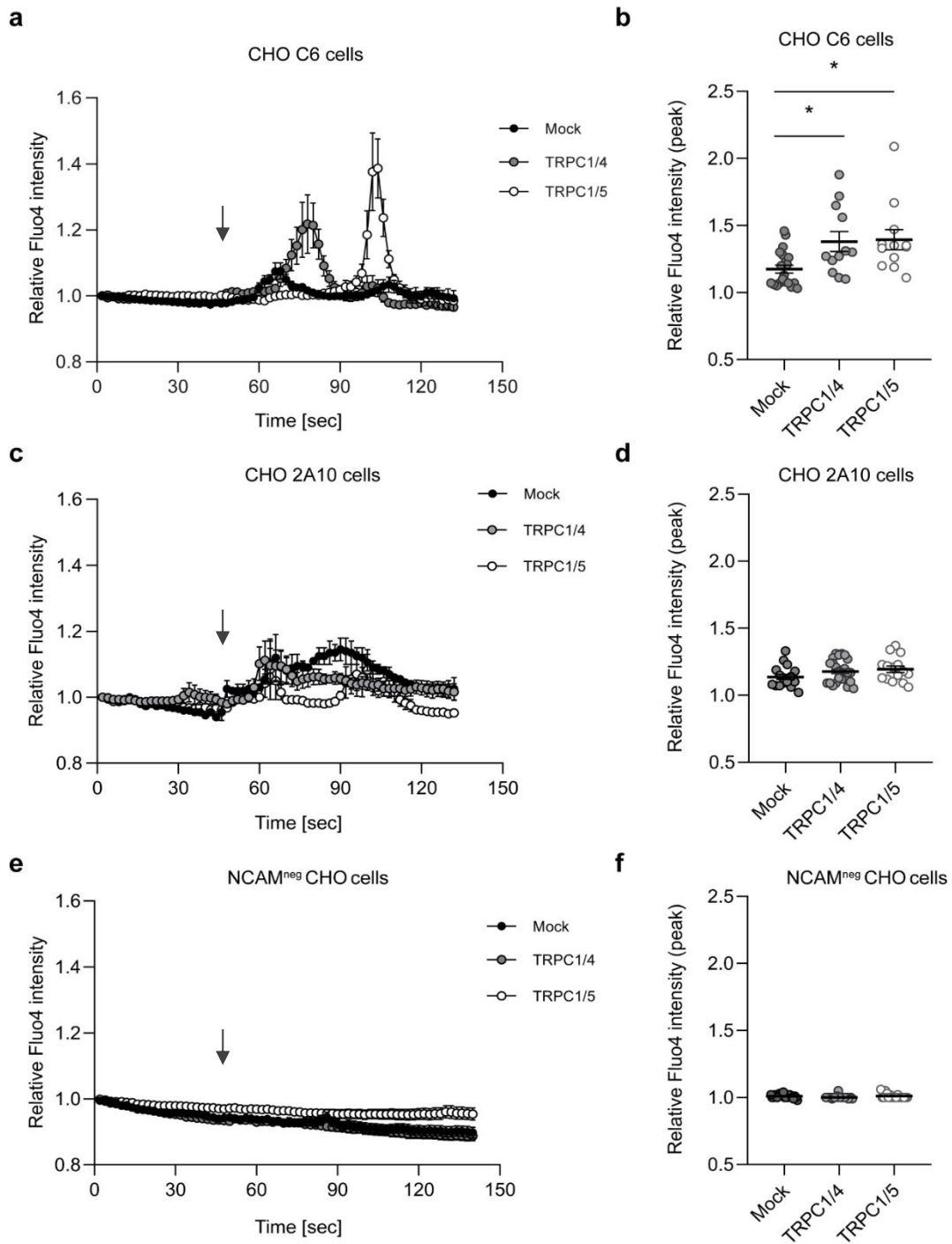


Figure 23. The expression of TRPC1/4 or TRPC1/5 in NCAM-PSA-expressing CHO cells results in an NCAM-dependent Ca^{2+} flux. Cultured CHO cells were transfected with TRPC1/4 or TRPC1/5 plasmids or mock-transfected, treated with an NCAM antibody, and incubated with Fluo4 to monitor calcium flux. **(a, c, e)** Representative time courses of CHO C6, CHO 2A10, and NCAM^{neg} CHO cells transfected with TRPC1/4, TRPC1/5, or mock-transfected after NCAM antibody treatment (the application of antibody is indicated by the grey arrow). **(b, d, f)** Quantification of Fluo4 signal intensity of 6-8 cells per condition from three independent cultures. Each dot indicates the peak value

of the Fluo4 signal in a cell. Scatter plots show mean values with \pm SEM. * $p < 0.05$ for a one-way ANOVA with Kruskal-Wallis post hoc test.

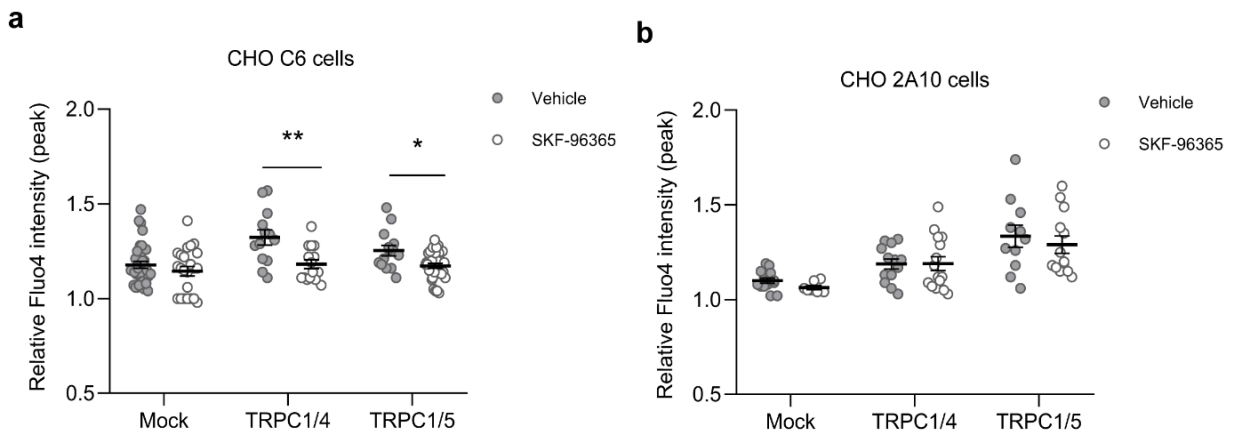


Figure 24. NCAM regulates the Ca^{2+} entry via TRPC1, -4, and -5 in transfected CHO cells that express NCAM-PSA. CHO C6 and CHO 2A10 cells were transfected with TRPC1/4 or TRPC1/5 or mock-transfected and then subjected to SKF-96365 treatment, loaded with Fluo4, and treated with NCAM antibody. **(a, b)** Quantification of the Fluo4 signal intensity of 6-8 cells per condition from three independent cultures. Each dot indicates the peak value of the Fluo4 signal in a cell. Scatter plots show mean values with \pm SEM. * $p < 0.05$ or ** $p < 0.01$ for an unpaired t-test between vehicle and SKF-96365 conditions.

3.6. Wild-type and NCAM-deficient mouse brains express similar levels of TRPC1, -4, and -5

The CHO cell experiments revealed that the interaction between NCAM-PSA and TRPC1, -4, and -5 is required for the NCAM-dependent Ca^{2+} flux. Before starting the calcium imaging experiments in neurons, it was necessary to determine if the TRPC1, -4, and -5 levels are similar in mouse brains from mice lacking and expressing NCAM. Western blot analysis of brain homogenates from NCAM $+/+$ (WT) and NCAM $-/-$ (KO) mice showed TRPC1-, TRPC4-, and TRPC5-positive bands at 90 kDa in both NCAM WT and NCAM KO brain homogenates. An α -tubulin antibody was used as a loading control (Figure 25a). The comparison of the relative TRPC1, -4, and -5 levels between NCAM WT and KO brain extracts did not show any differences (Figure 25b), suggesting that the expression of TRPC1, -4, and -5 is not altered in mice lacking NCAM.

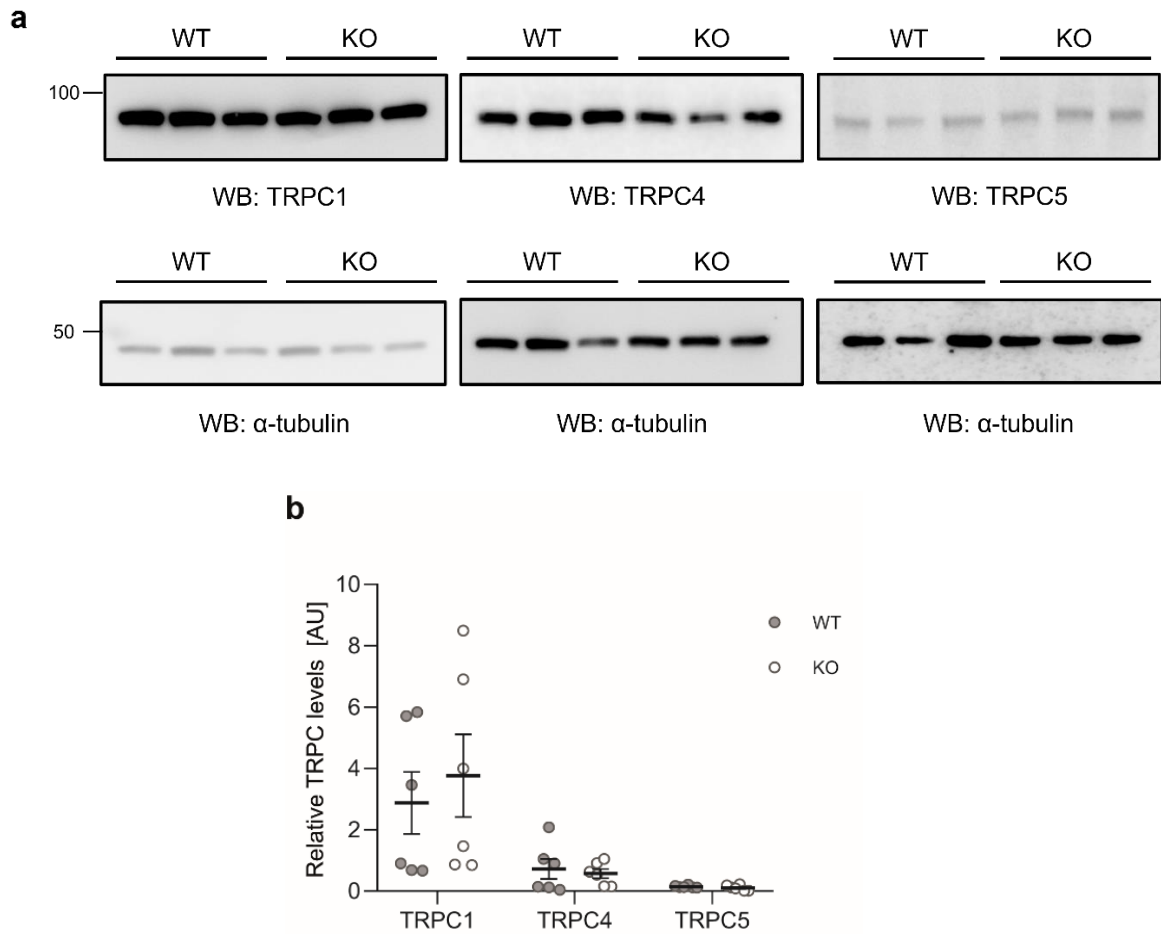


Figure 25. NCAM WT and NCAM KO brain homogenates express similar levels of TRPC1, -4, and -5. Brain homogenates from NCAM $+/+$ (WT) and NCAM $-/-$ (KO) mice were subjected to Western blot (WB) analysis with TRPC1 E6 (TRPC1), TRPC4 ACC-018 (TRPC4), TRPC5 IC8 (TRPC5), and α -tubulin TU-02 (α -tubulin) antibodies. **(a)** Representative WB images with samples from three mice per genotype are shown. **(b)** Quantification of the TRPC1, -4, and -5 levels relative to α -tubulin levels from brain homogenates from six mice. Each dot indicates the relative amount of TRPC in a brain homogenate. Scatter plots show mean values with \pm SEM. No differences were found comparing WT and KO brain extracts using an unpaired t-test.

3.7. NCAM regulates the Ca²⁺ influx via TRPC1, -4, and -5 in cortical neurons

3.7.1. The presence of NCAM-PSA is required for the NCAM-dependent function triggering

My previous PLA experiments showed that NCAM-PSA and TRPC1, -4, and -5 are in close proximity in cerebellar, hippocampal, and cortical neurons (Figures 11, 12, and 14). As the interaction appears in different neuronal types, the calcium imaging experiments were performed using cortical cells for technical reasons. Cortical neurons were isolated from embryonic day 16 brains from NCAM WT and NCAM KO mice, treated with a function-triggering NCAM antibody, and incubated with Fluo4 to monitor calcium flux. NCAM antibody addition to the imaging medium of NCAM WT cells triggered an increase in the Fluo4 signal after 20 seconds. This increase was not observed in NCAM KO neurons (Figure 26a). After NCAM antibody addition, a lag phase of 10-20 seconds was observed before the channels could open. Afterwards, the calcium intensities returned to background levels in 80-100 seconds (Figure 26b, c). The NCAM-dependent calcium response was present in NCAM WT neurons, while NCAM KO neurons showed a reduced Fluo4 signal increase (Figure 26b). Moreover, treatment of NCAM WT cortical cells with Endo N reduced the Fluo4 signal flux compared to vehicle-treated WT cells (Figure 26c). These results suggest that the presence of PSA on NCAM is required for NCAM-dependent calcium signaling in neurons.

3.7.2. The inhibition of TRPC1, -4, and -5 with pico145 reduces the NCAM-dependent Ca²⁺ flux

My previous results showed that NCAM antibody addition to the imaging medium triggers an NCAM-dependent Ca²⁺ flux in cortical neurons expressing NCAM-PSA (Figure 26). Moreover, I showed that the NCAM antibody-induced calcium flux is reduced after TRPC inhibition in CHO cells expressing NCAM-PSA and TRPC1, -4, and -5 (Figure 24). To investigate whether the NCAM-dependent neuronal calcium signaling is affected by TRPC inhibition, cultured cortical neurons were treated with HC-070 and M084, inhibitors of TRPC4- and -5-containing channels, pico145, an inhibitor of TRPC1, -4, and -5, GSK-417651A, an inhibitor of TRPC3, -6, and -7, and colominic acid, the bacterial homolog of PSA. After applying an NCAM antibody, the Fluo4 signal was reduced in neurons pre-treated with pico145 compared to vehicle-treated neurons (Figure 27a and Figure 28). Moreover, the pico145 treatment caused a concentration-dependent inhibition of the NCAM-dependent calcium flux (Figure 27b). The pre-treatment of wild-type cortical neurons with HC-070, M084, and GSK-417651A did not affect the NCAM antibody-dependent increase in Fluo4

intensity. In contrast, the Fluo4 intensity was reduced in wild-type cells pre-treated with colominic acid or Endo N and in KO cells (Figure 28). These results indicate that the inhibition of TRPC1, -4, and -5 with pico145 reduces the NCAM-dependent Ca^{2+} signaling.

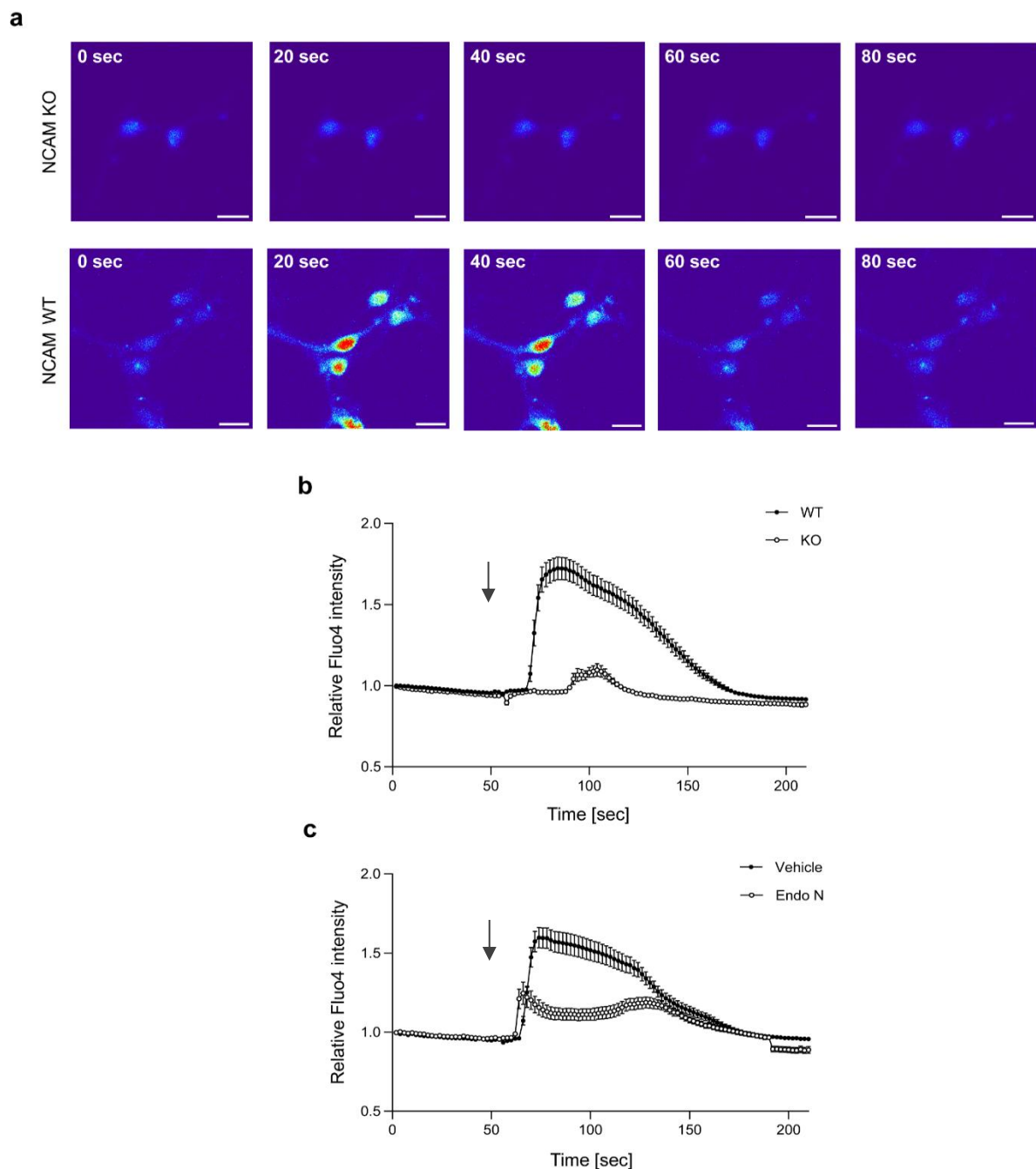


Figure 26. NCAM-PSA is required for the NCAM-dependent calcium response. Cultured cortical neurons were treated with an NCAM antibody and incubated with Fluo4 to monitor calcium flux. **(a)** Representative images from a live imaging recording of NCAM $+/+$ (WT) or NCAM $-/-$ (KO) cultured cortical cells after adding NCAM antibody at the time point 0. Scale bars: 10 μm . **(b, c)** Representative time-course of NCAM WT **(b, c)** or NCAM KO **(b)** cultured cortical cells without **(b, c)** or with Endo N treatment **(c)** after NCAM antibody treatment (the application of antibody is

indicated by the grey arrow). Mean values \pm SEM of Fluo4 signal intensity of 15 cells per condition from three independent cultures.

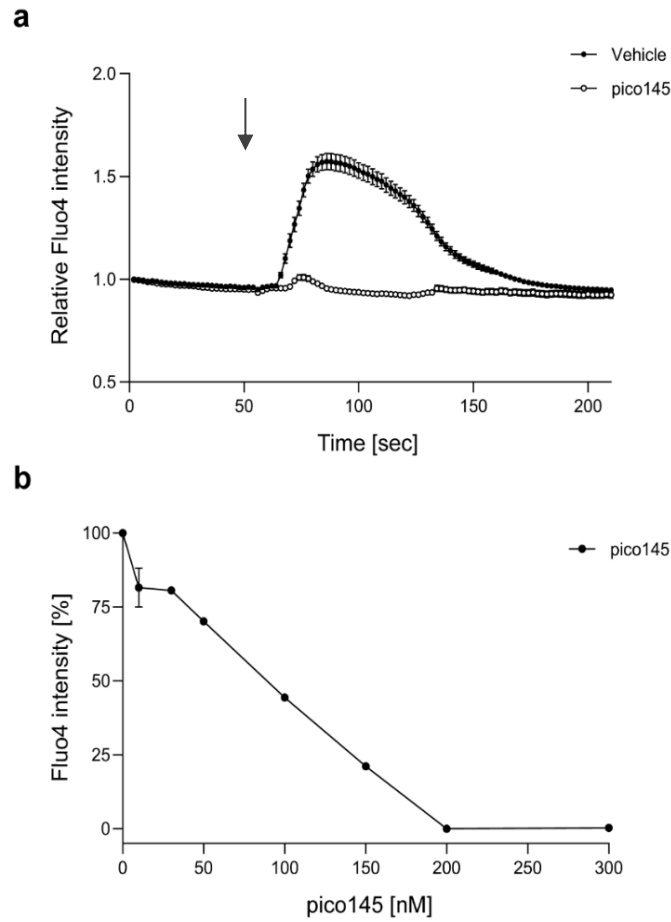


Figure 27. Pico145 inhibits the NCAM-dependent increase of Fluo4 intensity. Cultured cortical neurons were treated with an NCAM antibody and incubated with Fluo4 to monitor calcium flux. **(a)** Representative time-course of wild-type neurons after NCAM antibody treatment (the application of antibody is indicated by the grey arrow) in the absence (vehicle) or presence of pico145 inhibitor. **(b)** Representation of the Fluo4 intensity percentage after pre-treatment of cultured cortical cells with increasing concentrations of pico145 and NCAM antibody treatment. Mean values \pm SEM of Fluo4 signal intensity of 15 cells per condition from three independent cultures **(a)** and 10 cells per condition from two independent cultures **(b)**.

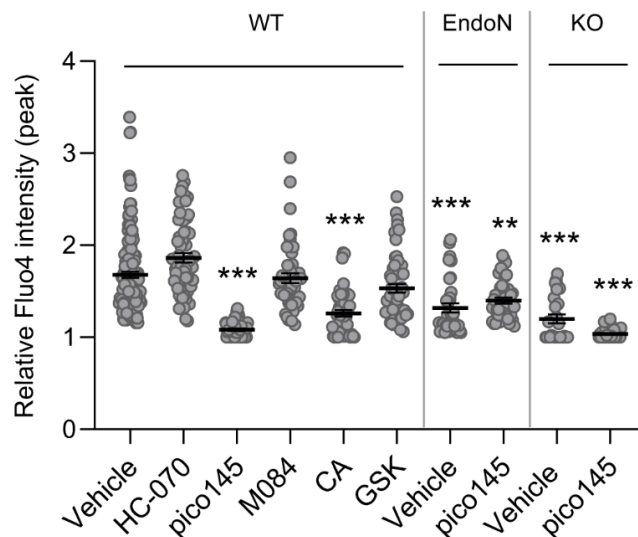


Figure 28. NCAM regulates the Ca^{2+} influx via TRPC1, -4, and -5 in cortical neurons. Cultured cortical NCAM $+/+$ (WT) neurons, Endo N pre-treated wild-type neurons (Endo N), and NCAM-deficient (KO) neurons were treated with NCAM antibody in the absence (vehicle) or presence of HC-070, pico145, M084, colominic acid (CA), and GSK-417651A (GSK) and incubated with Fluo4 to monitor calcium flux. Quantification of the peak Fluo4 values for wild-type neurons after NCAM antibody treatment. Each dot indicates the peak Fluo4 value per cell. Scatter plots show mean values \pm SEM and single values from three independent cultures analyzing 15 cells per treatment and experiment. One-way ANOVA with Kruskal-Wallis as post hoc test, ** $p < 0.01$, *** $p < 0.001$ relative to values of vehicle-treated wild-type neurons.

3.7.3. The treatment of cortical neurons with TRPC1 261-278 peptide increases the TRPC1-dependent Ca^{2+} flux

My ELISA experiments showed that the TRPC1 peptide comprising amino acids 261-278 of murine TRPC1 binds to NCAM140-ICD and colominic acid in a concentration-dependent manner (Figure 8b-d). Moreover, the mutated TRPC1 peptide showed a reduced binding capacity to NCAM140-ICD compared to the TRPC1 peptide, but these differences were not-significant (Figure 8e). Despite the lack of differences in the ELISA binding, the treatment of wild-type cortical neurons with the TRPC1 unmutated peptide induced a Ca^{2+} flux that was significantly lower after the treatment with the TRPC1 mutated peptide (Figure 29a, b). These results further support the hypothesis that the TRPC1 region 261-278 is involved in the binding between NCAM140 and TRPC1.

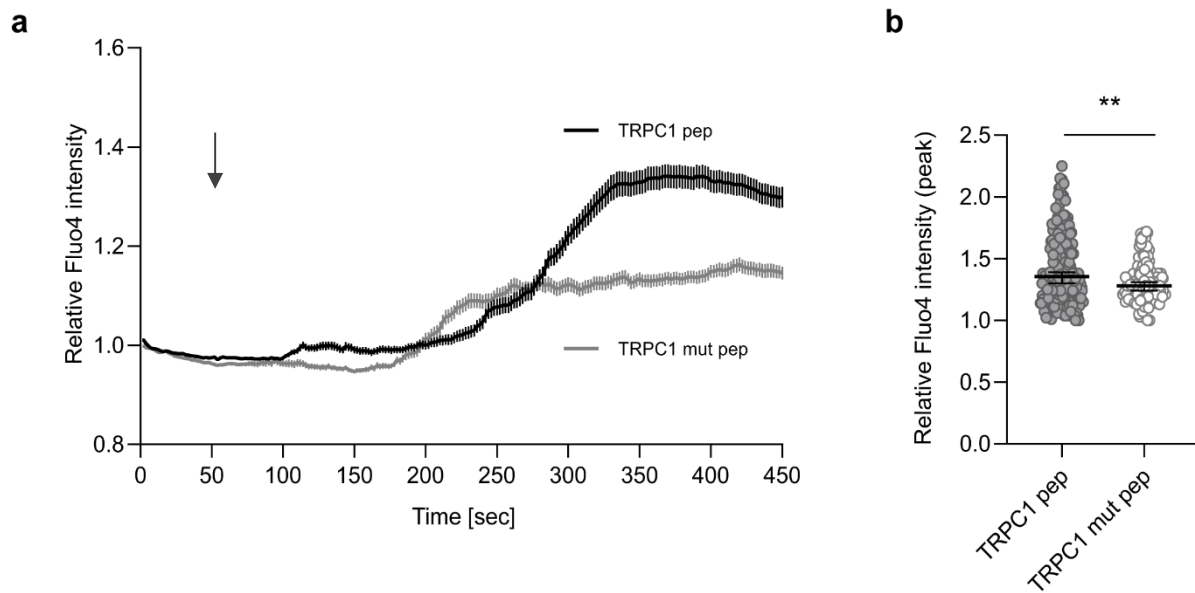


Figure 29. The TRPC1 261-278 peptide is involved in the binding between NCAM and TRPC1. Cultured cortical wild-type neurons were treated with TRPC1 peptide (TRPC1 pep) or TRPC1 mutated peptide (TRPC1 mut pep) and incubated with Fluo4 to monitor calcium flux. (a) Representative time-course of wild-type neurons after TRPC1 pep or TRPC1 mut pep treatment (the application of TRPC1 peptide is indicated by the grey arrow). (b) Quantification of the peak Fluo4 values for wild-type neurons after TRPC1 pep or TRPC1 mut pep treatment. Each dot indicates the peak Fluo4 value per cell. Scatter plots show median values with 95% CI and single values from three independent cultures analyzing 30 cells per treatment and experiment. Mann-Whitney test, ** $p < 0.01$.

3.8. The NCAM-dependent Ca^{2+} signaling depends on the influx of extracellular calcium and, to a lower extent, on the influx from intracellular stores

As previously seen, NCAM antibody treatment can trigger an NCAM-dependent Ca^{2+} flux regulated by the TRPC1, -4, and -5 channels (Figure 28). Next, I wanted to determine if the NCAM-triggered calcium signaling depends on the opening of intracellular calcium stores or the extracellular Ca^{2+} influx from the culture medium. To this aim, embryonic cortical neurons were pre-incubated with thapsigargin, a drug that inhibits the retrotranslocation of Ca^{2+} to the intracellular stores, in the absence or presence of Ca^{2+} in the imaging medium, and stimulated with NCAM antibody. The cells with extracellular Ca^{2+} availability and treated with thapsigargin showed an increased Ca^{2+} flux. On the contrary, the cells that only had intracellular Ca^{2+} availability, which were cells without incubation with thapsigargin,

showed a reduction in the Ca^{2+} flux. Finally, the Ca^{2+} flux was abolished in cells treated with thapsigargin and without extracellular Ca^{2+} availability (Figure 30a). The quantification of the Fluo4 intensity confirmed that the Ca^{2+} flux was increased in cells treated with thapsigargin and with extracellular Ca^{2+} availability (Figure 30b). These results suggest that the NCAM-regulated TRPC1, -4, and -5 channels function mainly as receptor-operated Ca^{2+} channels.

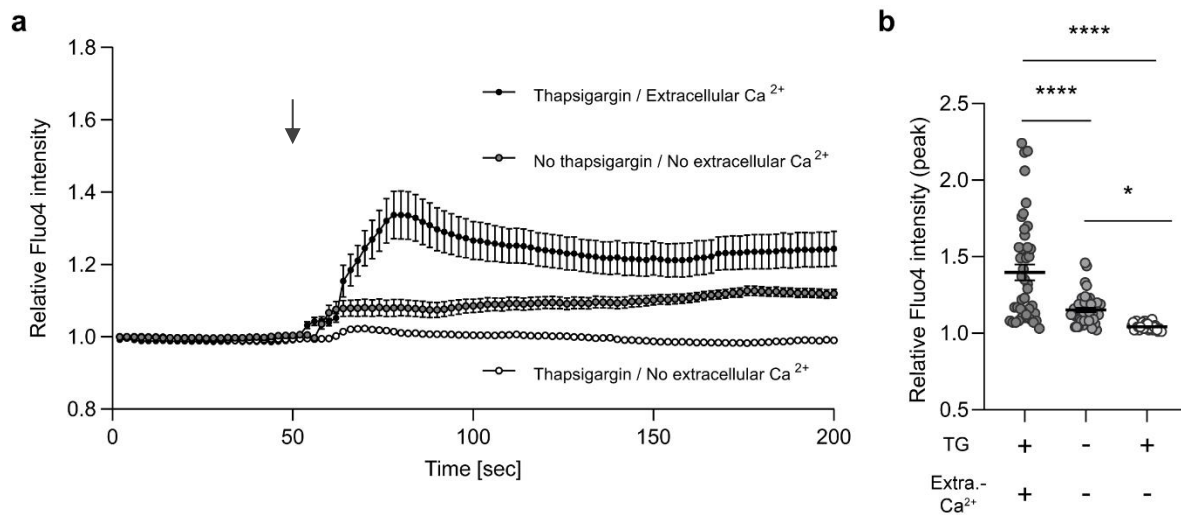


Figure 30. The NCAM-dependent Ca^{2+} signaling depends on the influx of extracellular calcium and, to a lower extent, on the influx from intracellular stores. Cultured wild-type cortical cells were pre-treated with thapsigargin, treated with an NCAM antibody, and incubated with Fluo4 to monitor calcium flux. **(a)** Representative time-course of wild-type neurons after NCAM antibody treatment (the application of antibody is indicated by the grey arrow) in the absence (no thapsigargin) or presence of thapsigargin (thapsigargin) and in the absence (no extracellular Ca^{2+}) or presence of Ca^{2+} in the extracellular medium (extracellular Ca^{2+}). Mean values \pm SEM of Fluo4 signal intensity of 15 cells per condition from three independent cultures. **(b)** Quantification of the Fluo4 peak value in wild-type neurons after NCAM antibody treatment in the absence (-) or presence (+) of thapsigargin (TG) or Ca^{2+} in the extracellular medium (Extra.- Ca^{2+}). Each dot indicates the Fluo4 peak value per cell. Scatter plots show mean values \pm SEM from three independent cultures analyzing 15 cells per treatment and experiment. One-way ANOVA with Kruskal-Wallis as post hoc test, * $p < 0.05$ and **** $p < 0.0001$.

3.9. The inhibition of TRPC1, -4, and -5 with pico145 reduces the NCAM-dependent Ca²⁺ flux in astrocytes

Glial cells express NCAM120 and NCAM140 (Jucker et al., 1995). To study if the astrocytic NCAM-dependent calcium signaling is affected by TRPC inhibitors similarly as in neurons, astrocytes were isolated from brains of wild-type mice, cultured, and pre-treated with HC-070, pico145, M084, colominic acid, and GSK-417651A. After applying an NCAM antibody, the Fluo4 signal was reduced only in astrocytes pre-treated with pico145, while pre-treatment with HC-070, M084, colominic acid, and GSK-417651A did not show any differences (Figure 31). These results suggest that the inhibition of TRPC1, -4, and -5 with pico145 reduces the NCAM-dependent Ca²⁺ flux in astrocytes.

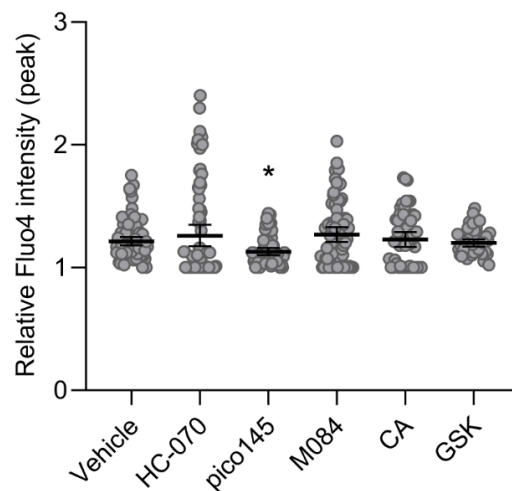


Figure 31. NCAM regulates the Ca²⁺ flux via TRPC1, -4, and -5 in astrocytes. Cultured wild-type astrocytes were treated with NCAM antibody in the absence (vehicle) or presence of HC-070, pico145, M084, colominic acid (CA), and GSK-417651A (GSK) and incubated with Fluo4 to monitor calcium flux. Quantification of the peak Fluo4 values for wild-type astrocytes after NCAM antibody treatment. Each dot indicates the peak Fluo4 value per cell. Scatter plots show mean values ± SEM and single values from three independent cultures analyzing 15 cells per treatment and experiment. One-way ANOVA with Kruskal-Wallis as post hoc test, * p < 0.05 relative to vehicle-treated astrocytes values.

3.10. The NCAM-dependent phosphorylation of Erk1/2 is modulated by TRPC1, -4, and -5

After establishing that NCAM and TRPC1, -4, and -5 interact and that the interaction is relevant for the NCAM-dependent Ca^{2+} flux, the next step was to study the functional relevance of this association in cortical neurons. Since NCAM regulates the phosphorylation of PKC and Erk1/2 (Kolkova et al., 2005; Niethammer et al., 2002), cultured embryonic cortical neurons were pre-treated with HC-070, pico145, or colominic acid and then treated with NCAM antibody to analyze the Erk1/2 and PKC phosphorylation state by Western blot.

3.10.1. The NCAM antibody treatment leads to Erk1/2 and PKC phosphorylation

First, cultured cortical neurons were lysed after 5, 10, 15, 20, 30, or 40 minutes-treatment with NCAM antibody to determine the optimal phosphorylation time for pErk1/2 and pPKC. Western blot analysis of lysed cortical neurons using phosphorylated and total Erk1/2 and phosphorylated and total PKC antibodies showed Erk1/2-positive bands at 42 and 44 kDa corresponding to phosphorylated and total Erk1 and Erk2, respectively, and a PKC-positive band at ~80 kDa corresponding to phosphorylated and total PKC (Figure 32a, b). After quantification, the phosphorylation levels of Erk1/2 were higher after 20 minutes (Figure 32c), while the phosphorylation levels of PKC were higher after 15 minutes of treatment with NCAM antibody (Figure 32d).

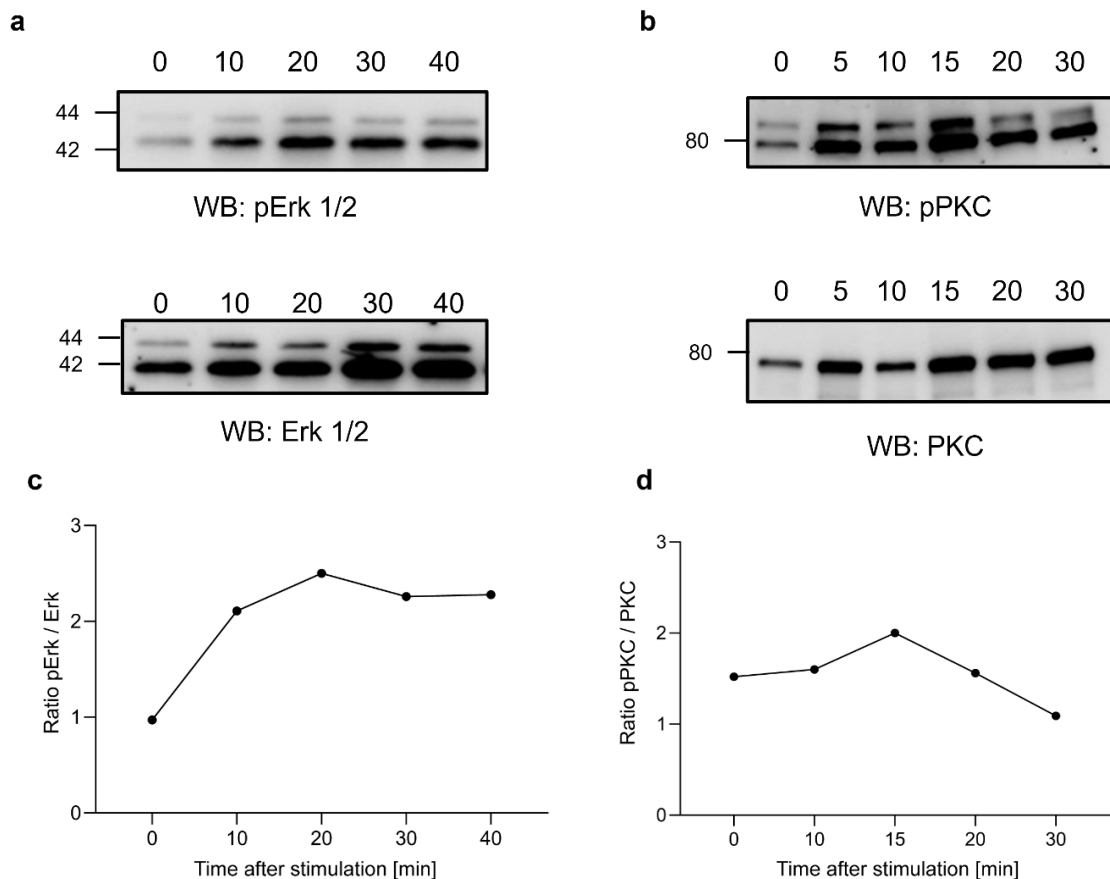


Figure 32. The Erk1/2 and PKC phosphorylation peaks are 15-20 minutes after the NCAM antibody treatment. Cortical neurons were lysed, and lysates were subjected to Western blot (WB) analysis with phosphorylated and total Erk1/2 (**a**), and phosphorylated and total PKC (**b**) antibodies after 0 min (0), 5 min (5), 10 min (10), 15 min (15), 20 min (20), 30 min (30), and 40 min (40) stimulation with NCAM antibody. (**a**, **b**) Representative WB images are shown. (**c**, **d**) Quantification of the relative levels of Erk1/2 (**c**) and PKC (**d**) phosphorylation after NCAM antibody treatment from two independent cultures.

3.10.2. The NCAM-dependent Erk1/2 phosphorylation is affected by TRPC1, -4, and -5 inhibition

As mentioned above, I studied the role of TRPC1, -4, and -5 in the NCAM-dependent Erk1/2 and PKC phosphorylation by pre-treating cortical neurons for 20 minutes with HC-070, pico145, or colominic acid, treating with NCAM an antibody and analyzing the phosphorylation state by Western blot. After lysis, 42 and 44 kDa Erk1/2-positive and ~80 kDa PKC-positive bands were observed in the Western blot membranes for the phosphorylated and the total Erk1/2 and PKC proteins for all the conditions. γ -adapatin was used as a loading control (Figure 33a, b).

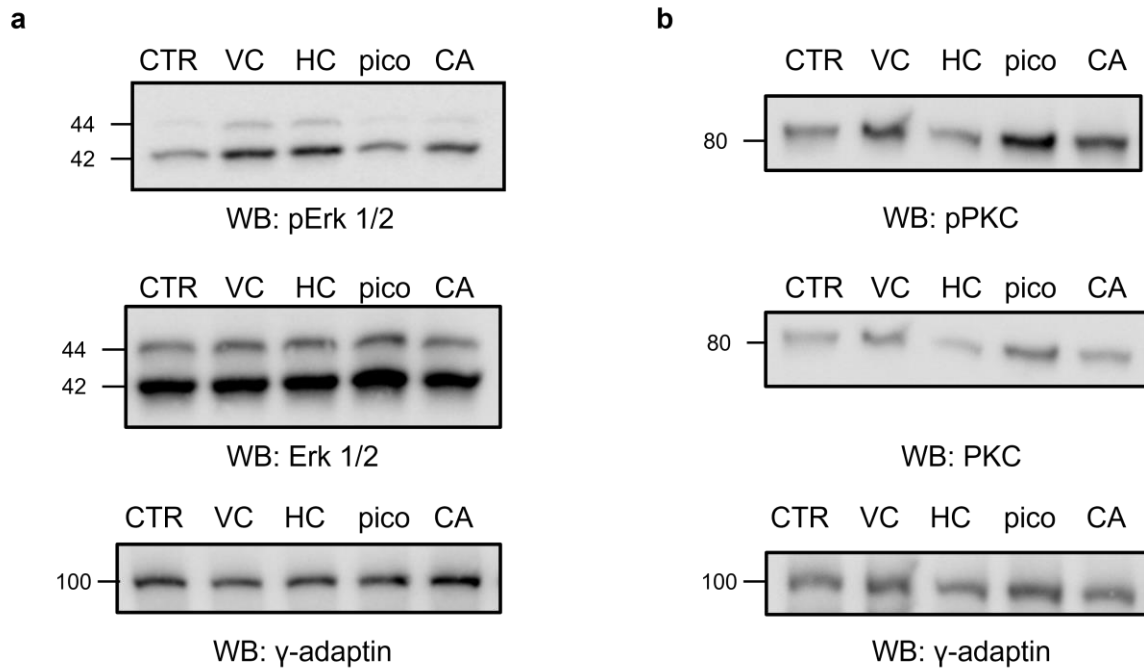


Figure 33. Western-blot analysis of NCAM-dependent phosphorylation of Erk1/2 and PKC expression in cortical neurons. **(a, b)** Cultured cortical neurons were treated without (CTR) or with NCAM antibody in the absence (vehicle, VC) or presence of HC-070 (HC), pico145 (pico), or colominic acid (CA), lysed, and subjected to WB analysis with antibodies against phosphorylated and total Erk1/2 **(a)**, phosphorylated and total PKC **(b)** and γ -adapatin **(a, b)**.

On the one hand, the pre-treatment of cultured cortical neurons with pico145 or colominic acid decreased the NCAM-dependent Erk1/2 phosphorylation compared to vehicle-treated neurons; this reduction was not observed in cells pre-treated with HC-070 (Figure 34a). The differences in the phosphorylation state of Erk1/2 after pre-treatment with pico145 or colominic acid were not seen in NCAM KO cells compared to vehicle-treated neurons (Figure 34b). On the other hand, the NCAM-dependent PKC phosphorylation was not affected by the pre-treatment of cells with HC-070, pico145, or colominic acid neither when analyzing the Ser660 phosphorylation present in all PKC isoforms (Figure 35a) nor the specific Thr638/641 phosphorylation only present in PKC α and PKC β II (Figure 35b). These results suggest that the NCAM-dependent phosphorylation of Erk1/2 depends on TRPC1, -4, and -5 but not the NCAM-dependent PKC phosphorylation.

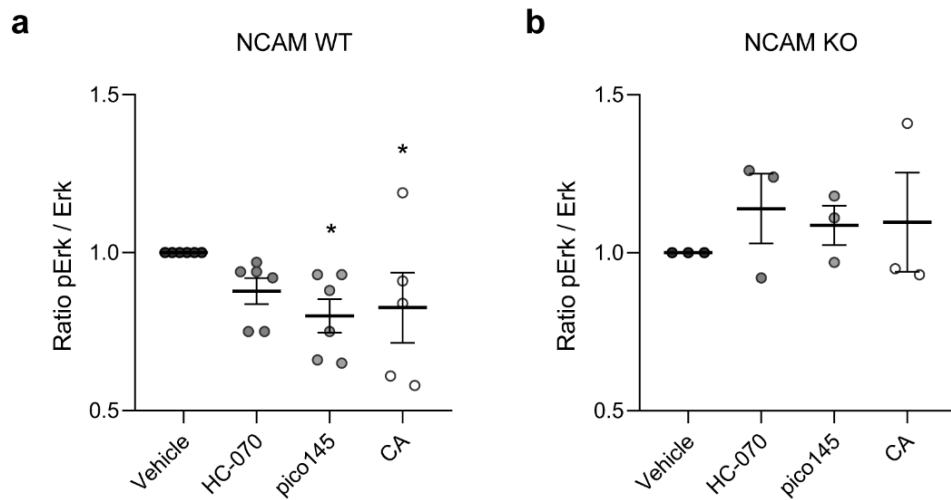


Figure 34. The NCAM-dependent Erk1/2 phosphorylation partially depends on TRPC1, -4, and -5. Cultured cortical neurons were vehicle-treated or pre-treated with HC-070, pico145, or colominic acid (CA), treated with NCAM antibody for 20 minutes and lysed. Quantification of the levels of pErk/Erk in lysates from NCAM +/+ (NCAM WT) (a) and NCAM -/- (NCAM KO) (b) cortical neurons. Mean values \pm SEM are shown for the phosphorylated Erk1/2 versus total Erk1/2 levels. The quantification is relative to the values obtained from NCAM antibody-treated neurons in the absence of inhibitors (vehicle, set to 1) from six (a) or three (b) independent cultures. One-way ANOVA with Kruskal-Wallis as post hoc test, * $p < 0.05$.

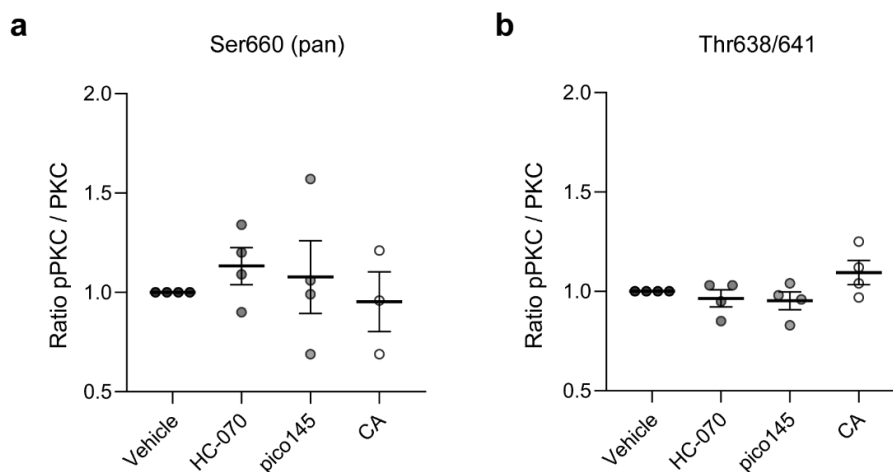


Figure 35. The NCAM-dependent PKC phosphorylation does not depend on TRPC1, -4, and -5. Cultured cortical neurons were vehicle-treated or pre-treated with HC-070, pico145, or colominic acid (CA), treated with NCAM antibody for 15 minutes and lysed. (a, b) Quantification of the levels of pPKC/PKC in lysates from cortical neurons. Mean values \pm SEM are shown for the phosphorylated PKC at the Ser660 (pan) (a) or the Thr638/641 (b) versus total PKC levels. The quantification is relative to the values obtained from NCAM antibody-treated neurons in the absence of inhibitors

(vehicle, set to 1) from four independent cultures. No differences were found in one-way ANOVA with Kruskal-Wallis as post hoc test.

3.11. The NCAM-dependent promotion of neurite outgrowth depends on TRPC1, -4, and -5

In the developing nervous system, NCAM was shown to be essential for the promotion of neurite outgrowth (Maness & Schachner, 2007; Rønn et al., 2000). To address if the inhibition of the TRPC channels affects the NCAM-mediated neurite outgrowth, embryonic cortical neurons were pre-treated with HC-070, pico145, M084, and GSK-417651A and stimulation of neurite outgrowth was accomplished by treatment with NCAM antibody or colominic acid. The TRPC inhibitors did not change the basal neurite outgrowth of neurons, whereas the total neurite length was decreased in cells pre-treated with HC-070, pico145, and M084 and stimulated with NCAM antibody compared to vehicle and NCAM antibody-treated cells. In contrast, the outgrowth of cells pre-treated with GSK-417651A and treated with NCAM antibody was similar to those only stimulated with NCAM antibody (Figure 36a). Moreover, NCAM KO cells did not increase the total neurite length after NCAM antibody treatment (Figure 36b). The treatment of cells with colominic acid also led to an increase in neurite length compared to the untreated cells, but the pre-treatment with TRPC inhibitors did not reduce the colominic acid-stimulated enhancement in neurite length (Figure 37). Additionally, the total neurite length was not increased in NCAM KO cells treated with colominic acid (Figure 36b). These results suggest that NCAM-, but not colominic acid-promoted neurite outgrowth depends on TRPC1, -4, and -5.

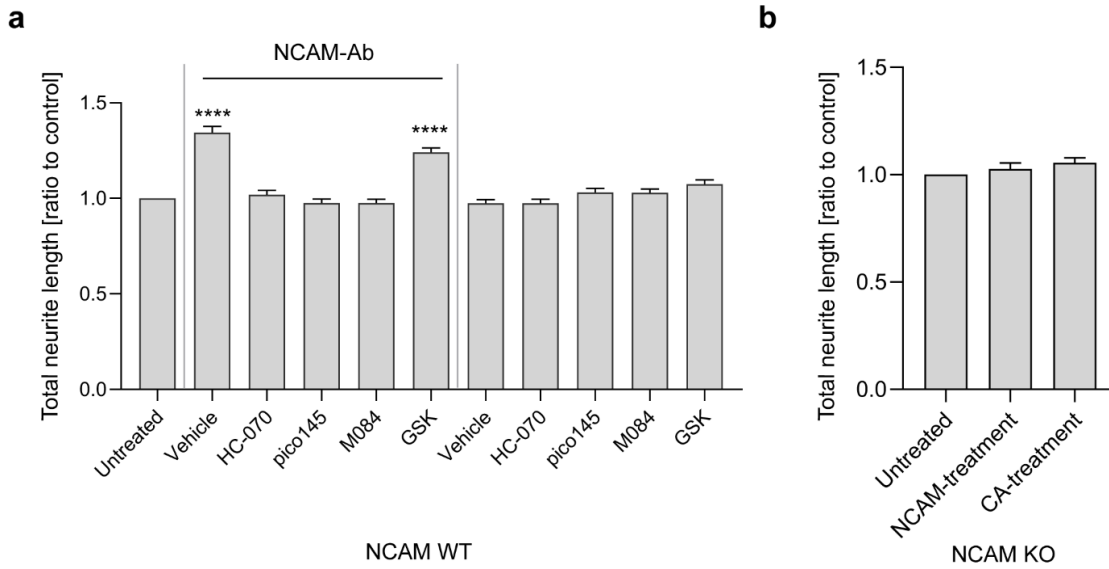


Figure 36. The NCAM-dependent neurite outgrowth requires TRPC1, -4, and -5. Cortical neurons from NCAM +/+ (WT) (**a**) and NCAM -/- (KO) (**b**) mice were treated with vehicle alone (Untreated) or together with NCAM antibody (NCAM-Ab) (**a, b**) or colominic acid (CA) (**b**) in the absence (**a, b**) or presence of HC-070, pico145, M084, and GSK-417651A (GSK) (**a**). Total neurite lengths per neuron relative to the untreated cells were measured to determine neurite outgrowth. Mean values \pm SEM from three independent experiments with duplicates are shown. **** $p < 0.0001$ for a one-way ANOVA with Kruskal-Wallis post hoc test.

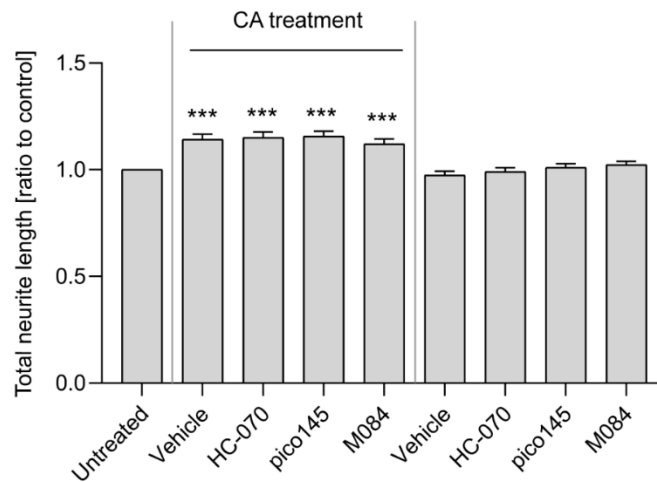


Figure 37. The colominic acid-dependent neurite outgrowth does not depend on TRPC1, -4, and -5. Cortical neurons from wild-type mice were treated with vehicle alone (Untreated) or together with colominic acid (CA) in the absence or presence of HC-070, pico145, and M084. Total neurite lengths per neuron relative to the untreated cells were measured to determine neurite outgrowth. Mean values \pm SEM from three independent experiments with duplicates are shown. *** $p < 0.001$ for a one-way ANOVA with Kruskal-Wallis post hoc test.

4. Discussion

In the present thesis, the interaction between NCAM and TRPC1, -4, and -5 was characterized, and the modulatory effects of this association were studied on the NCAM-dependent Ca^{2+} flux and NCAM-dependent neurite outgrowth. I showed by ELISA experiments that the N-terminal fragments of TRPC1, -4, and -5 directly bind to the ICDs of NCAM140 and NCAM180 and the bacterial homolog of PSA, colominic acid. Moreover, the immunoprecipitation and pull-down experiments showed that binding between NCAM and TRPC is independent of the presence of PSA on NCAM. The data from immunostainings and proximity ligation assays in cultured neurons confirmed the close proximity of NCAM-PSA with TRPC1, -4, and -5, and TIRF microscopy revealed that the association occurs at or close to the neuronal plasma membrane.

The analysis of the Ca^{2+} flux after triggering NCAM with an antibody in the absence or presence of TRPC inhibitors supported the notion that interactions between NCAM-PSA and TRPC1, -4, and -5 modulate the NCAM-dependent Ca^{2+} entry into neurons. Moreover, the NCAM-dependent Ca^{2+} flux was mainly dependent on extracellular calcium and required the presence of PSA on NCAM. Finally, an alteration of the Erk1/2 phosphorylation state and a reduction of the NCAM-dependent neurite outgrowth were observed after using TRPC1, -4, and -5 inhibitors.

4.1. NCAM and colominic acid directly bind to TRPC1, -4, and -5

Previous studies in our group suggested an interaction between NCAM and TRPC1, -4, and -5, but not TRPC3, -6, and -7 using immunoprecipitation and pull-down experiments (Theis, 2011). In my thesis, I confirmed the association between NCAM-PSA and TRPC channels through ELISA experiments and identified the specific region of the N-terminal domain of TRPC1 involved in the interaction. Data from Theis et al. (2013) show that PSA can bind to the effector domain of MARCKS at the plane of the plasma membrane, and this interaction takes place from opposite sides. On the one hand, the PSA-MARCKS association is possible because the effector domain of MARCKS is highly basic, in contrast to the rest of the protein, which is highly acidic (Scarlett, 2003; Swierczynski et al., 1996). Moreover, with its effector domain, MARCKS is suggested to dip into the membrane (Bähr et al., 1998). In contrast, PSA is a negatively charged glycan that can adopt highly ordered left-handed helical structures, and it is also suggested to dip into the plasma membrane from the outside of the

cell (Brisson et al., 1992; Janas et al., 2010). On the other hand, the formation of signaling complexes and a direct binding between TRPC1 and MARCKS have also been described (Shi et al., 2014).

In this thesis, the sequence analysis of the amino acids 261-278 from the N-terminal domain of murine TRPC1 predicted an amphipathic helical structure characterized by four positively charged amino acids embedded by hydrophobic amino acids. The insertion of the hydrophobic amino acids into the plasma membrane could facilitate the binding between the positively charged amino acids of TRPC and the negatively charged PSA, as seen in the interaction between PSA and the effector domain of MARCKS. Interestingly, the same region in the N-terminal domain of TRPC1 is also responsible for the binding with NCAM140.

In line with the idea of a possible PSA-TRPC interaction, the stimulation of cells with a TRPC1-penetrating peptide resulted in a TRPC1-dependent Ca^{2+} entry into neurons that was reduced after using a mutated TRPC1 peptide without the amphipathic structure. Taking into account that the binding of MARCKS to TRPC1 inhibits the channel (Jahan et al., 2020; Shi et al., 2014), it is conceivable that the TRPC1 peptide competes with TRPC1 for the binding to MARCKS, thus allowing the release of TRPC1 and the consequent Ca^{2+} influx due to the opening of the channel. In contrast, the treatment of cells with a mutated TRPC1 peptide does not result in binding to MARCKS, so the competition will not take place, and the Ca^{2+} flux will be reduced. Given the interaction between MARCKS and PSA (Theis et al., 2013), other possibilities are that the TRPC1 peptide interacts with NCAM, thus allowing the PSA covalently bound to NCAM to interact with the N-terminal domain of the TRPCs and trigger the opening of these channels or that PSA binds to MARCKS thus inducing the release of TRPC1 and the subsequent Ca^{2+} flux. Since MARCKS associates with TRPC1 and PSA (Shi et al., 2014; Theis et al., 2013), it may mediate or contribute to the interaction between TRPC1 and PSA.

Finally, it has to be considered that the cell-penetrating peptide used for the calcium imaging experiments contained a TAT sequence, which is known to be cationic (Green et al., 1989). Since PSA is a highly negatively charged glycan (Johnson et al., 2005), a possible unspecific interaction of the TAT-containing peptide and PSA cannot be excluded due to the attraction of opposite charges. Further experiments should be performed using non-cationic cell-penetrating peptides (CPPs), such as Pep1 or MPG (Xie et al., 2020), to clarify the exact role of NCAM-PSA – TRPC1 – MARCKS in the TRPC1-dependent Ca^{2+} entry.

4.2. NCAM and TRPC1, -4, and -5 interact at the neuronal plasma membrane in a PSA-independent manner

The association between TRPC channels and NCAM takes place in neurons from the cerebellum, hippocampus, and cortex. These regions express NCAM at high levels during the maturation of the brain (Goldowitz et al., 1990; Seki & Arai, 1991) and share a similar gene expression pattern for TRPC channels (Formoso et al., 2020). The fact that TRPC channels function through the plasma membrane, allowing the entrance of Ca^{2+} into the cell or through the endoplasmic reticulum, participating in the store-operated calcium entry (SOCE) (Wang et al., 2020), pointed out the need to determine the specific localization of the interaction between NCAM and TRPC. The data from TIRF microscopy showed that the association is taking place at or near the plasma membrane, while there is little participation of the endoplasmic reticulum. The interaction between TRPC1, -4, and -5 with NCAM at the plasma membrane is in line with the knowledge that TRPC1 is mainly found in this location forming heteromers together with TRPC4 and -5 (Alfonso et al., 2008; Hofmann et al., 2002).

Moreover, the TIRF experiments confirmed that removal of PSA from NCAM does not affect the NCAM-TRPC interaction or its localization. The notion that NCAM and TRPC interact in a PSA-independent manner was further supported by experiments in CHO cells where TRPC antibodies could precipitate NCAM in NCAM- and NCAM-PSA-expressing cells. Despite this, PSA was found in close proximity to TRPC1 and -4, which suggests that even though the presence of PSA is not strictly necessary for the NCAM-TRPC interaction, it participates in the regulation of it due to its distinct modulatory roles on NCAM binding properties (Johnson et al., 2005).

Finally, TIRF experiments showed that the NCAM-triggered Ca^{2+} flux in cells does not affect the plasma membrane localization of the NCAM-TRPC interaction, which reinforces the hypothesis of a calcium flux acting through the plasma membrane and not the endoplasmic reticulum. Furthermore, the calcium imaging experiments with a pre-treatment of cells with the non-competitive inhibitor of the sarco/endoplasmic reticulum Ca^{2+} -ATPase, thapsigargin, further supported the hypothesis that TRPC channels work as receptor-operated channels when associated with NCAM-PSA.

When cortical neurons were cultured in the presence of thapsigargin and extracellular Ca^{2+} , an immediate increase in the Ca^{2+} level was observed in the cytosol after triggering NCAM with an antibody. This Ca^{2+} increase was characterized by an intense peak followed by a slow

decline to basal levels. In contrast, neurons cultured in the absence of thapsigargin and extracellular Ca^{2+} showed a slight increase of Ca^{2+} after NCAM-triggering. This slight increase lacked the characteristic peak of the extracellular Ca^{2+} flux. An explanation for the two different calcium waves would be that when extracellular Ca^{2+} is available, the direct binding between NCAM-PSA and TRPC mediates the opening of the channels and the corresponding Ca^{2+} influx into the cells. On the contrary, the only availability of intracellular Ca^{2+} leads to the activation of indirect signaling pathways mediated through NCAM that do not necessarily include the TRPC channels. NCAM, through its binding partners such as the FGFR, could mediate the activation of the PLC and PKC pathway, which in turn induces the release of IP_3 and its binding to its endoplasmic reticulum receptors. The binding of IP_3 induces the release of Ca^{2+} from the intracellular stores (Clapham, 2007; Kiselyov, 2010; Lock & Parker, 2020), which could correspond to the smaller Ca^{2+} wave seen in the experiment.

4.3. NCAM-triggered Ca^{2+} flux mediated by TRPC1, -4, and -5 requires the presence of PSA on NCAM

With the calcium imaging experiments in CHO cells, I demonstrated that PSA on NCAM is required to induce the NCAM-dependent Ca^{2+} flux mediated by TRPC1, -4, and -5. The importance of the polysialylated form of NCAM was further supported by the experiments in cortical cells, where I saw a reduced Ca^{2+} flux in cells where PSA was degraded by Endo N treatment. The need for PSA as a regulator of NCAM signaling cascades is not a novel suggestion. It is known that PSA can modulate the adhesive properties of NCAM to heterophilic binding partners, thereby regulating NCAM-mediated Ca^{2+} signaling (Johnson et al., 2005). A clear example where PSA on NCAM modulates a signaling cascade is the regulation of the N-methyl-D-aspartate (NMDA) receptors. PSA-carrying NCAM, but not non-polysialylated NCAM, inhibited the GluN2B-containing NMDA receptors, thus blocking the excitotoxic cell death induced by glutamate (Hammond et al., 2006). Moreover, hippocampal neurons from NCAM-deficient mice show increased GluN2B levels and Ca^{2+} transients leading to impaired long-term potentiation that is reversed after the application of an antagonist of GluN2B. The findings of the involvement of NCAM-PSA in the GluN2B-Ras-GRF1-p38 mitogen-activated protein kinase (MAPK) pathway support the role of PSA as a regulator of signaling cascades (Kochlamazashvili et al., 2010).

My results obtained from experiments with CHO cells showed that the pre-treatment of these cells with a general inhibitor for the TRPC channels reduced the NCAM-dependent Ca^{2+} flux only when NCAM-PSA was expressed by the cells. These results are in accordance with previous studies by Kiryushko et al. (2006), showing that the inhibition of the NSCCs channels, but not the VDCCs channels, blocks the NCAM-dependent Ca^{2+} influx.

The calcium imaging experiments in cortical cells allow a deeper understanding of the regulatory role of TRPC channels in the NCAM-dependent Ca^{2+} flux. The TRPC3, -6, and -7 inhibitor GSK-417651A did not block the NCAM-dependent Ca^{2+} flux, confirming previous results in our group indicating that TRPC3, -6, and -7 do not interact with NCAM (Theis, 2011). Surprisingly, the xanthine derivatives pico145 and HC-070, which inhibit TRPC1, -4, and -5 heteromers and homomers similarly (Just et al., 2018; Rubaiy, Ludlow, Bon, & Beech, 2017; Rubaiy, Ludlow & Henrot, et al., 2017), exhibited different effects on the NCAM-dependent Ca^{2+} flux. While pico145 inhibited the Ca^{2+} flux in wild-type cortical neurons, HC-070 had no effect. An explanation for this difference could be that the binding region of the two inhibitors differs. Pico145 binds to a lipid-binding site between the transmembrane domains of two TRPC subunits and displaces the phospholipids (Wright et al., 2020), while HC-070 binding replaces the glycerol group of DAG, which stabilizes TRPC channels in a closed state (Song et al., 2021). Thus, it is tempting to speculate that the displacement of phospholipids by pico145 is necessary for the NCAM-PSA-dependent Ca^{2+} flux mediated by TRPC1, -4, and -5, but not the displacement of the glycerol group of DAG by HC-070.

In the same experiments, the TRPC4- and -5 channel inhibitor M084 did not block the Ca^{2+} response. One possibility for the lack of effect is that although M084 inhibits TRPC1, -4, and -5 heteromers and homomers, its inhibitory potency is lower than that of pico145 or HC-070 (Minard et al., 2018; Zhu et al., 2015). Another possibility could be that the M084 binding region in the TRPC channels differs from pico145 and HC-070. Structural analysis of the binding of M084 to TRPC is required, but Song et al. (2021) showed that clemizole, another member of the M084 class of inhibitors, binds to the voltage sensor-like domain of TRPC subunits.

Interestingly, the NCAM-dependent Ca^{2+} flux was also reduced after pre-treatment of cultured cortical cells with colominic acid. Two possible explanations for this effect are: 1. The binding of colominic acid to the N-terminal domain of TRPC blocks the binding between TRPC and NCAM. Thereby, the NCAM-TRPC interaction is impaired, and the addition of an NCAM antibody does not trigger the Ca^{2+} flux. These results are in line with my ELISA experiments that showed that the NCAM140-ICD and colominic acid compete for the same binding region in the N-terminal domain of TRPC1, -4, and -5. 2. The binding of colominic acid to the N-terminal domain of TRPC may block the PSA binding to TRPC1, -4, and -5 induced by NCAM triggering, thus blocking the NCAM-dependent Ca^{2+} flux. Further experiments are required to gain a deeper insight into the signaling complex of NCAM-PSA-TRPC in the NCAM-dependent Ca^{2+} flux.

Of note, not only neurons but also astrocytes express TRPC channels (Beskina et al., 2007; Malarkey et al., 2008; Miyano et al., 2010) and, predominantly, NCAM120 and NCAM140 isoforms (Jucker et al., 1995). Despite the expression of different NCAM isoforms in astrocytes compared to neurons, the calcium imaging experiments with cultured astrocytes and TRPC inhibitors showed similar results as those with cortical neurons. While pico145 inhibited the NCAM-dependent Ca^{2+} flux, HC-070 did not affect it. Also, these results can be explained here due to the different binding regions of both inhibitors (Song et al., 2021; Wright et al., 2020).

4.4. NCAM-dependent neurite outgrowth is affected by TRPC1, -4, and -5 inhibition

The NCAM antibody-induced Ca^{2+} flux results in an increase of intracellular Ca^{2+} levels that could trigger different signaling pathways, including activation of kinases and phosphorylation-dependent cascades (Aonurm-Helm et al., 2008; Kiryushko et al., 2006; Kolkova et al., 2000; Kolkova et al., 2005; Niethammer et al., 2002). Moreover, the Ca^{2+} flux is involved in NCAM-dependent neuritogenesis (Cassens et al., 2010; Kiselyov, 2010; Kleene & Cassens, et al., 2010; Sheng et al., 2015). Independently of NCAM activation, TRPC channels are also modulators of neurite outgrowth (Heiser et al., 2013; Kumar et al., 2012; Yao et al., 2009). In this thesis, I show a new role for TRPC channels as mediators in NCAM-dependent neurite elongation. The inhibitor pico145 blocked the NCAM-dependent Erk1/2 phosphorylation, and pre-treatment of cortical cells with TRPC1, -4, and -5 inhibitors reduced the NCAM-dependent neurite outgrowth.

Despite the activation of Erk1/2, no differences were found in the PKC phosphorylation state after pre-treatment of cells with the TRPC inhibitors and after NCAM-antibody triggering. The gating of TRPC channels is highly regulated by PKC activation, but its function is still controversial. While the DAG-induced PKC activation inhibits the receptor-operated Ca^{2+} entry by TRPC1, -4, and -5 channels (Ningoo et al., 2021; Soboloff et al., 2007; Venkatachalam et al., 2003), it leads to phosphorylation of the TRPCs that participate in the store-operated Ca^{2+} entry resulting in an enhanced Ca^{2+} flux (Baudel et al., 2020; Bodiga et al., 2015). Considering that the TRPC channels act as receptor-operated channels when interacting with NCAM, it is tempting to speculate that the NCAM-dependent PKC phosphorylation occurs independently of the TRPC channels. Moreover, other NCAM binding partners, such as the FGFR, are already known activators of the NCAM-dependent PKC signaling pathway (Fujita-Hamabe et al., 2011; Westphal et al., 2017).

Taking into account all the experiments mentioned, the NCAM-dependent Ca^{2+} flux mediated by TRPC1, -4, and -5 could regulate NCAM-dependent neurite elongation and synaptogenesis during the development of the CNS and NCAM-dependent synaptic plasticity associated with learning, memory, and behavior in the mature nervous system.

4.5. NCAM-PSA and TRPC1, -4, and -5 modulate fear memory formation and consolidation

Focusing on behavior, NCAM, PSA, and TRPC1, -4, and -5 are regulators of the consolidation and formation of fear memories and innate fear, especially involving anxiety-like behaviors. NCAM-deficient mice display anxiety-like behaviors (Brandewiede et al., 2013; Stork et al., 1999), which are abolished in NCAM-deficient mice with transgenic expression of NCAM180 (Stork et al., 2000). Furthermore, NCAM-deficient mice exhibit deficits in the consolidation of fear memories due to impairments in the amygdala-mediated regulation of the hippocampus-dependent contextual fear memory formation (Albrecht et al., 2010). Moreover, chronic unpredictable stress increases the NCAM levels in the amygdala and enhances fear conditioning and anxiety-like behavior (Bisaz & Sandi, 2010). Similar to these findings, mice overexpressing a soluble extracellular NCAM fragment show impairments in contextual and cued fear conditioning (Pillai-Nair et al., 2005). Mice conditionally deficient in NCAM in post-migratory forebrain neurons show reduced NCAM levels in the amygdala and impaired innate and learned avoidance behaviors (Bisaz & Sandi, 2010; Brandewiede et al., 2014). Finally, acute stress induction in rats reduces the NCAM

expression in the hippocampus and the prefrontal cortex and impairs spatial memory formation (Sandi et al., 2005).

Several studies also pointed out the importance of NCAM-PSA in consolidating contextual memories. NCAM-PSA expression is increased in the dorsal hippocampus after contextual fear conditioning, and the treatment with Endo N reduces the behavioral responses to the conditioned stimulus (Lopez-Fernandez et al., 2007). Moreover, the application of colominic acid and recombinant NCAM-PSA in the CA1 hippocampal region before a fear-conditioned stimulus impairs the formation of hippocampal-dependent contextual memories (Senkov et al., 2006). Mice with a deficiency in ST8Sia-II show higher exploratory behaviors, a reduced response to Pavlovian fear conditioning, which is a parameter used to study the formation of fear memories (Angata et al., 2004), and reduced anxiety-like behaviors (Calandreau et al., 2010). Despite this, mice either overexpressing or with a deficit in ST8Sia-IV do not show impairments in anxiety-like behaviors but display reduced exploratory behaviors (Calandreau et al., 2010; Fewou et al., 2019).

Recent studies also pointed to the participation of the TRPC channels in fear-related responses (Neuner et al., 2015; Riccio et al., 2009; Riccio et al., 2014). TRPC4- and -5-deficient mice exhibit reduced innate fear and increased exploratory behavior (Riccio et al., 2009; Riccio et al., 2014), and the local ablation of TRPC4 in the amygdala reproduced the observed anxiety-like behaviors (Riccio et al., 2014). Moreover, TRPC1, -4, and -5 knockout mice show deficits in spatial working memory (Bröker-Lai et al., 2017; Lepannetier et al., 2018). Finally, the application of TRPC1, -4, and -5 inhibitors in mice exerts anxiolytic-like and antidepressant effects (Yang et al., 2015) and attenuates the anxiogenic effects of a panic-inducing peptide as well as the fear memory induced by chronic social stress (Just et al., 2018).

The participation in fear memory formation and anxiety-like behaviors of NCAM-PSA and TRPC in mice and rats suggests that their emotional behavior is modulated by the NCAM-PSA-TRPC interaction described in this thesis. The question now arises whether these molecules work together with other proteins to regulate emotional behavior. Here I propose candidates that could participate in this process: the dopamine D2 receptor and BDNF and its receptor TrkB (TrkB-BDNF).

First, the NCAM-PSA-TRPC complex could modulate the interaction between NCAM or TRPC with the dopamine D2 receptor (Hannan et al., 2008; Xiao et al., 2009) and influence the dopamine-dependent emotional behavior, which includes fear conditioning (Oliveira et al., 2006; Vita et al., 2021). On the one hand, the modulation of dopaminergic neurons by TRPC1 has been reported. While TRPC1-deficient mice exhibit a reduced number of dopaminergic neurons, the overexpression of TRPC1 increases the survival of these neurons after the administration of a neurotoxin (Selvaraj et al., 2012). On the other hand, the administration of a dopamine inhibitor reduces the NCAM-PSA expression in the prefrontal cortex (Castillo-Gómez et al., 2008). Second, the direct NCAM and TrkB interaction mediates NCAM-dependent neurite outgrowth (Cassens et al., 2010) and NCAM-deficient mice show a dramatic reduction of BDNF in the prefrontal cortex and the hippocampus together with a reduction of TrkB phosphorylation (Aonurm-Helm et al., 2015). Regarding TRPC, recent studies show that the administration of a TRPC4 and -5 inhibitor in mice increases the protein and mRNA levels of BDNF in the prefrontal cortex and hippocampus, inducing anxiolytic-like effects (Yang et al., 2015). Finally, deficits in the recruitment of TrkB to the plasma membrane lead to impaired hippocampal memory acquisition and consolidation (Li et al., 2021). Moreover, mice with a mutation in the BDNF gene exhibit increased anxiety-related behaviors and impaired extinction of conditioned fear (Chen et al., 2006; Heldt et al., 2007).

The interplay among NCAM-PSA, TRPC1, -4, and -5, and dopamine D2 receptors or the BDNF-TrkB system should be further investigated with different behavioral tests in healthy and diseased animals to determine the participation of NCAM-TRPC-dopamine D2 receptor/TrkB-BDNF interactions in psychiatric disorders, such as schizophrenia and bipolar and anxiety disorders.

4.6. Conclusions

In this thesis, I show that NCAM-PSA is in close proximity with TRPC1, -4, and -5 in cultured cerebellar, hippocampal, and cortical neurons. The N-terminal domain of TRPC1, -4, and -5 can interact with the ICD of NCAM and colominic acid. Based on my thesis's results, it is not possible to determine the exact NCAM-PSA-TRPC association complex, so I propose two different interaction models. In both models, the NCAM antibody binding to NCAM will mimic an NCAM interaction partner inducing a conformational change in NCAM that will affect the NCAM-PSA-TRPC complex.

First model: Under basal conditions, NCAM140 or NCAM180 ICDs will bind to the N-terminal domain of TRPCs, thus blocking its binding to PSA. The addition of an NCAM antibody will induce a conformational change in NCAM, leading to the dissociation of the NCAM-ICD from the N-terminal domain of TRPCs. Afterwards, the TRPCs will transiently bind to the PSA moiety of NCAM-PSA and trigger the NCAM-dependent Ca^{2+} flux (Figure 38).

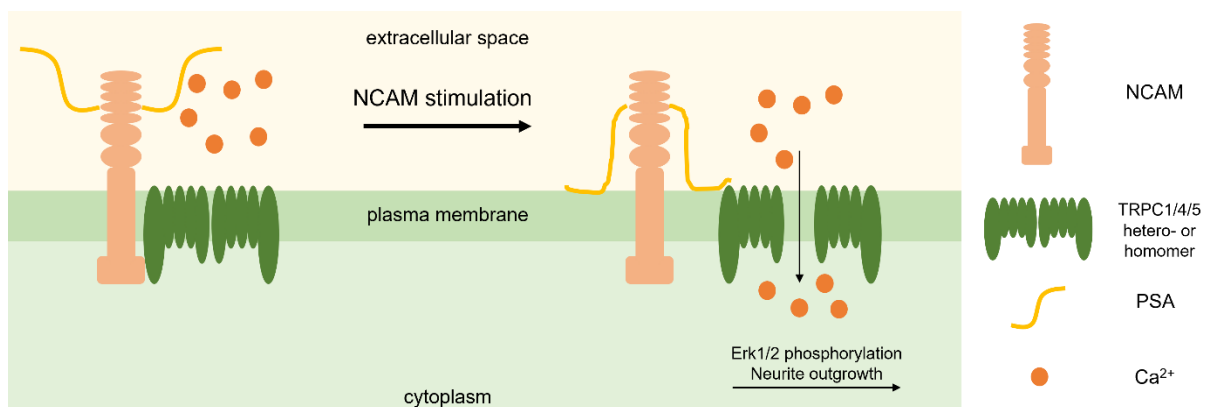


Figure 38. Schematic representation of the NCAM-dependent Ca^{2+} flux triggered by the binding of PSA to TRPC. Under basal conditions, NCAM is associated with TRPC in the plasma membrane. After NCAM stimulation, NCAM dissociates from TRPC, which then binds to PSA. The binding of PSA to TRPC triggers a Ca^{2+} flux that leads to the NCAM-dependent Erk1/2 phosphorylation and neurite outgrowth. Scheme adapted from (Amores-Bonet et al., 2022).

Second model: Under basal conditions, NCAM140 or NCAM180 ICDs are associated with the N-terminal domain of TRPCs, which are in a closed state. The addition of an NCAM antibody will induce a conformational change in NCAM that will allow the opening of the TRPC channels, thereby inducing an NCAM-dependent Ca^{2+} flux. The presence of PSA on NCAM will be necessary to modulate the NCAM-TRPC interaction and the TRPC channel gating (Figure 39).

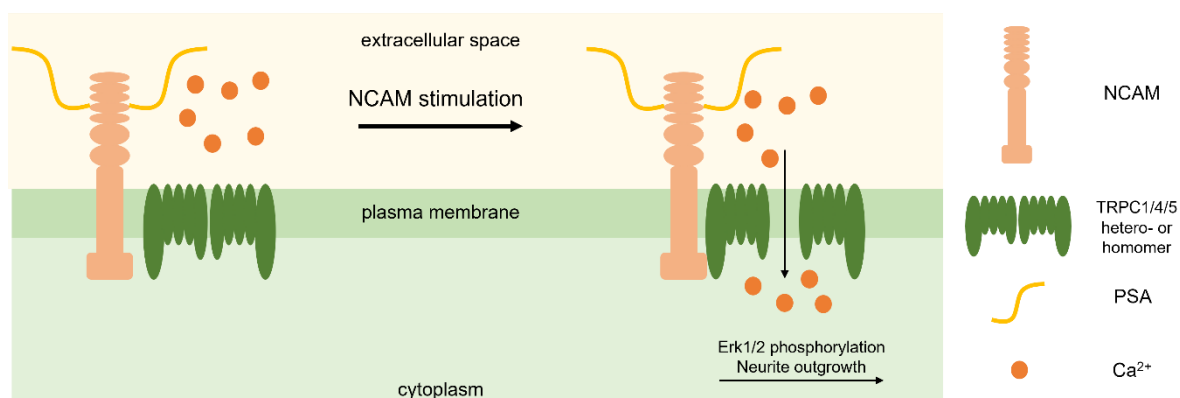


Figure 39. Schematic representation of the NCAM-dependent Ca^{2+} flux triggered by the binding of NCAM to TRPC. NCAM is associated with TRPC at the plasma membrane. After NCAM stimulation, a conformational change on polysialylated NCAM leads to the TRPC channels opening and induction of Ca^{2+} flux. This Ca^{2+} flux triggers the NCAM-dependent Erk1/2 phosphorylation and neurite outgrowth.

Further experiments are required to determine which of the interaction models is correct. An option to solve this question would be to perform an immunoprecipitation experiment with cultured cortical cells lysed immediately after the addition of an NCAM antibody. This experiment could determine if the TRPC channels bind to NCAM or PSA when they are in an open state.

Finally, NCAM-triggering will induce a Ca^{2+} flux into cells, leading to the phosphorylation of Erk1/2 and NCAM-dependent neurite outgrowth. The NCAM-PSA-TRPC binding complex could also include other binding partners, such as the dopamine D2 receptor or TrkB-BDNF, and modulate the NCAM-PSA-TRPC participation in neuropsychiatric diseases like bipolar and anxiety disorders or schizophrenia.

5. Summary

5.1. Summary

In this thesis, I show that the intracellular domain (ICD) of the neural cell adhesion molecule (NCAM) and the bacterial homolog of polysialic acid (PSA), colominic acid (CA), interact with the N-terminal domain of the transient receptor potential canonical (TRPC) channels 1, -4, and -5.

The NCAM-PSA-TRPC interaction is shown by immunoprecipitation, pull-down, and ELISA experiments, confirming that NCAM140, NCAM180, and CA interact with TRPC1, -4, and -5. Moreover, the interaction between NCAM-PSA and TRPC1, -4, and -5 is further verified by co-localization experiments and proximity ligation assay (PLA) using cultured cerebellar, hippocampal, and cortical neurons. By total internal reflection fluorescence microscopy, I show that those interactions occur at the plane or near the plasma membrane but not in the endoplasmic reticulum. Furthermore, the interaction of NCAM with TRPC1, -4, and -5 occurs independently of PSA on NCAM because the treatment of cells with Endo N, which degrades PSA, does not affect the localization of the interaction.

In NCAM-expressing CHO 2A10 cells or NCAM-PSA-expressing CHO C6 cells, the treatment with an NCAM-triggering antibody (NCAM-Ab) only increases the Ca^{2+} flux in CHO C6 cells overexpressing TRPC1/4 or TRPC1/5. Moreover, the application of a general TRPC inhibitor, SKF-96365, reduces the NCAM-dependent Ca^{2+} flux after overexpression of TRPC1/4 or TRPC1/5, suggesting that the Ca^{2+} flux induced by NCAM-Ab treatment in NCAM-PSA-expressing CHO cells is modulated by TRPC1, -4, and -5.

The calcium imaging experiments in cortical cells show that the NCAM-dependent Ca^{2+} flux is only triggered in cells expressing NCAM-PSA. NCAM-deficient cells and wild-type cells treated with Endo N show a reduction in the Ca^{2+} flux. Furthermore, pre-treatment of wild-type cells with the TRPC1, -4, and -5 inhibitor, pico145, and CA reduce the NCAM-dependent Ca^{2+} flux. The pre-treatment of cells with thapsigargin, an inhibitor of the retrotranslocation of calcium to the intracellular stores, in the absence or presence of Ca^{2+} in the medium, reveals that the NCAM-dependent signaling is mainly triggered by extracellular calcium.

Finally, the NCAM-dependent Erk1/2 phosphorylation and the NCAM-dependent neurite outgrowth are also reduced in cells pre-treated with TRPC1, -4, and -5 inhibitors. Altogether, these results suggest a role of TRPC1, -4, and -5 in the regulation of NCAM-dependent neurite outgrowth.

5.2. Zusammenfassung

In dieser Arbeit zeige ich, dass die intrazelluläre Domäne (ICD) des neuronalen Zelladhäsionsmoleküls (NCAM) und das bakterielle Homolog der Polysialinsäure (PSA), die Colominsäure (CA), mit den N-terminalen Domänen der *transient receptor potential canonical* (TRPC) Kanäle-1, -4 und -5 interagieren.

Die NCAM-TRPC-Interaktion wird durch Immunpräzipitations-, Pull-Down- und ELISA-Experimente nachgewiesen. Diese Experimente bestätigen, dass NCAM140, NCAM180 und CA mit TRPC1, -4 und -5 interagieren. Darüber hinaus wird die Interaktion zwischen NCAM-PSA und TRPC1, -4 und -5 durch Ko-Lokalisierungsexperimente und Proximity Ligation Assay (PLA) mit kultivierten Kleinhirn-, Hippocampus-Neuronen und kortikalen Neuronen bestätigt. Mit Hilfe der Fluoreszenzmikroskopie mit totaler interner Reflexion zeige ich, dass diese Interaktionen in der Ebene oder in der Nähe der Plasmamembran, nicht aber im endoplasmatischen Retikulum stattfinden. Darüber hinaus erfolgt die Interaktion von NCAM und TRPC1, -4 und -5 unabhängig davon ob NCAM PSA trägt, da die Behandlung der Zellen mit Endo N, welches PSA abbaut, keinen Einfluss auf die Lokalisation der Interaktion hat.

In NCAM-exprimierenden CHO 2A10-Zellen oder NCAM-PSA-exprimierenden CHO C6-Zellen erhöht die Behandlung mit einem NCAM-stimulierenden Antikörper (NCAM-Ab) den Ca^{2+} -Fluss nur in CHO C6-Zellen, die TRPC1/4 oder TRPC1/5 überexprimieren. Darüber hinaus reduziert die Anwendung eines allgemeinen TRPC-Inhibitors, SKF-96365, den NCAM-abhängigen Ca^{2+} -Fluss nach Überexpression von TRPC1/4 oder TRPC1/5, was darauf hindeutet, dass der durch NCAM-Ab in NCAM-PSA-exprimierenden CHO-Zellen induzierte Ca^{2+} -Fluss durch TRPC1, -4 und -5 moduliert wird.

Die *Calcium Imaging*-Experimente in kortikalen Zellen zeigen, dass der NCAM-abhängige Ca^{2+} -Fluss nur in Zellen ausgelöst wird, die NCAM-PSA exprimieren. NCAM-defiziente Zellen und Wildtyp-Zellen, die mit Endo N behandelt wurden zeigen eine Verringerung des Ca^{2+} -Flusses. Darüber hinaus reduziert die Vorbehandlung von Wildtyp-Zellen mit dem

TRPC1-, -4- und -5 Inhibitor pico145 und CA den NCAM-abhängigen Ca^{2+} -Fluss. Die Vorbehandlung der Zellen mit Thapsigargin, einem Inhibitor der Retrotranslokation von Kalzium in die intrazellulären Speicher, in Abwesenheit oder Anwesenheit von Ca^{2+} im Medium, zeigt, dass die NCAM-abhängige Signalübertragung hauptsächlich durch extrazelluläres Kalzium ausgelöst wird.

Weiterhin sind auch die NCAM-abhängige Erk1/2-Phosphorylierung und das NCAM-abhängige Neuritenwachstum in Zellen, die mit TRPC1-, -4- und -5-Inhibitoren vorbehandelt wurden, reduziert. Insgesamt deuten die Ergebnisse auf eine Rolle von TRPC1, -4 und -5 bei der Regulierung des NCAM-vermittelten Neuritenwachstums hin.

6. Abbreviations

Ab: Antibody

APS: Ammonium persulfate

ARD: Ankyrin-like repeats domain

BCA: Bicinchoninic acid assay

BDNF: Brain-derived neurotrophic factor

BFP: Blue fluorescent protein

BSA: Bovine serum albumin

CAM: Cell adhesion molecule

CaMKII β : calcium/calmodulin-dependent kinase II β

CHL1: Cell adhesion molecule L1 like

CHO: Chinese hamster ovary cell

CI: Confidence interval

CNS: Central nervous system

Co-IP: Co-immunoprecipitation

CPP: Cell-penetrating peptide

CREB: cAMP response element-binding protein

DAG: Diacylglycerol

DAPI: 4',6-diamidino-2-phenylindole

DMEM: Dulbecco's modified eagle medium

ECM: Extracellular matrix

EDTA: Ethylenediaminetetraacetic acid

ELISA: Enzyme-linked immunosorbent assay

Endo N: Endoneuramidase N

ER: Endoplasmic reticulum

Erk1/2: Extracellular signal-regulated kinase 1/2

FBS: Fetal bovine serum

FGF: Fibroblast growth factor

FGFR: Fibroblast growth factor receptor

FHS: Fetal horse serum

FNIII: Fibronectin type III

GDNF: Glial cell-derived neurotrophic factor

GFP: Green fluorescent protein

GPCRs: G protein-coupled receptors

GPI: Glycosylphosphatidylinositol

GST: Glutathione s-transferase

HBSS: Hank's balanced salt solution

HNK-1: Human natural killer cell glycan 1

HRP: Horseradish peroxidase

ICD: Intracellular domain

Ig: Immunoglobulin

IP: Immunoprecipitation

IP₃: Inositol trisphosphate

IP₃R: Inositol trisphosphate receptor

IPTG: Isopropyl β-d-1-thiogalactopyranoside

LB: Lysogeny broth

LTP: Long-term potentiation

L1: Cell adhesion molecule L1

MAPK: Mitogen-activated protein kinase

MARCKS: Myristoylated alanine-rich C-kinase substrate

NCAM: Neural cell adhesion molecule

NCAM-Ab: Function-triggering NCAM antibody

NCAM-PSA: NCAM carrying PSA

NHERF: Na⁺/H⁺ exchanger regulatory factor

NMDA: N-methyl-D-aspartate

NSC: Neural stem cell

NSCC: Non-selective cation channels

NT: N-terminal

OD: Optical density

OPD: O-phenylenediamine dihydrochloride

PBS: Phosphate buffer saline

PCR: Polymerase chain reaction

PDGF: Platelet-derived growth factor-BB

PIP₂: phosphatidylinositol (4,5) bisphosphate

PKC: Protein kinase C

PLA: Proximity ligation assay

PLC: Phospholipase C

PLL: Poly-l-lysine

PSA: Polysialic acid

PST: ST8SiaIV

Pyk2: Proline-rich tyrosine kinase 2

RT: Room temperature

SDS-PAGE: Sodium dodecyl sulfate-polyacrylamide gel electrophoresis

SERCA: Sarco/endoplasmic reticulum Ca²⁺-ATPases

SOC: Super optimal catabolite

SOCE: Store-operated calcium entry

STM2: Stathmin 2

STX: ST8SiaII

SynCAM: Synaptic cell adhesion molecule

TAE: Tris-acetate-EDTA

TAT: Transactivator of transcription

TBS: Tris-buffered saline

TEMED: Tetramethylethylenediamin

TIRF: Total internal reflection fluorescence

TrkB: Tropomyosin receptor kinase B

TRP: Transient receptor potential

TRPC: Transient receptor potential canonical channel

TRPC1 peptide: TRPC1 261-278 peptide

TRPP: Transient receptor potential polycystic

TRPV: Transient receptor potential vanilloid

VDDCs: Voltage-dependent calcium channels

7. Bibliography

- Abramowitz, J., & Birnbaumer, L (2009). Physiology and pathophysiology of canonical transient receptor potential channels. *FASEB Journal : Official Publication of the Federation of American Societies for Experimental Biology*, 23(2), 297–328. <https://doi.org/10.1096/fj.08-119495>
- Albach, C., Damoc, E., Denzinger, T., Schachner, M., Przybylski, M., & Schmitz, B. (2004). Identification of N-glycosylation sites of the murine neural cell adhesion molecule NCAM by MALDI-TOF and MALDI-FTICR mass spectrometry. *Analytical and Bioanalytical Chemistry*, 378(4), 1129–1135. <https://doi.org/10.1007/s00216-003-2383-2>
- Albrecht, A., Bergado-Acosta, J. R., Pape, H.-C., & Stork, O. (2010). Role of the neural cell adhesion molecule (NCAM) in amygdalo-hippocampal interactions and salience determination of contextual fear memory. *The International Journal of Neuropsychopharmacology*, 13(5), 661–674. <https://doi.org/10.1017/S1461145709991106>
- Alfonso, S., Benito, O., Alicia, S., Angélica, Z., Patricia, G., Diana, K., Vaca, L., & Luis, V. (2008). Regulation of the cellular localization and function of human transient receptor potential channel 1 by other members of the TRPC family. *Cell Calcium*, 43(4), 375–387. <https://doi.org/10.1016/j.ceca.2007.07.004>
- Amores-Bonet, L., Kleene, R., Theis, T., & Schachner, M. (2022). Interactions between the Polysialylated Neural Cell Adhesion Molecule and the Transient Receptor Potential Canonical Channels 1, 4, and 5 Induce Entry of Ca²⁺ into Neurons. *International Journal of Molecular Sciences*, 23(17). <https://doi.org/10.3390/ijms231710027>
- Angata, K., Long, J. M., Bukalo, O., Lee, W., Dityatev, A., Wynshaw-Boris, A., Schachner, M., Fukuda, M., & Marth, J. D. (2004). Sialyltransferase ST8Sia-II assembles a subset of polysialic acid that directs hippocampal axonal targeting and promotes fear behavior. *Journal of Biological Chemistry*, 279(31), 32603–32613. <https://doi.org/10.1074/jbc.M403429200>
- Aonurm-Helm, A., Anier, K., Zharkovsky, T., Castrén, E., Rantamäki, T., Stepanov, V., Järvi, J., & Zharkovsky, A. (2015). Ncam-deficient mice show prominent abnormalities in serotonergic and BDNF systems in brain - Restoration by chronic

- amitriptyline. *European Neuropsychopharmacology : The Journal of the European College of Neuropsychopharmacology*, 25(12), 2394–2403. <https://doi.org/10.1016/j.euroneuro.2015.10.001>
- Aonurm-Helm, A., Berezin, V., Bock, E., & Zharkovsky, A. (2010). Ncam-mimetic, FGL peptide, restores disrupted fibroblast growth factor receptor (FGFR) phosphorylation and FGFR mediated signaling in neural cell adhesion molecule (NCAM)-deficient mice. *Brain Research*, 1309, 1–8. <https://doi.org/10.1016/j.brainres.2009.11.003>
- Aonurm-Helm, A., Zharkovsky, T., Jürgenson, M., Kalda, A., & Zharkovsky, A. (2008). Dysregulated CREB signaling pathway in the brain of neural cell adhesion molecule (NCAM)-deficient mice. *Brain Research*, 1243, 104–112. <https://doi.org/10.1016/j.brainres.2008.08.091>
- Aplin, A. E., Howe, A., Alahari, S. K., & Juliano, R. L. (1998). Signal transduction and signal modulation by cell adhesion receptors: The role of integrins, cadherins, immunoglobulin-cell adhesion molecules, and selectins. *Pharmacological Reviews*, 50(2), 197–263.
- Arai, M., Itokawa, M., Yamada, K., Toyota, T., Arai, M., Haga, S., Ujike, H., Sora, I., Ikeda, K., & Yoshikawa, T. (2004). Association of neural cell adhesion molecule 1 gene polymorphisms with bipolar affective disorder in Japanese individuals. *Biological Psychiatry*, 55(8), 804–810. <https://doi.org/10.1016/j.biopsych.2004.01.009>
- Arai, M., Yamada, K., Toyota, T., Obata, N., Haga, S., Yoshida, Y., Nakamura, K., Minabe, Y., Ujike, H., Sora, I., Ikeda, K., Mori, N., Yoshikawa, T., & Itokawa, M. (2006). Association between polymorphisms in the promoter region of the sialyltransferase 8B (SIAT8B) gene and schizophrenia. *Biological Psychiatry*, 59(7), 652–659. <https://doi.org/10.1016/j.biopsych.2005.08.016>
- Atz, M. E., Rollins, B., & Vawter, M. P. (2007). Ncam1 association study of bipolar disorder and schizophrenia: Polymorphisms and alternatively spliced isoforms lead to similarities and differences. *Psychiatric Genetics*, 17(2), 55–67. <https://doi.org/10.1097/YPG.0b013e328012d850>
- Bähr, G., Diederich, A., Vergères, G., & Winterhalter, M. (1998). Interaction of the effector domain of MARCKS and MARCKS-related protein with lipid membranes revealed by electric potential measurements. *Biochemistry*, 37(46), 16252–16261. <https://doi.org/10.1021/bi981765a>

- Baudel, M. A. S. M.-A., Shi, J., Large, W. A., & Albert, A. P. (2020). Insights into Activation Mechanisms of Store-Operated TRPC1 Channels in Vascular Smooth Muscle. *Cells*, 9(1). <https://doi.org/10.3390/cells9010179>
- Becker, C. G., Artola, A., Gerardy-Schahn, R., Becker, T., Welzl, H., & Schachner, M. (1996). The polysialic acid modification of the neural cell adhesion molecule is involved in spatial learning and hippocampal long-term potentiation. *Journal of Neuroscience Research*, 45(2), 143–152. [https://doi.org/10.1002/\(SICI\)1097-4547\(19960715\)45:2<143::AID-JNR6>3.0.CO;2-A](https://doi.org/10.1002/(SICI)1097-4547(19960715)45:2<143::AID-JNR6>3.0.CO;2-A)
- Beggs, H. E., Baragona, S. C., Hemperly, J. J., & Maness, P. F. (1997). Ncam140 interacts with the focal adhesion kinase p125(fak) and the SRC-related tyrosine kinase p59(fyn). *Journal of Biological Chemistry*, 272(13), 8310–8319. <https://doi.org/10.1074/jbc.272.13.8310>
- Beggs, H. E., Soriano, P., & Maness, P. F. (1994). Ncam-dependent neurite outgrowth is inhibited in neurons from Fyn-minus mice. *The Journal of Cell Biology*, 127(3), 825–833. <https://doi.org/10.1083/jcb.127.3.825>
- Benson, D. L., Colman, D. R., & Huntley, G. W. (2001). Molecules, maps and synapse specificity. *Nature Reviews. Neuroscience*, 2(12), 899–909. <https://doi.org/10.1038/35104078>
- Beskina, O., Miller, A., Mazzocco-Spezia, A., Pulina, M. V., & Golovina, V. A. (2007). Mechanisms of interleukin-1 β -induced Ca²⁺ signals in mouse cortical astrocytes: Roles of store- and receptor-operated Ca²⁺ entry. *American Journal of Physiology. Cell Physiology*, 293(3), C1103-11. <https://doi.org/10.1152/ajpcell.00249.2007>
- Bisaz, R., & Sandi, C. (2010). The role of NCAM in auditory fear conditioning and its modulation by stress: A focus on the amygdala. *Genes, Brain, and Behavior*, 9(4), 353–364. <https://doi.org/10.1111/j.1601-183X.2010.00563.x>
- Bisaz, R., Boadas-Vaello, P., Genoux, D., & Sandi, C. (2013). Age-related cognitive impairments in mice with a conditional ablation of the neural cell adhesion molecule. *Learning & Memory (Cold Spring Harbor, N.Y.)*, 20(4), 183–193. <https://doi.org/10.1101/lm.030064.112>
- Bodiga, V. L., Kudle, M. R., & Bodiga, S. (2015). Silencing of PKC- α , TRPC1 or NF- κ B expression attenuates cisplatin-induced ICAM-1 expression and endothelial dysfunction. *Biochemical Pharmacology*, 98(1), 78–91. <https://doi.org/10.1016/j.bcp.2015.08.101>

- Bollimuntha, S., Singh, B. B., Shavali, S., Sharma, S. K., & Ebadi, M. (2005). Trpc1-mediated inhibition of 1-methyl-4-phenylpyridinium ion neurotoxicity in human SH-SY5Y neuroblastoma cells. *Journal of Biological Chemistry*, *280*(3), 2132–2140. <https://doi.org/10.1074/jbc.M407384200>
- Bonfanti, L., & Theodosis, D. T. (2009). Polysialic acid and activity-dependent synapse remodeling. *Cell Adhesion & Migration*, *3*(1), 43–50. <https://doi.org/10.4161/cam.3.1.7258>
- Brandewiede, J., Stork, O., & Schachner, M. (2014). Ncam deficiency in the mouse forebrain impairs innate and learned avoidance behaviours. *Genes, Brain, and Behavior*, *13*(5), 468–477. <https://doi.org/10.1111/gbb.12138>
- Brandewiede, J., Jakovcevski, M., Stork, O., & Schachner, M. (2013). Role of stress system disturbance and enhanced novelty response in spatial learning of NCAM-deficient mice. *Stress (Amsterdam, Netherlands)*, *16*(6), 638–646. <https://doi.org/10.3109/10253890.2013.840773>
- Brenneman, L. H., Kochlamazashvili, G., Stoenica, L., Nonneman, R. J., Moy, S. S., Schachner, M., Dityatev, A., & Maness, P. F. (2011). Transgenic mice overexpressing the extracellular domain of NCAM are impaired in working memory and cortical plasticity. *Neurobiology of Disease*, *43*(2), 372–378. <https://doi.org/10.1016/j.nbd.2011.04.008>
- Brisson, J. R., Baumann, H., Imberty, A., Pérez, S., & Jennings, H. J. (1992). Helical epitope of the group B meningococcal alpha(2-8)-linked sialic acid polysaccharide. *Biochemistry*, *31*(21), 4996–5004. <https://doi.org/10.1021/bi00136a012>
- Bröker-Lai, J., Kollwe, A., Schindeldecker, B., Pohle, J., Nguyen Chi, V., Mathar, I., Guzman, R., Schwarz, Y., Lai, A., Weißgerber, P., Schwegler, H., Dietrich, A., Both, M., Sprengel, R., Draguhn, A., Köhr, G., Fakler, B., Flockerzi, V., Bruns, D., & Freichel, M. (2017). Heteromeric channels formed by TRPC1, TRPC4 and TRPC5 define hippocampal synaptic transmission and working memory. *The EMBO Journal*, *36*(18), 2770–2789. <https://doi.org/10.15252/embj.201696369>
- Bukalo, O., Fentrop, N., Lee, A. Y. W., Salmen, B., Law, J. W. S., Wotjak, C. T., Schweizer, M., Dityatev, A., & Schachner, M. (2004). Conditional ablation of the neural cell adhesion molecule reduces precision of spatial learning, long-term potentiation, and depression in the CA1 subfield of mouse hippocampus. *Journal*

- of Neuroscience*, 24(7), 1565–1577. <https://doi.org/10.1523/JNEUROSCI.3298-03.2004>
- Calandreau, L., Márquez, C., Bisaz, R., Fantin, M., & Sandi, C. (2010). Differential impact of polysialyltransferase ST8SiaII and ST8SiaIV knockout on social interaction and aggression. *Genes, Brain, and Behavior*, 9(8), 958–967. <https://doi.org/10.1111/j.1601-183X.2010.00635.x>
- Cassens, C., Kleene, R., Xiao, M.-F., Friedrich, C., Dityateva, G., Schafer-Nielsen, C., & Schachner, M. (2010). Binding of the receptor tyrosine kinase TrkB to the neural cell adhesion molecule (NCAM) regulates phosphorylation of NCAM and NCAM-dependent neurite outgrowth. *The Journal of Biological Chemistry*, 285(37), 28959–28967. <https://doi.org/10.1074/jbc.M110.114835>
- Castillo-Gómez, E., Gómez-Climent, M. A., Varea, E., Guirado, R., Blasco-Ibáñez, J. M., Crespo, C., Martínez-Guijarro, F. J., & Náchter, J. (2008). Dopamine acting through D2 receptors modulates the expression of PSA-NCAM, a molecule related to neuronal structural plasticity, in the medial prefrontal cortex of adult rats. *Experimental Neurology*, 214(1), 97–111. <https://doi.org/10.1016/j.expneurol.2008.07.018>
- Chen, Z.-Y., Jing, D., Bath, K. G., Ieraci, A., Khan, T., Siao, C.-J., Herrera, D. G., Toth, M., Yang, C., McEwen, B. S., Hempstead, B. L., & Lee, F. S. (2006). Genetic variant BDNF (Val66Met) polymorphism alters anxiety-related behavior. *Science (New York, N.Y.)*, 314(5796), 140–143. <https://doi.org/10.1126/science.1129663>
- Chuong, C. M., & Edelman, G. M. (1984). Alterations in neural cell adhesion molecules during development of different regions of the nervous system. *Journal of Neuroscience*, 4(9), 2354–2368.
- Clapham, D. E. (2003). Trp channels as cellular sensors. *Nature*, 426(6966), 517–524. <https://doi.org/10.1038/nature02196>
- Clapham, D. E. (2007). Calcium signaling. *Cell*, 131(6), 1047–1058. <https://doi.org/10.1016/j.cell.2007.11.028>
- Cremer, H., Lange, R., Christoph, A., Plomann, M., Vopper, G., Roes, J., Brown, R., Baldwin, S., Kraemer, P., & Scheff, S. (1994). Inactivation of the N-CAM gene in mice results in size reduction of the olfactory bulb and deficits in spatial learning. *Nature*, 367(6462), 455–459. <https://doi.org/10.1038/367455a0>

- Cunningham, B. A., Hemperly, J. J., Murray, B. A., Prediger, E. A., Brackenbury, R., & Edelman, G. M. (1987). Neural cell adhesion molecule: Structure, immunoglobulin-like domains, cell surface modulation, and alternative RNA splicing. *Science (New York, N.Y.)*, *236*(4803), 799–806. <https://doi.org/10.1126/science.3576199>
- Curreli, S., Arany, Z., Gerardy-Schahn, R., Mann, D., & Stamatou, N. M. (2007). Polysialylated neuropilin-2 is expressed on the surface of human dendritic cells and modulates dendritic cell-T lymphocyte interactions. *Journal of Biological Chemistry*, *282*(42), 30346–30356. <https://doi.org/10.1074/jbc.M702965200>
- Davare, M. A., Fortin, D. A., Saneyoshi, T., Nygaard, S., Kaech, S., Banker, G., Soderling, T. R., & Wayman, G. A. (2009). Transient receptor potential canonical 5 channels activate Ca²⁺/calmodulin kinase Iγ to promote axon formation in hippocampal neurons. *Journal of Neuroscience*, *29*(31), 9794–9808. <https://doi.org/10.1523/JNEUROSCI.1544-09.2009>
- Diestel, S., Schaefer, D., Cremer, H., & Schmitz, B. (2007). Ncam is ubiquitinated, endocytosed and recycled in neurons. *Journal of Cell Science*, *120*(Pt 22), 4035–4049. <https://doi.org/10.1242/jcs.019729>
- Dionisio, N., Albarran, L., Berna-Erro, A., Hernandez-Cruz, J. M., Salido, G. M., & Rosado, J. A. (2011). Functional role of the calmodulin- and inositol 1,4,5-trisphosphate receptor-binding (CIRB) site of TRPC6 in human platelet activation. *Cellular Signalling*, *23*(11), 1850–1856. <https://doi.org/10.1016/j.cellsig.2011.06.022>
- Ditlevsen, D. K., Owczarek, S., Berezin, V., & Bock, E. (2008). Relative role of upstream regulators of Akt, ERK and CREB in NCAM- and FGF2-mediated signalling. *Neurochemistry International*, *53*(5), 137–147. <https://doi.org/10.1016/j.neuint.2008.06.011>
- Doherty, P., Ashton, S. V., Moore, S. E., & Walsh, F. S. (1991). Morphoregulatory activities of NCAM and N-cadherin can be accounted for by G protein-dependent activation of L- and N-type neuronal Ca²⁺ channels. *Cell*, *67*(1), 21–33. [https://doi.org/10.1016/0092-8674\(91\)90569-k](https://doi.org/10.1016/0092-8674(91)90569-k)
- Du, J., Ma, X., Shen, B., Huang, Y., Birnbaumer, L., & Yao, X. (2014). Trpv4, TRPC1, and TRPP2 assemble to form a flow-sensitive heteromeric channel. *FASEB Journal : Official Publication of the Federation of American Societies for Experimental Biology*, *28*(11), 4677–4685. <https://doi.org/10.1096/fj.14-251652>

- Fedorkova, L., Rutishauser, U., Prosser, R., Shen, H., & Glass, J. (2002). Removal of polysialic acid from the SCN potentiates nonphotic circadian phase resetting. *Physiology & Behavior*, *77*(2-3), 361–369. [https://doi.org/10.1016/s0031-9384\(02\)00880-6](https://doi.org/10.1016/s0031-9384(02)00880-6)
- Fewou, S. N., Röckle, I., Hildebrandt, H., & Eckhardt, M. (2019). Transgenic overexpression of polysialyltransferase ST8SiaIV under the control of a neuron-specific promoter does not affect brain development but impairs exploratory behavior. *Glycobiology*, *29*(9), 657–668. <https://doi.org/10.1093/glycob/cwz040>
- Finne, J., Finne, U., Deagostini-Bazin, H., & Goriadis, C. (1983). Occurrence of α 2–8 linked polysialosyl units in a neural cell adhesion molecule. *Biochemical and Biophysical Research Communications*, *112*(2), 482–487. [https://doi.org/10.1016/0006-291X\(83\)91490-0](https://doi.org/10.1016/0006-291X(83)91490-0)
- Fiorio Pla, A., Maric, D., Brazer, S.-C., Giacobini, P., Liu, X., Chang, Y. H., Ambudkar, I. S., & Barker, J. L. (2005). Canonical transient receptor potential 1 plays a role in basic fibroblast growth factor (bFGF)/FGF receptor-1-induced Ca²⁺ entry and embryonic rat neural stem cell proliferation. *Journal of Neuroscience*, *25*(10), 2687–2701. <https://doi.org/10.1523/JNEUROSCI.0951-04.2005>
- Formoso, K., Susperreguy, S., Freichel, M., & Birnbaumer, L. (2020). Rna-seq analysis reveals TRPC genes to impact an unexpected number of metabolic and regulatory pathways. *Scientific Reports*, *10*(1), 7227. <https://doi.org/10.1038/s41598-020-61177-x>
- Fowler, M. A., Sidiropoulou, K., Ozkan, E. D., Phillips, C. W., & Cooper, D. C. (2007). Corticolimbic expression of TRPC4 and TRPC5 channels in the rodent brain. *PLOS ONE*, *2*(6), e573. <https://doi.org/10.1371/journal.pone.0000573>
- Freichel, M., Vennekens, R., Olausson, J., Hoffmann, M., Müller, C., Stolz, S., Scheunemann, J., Weissgerber, P., & Flockerzi, V. (2004). Functional role of TRPC proteins in vivo: Lessons from TRPC-deficient mouse models. *Biochemical and Biophysical Research Communications*, *322*(4), 1352–1358. <https://doi.org/10.1016/j.bbrc.2004.08.041>
- Frosch, M., Görden, I., Boulnois, G. J., Timmis, K. N., & Bitter-Suermann, D. (1985). Nzb mouse system for production of monoclonal antibodies to weak bacterial antigens: Isolation of an IgG antibody to the polysaccharide capsules of Escherichia coli K1 and group B meningococci. *Proceedings of the National*

- Academy of Sciences of the United States of America*, 82(4), 1194–1198.
<https://doi.org/10.1073/pnas.82.4.1194>
- Fujita-Hamabe, W., Nakamoto, K., & Tokuyama, S. (2011). Involvement of NCAM and FGF receptor signaling in the development of analgesic tolerance to morphine. *European Journal of Pharmacology*, 672(1-3), 77–82.
<https://doi.org/10.1016/j.ejphar.2011.04.029>
- Gascon, E., Vutskits, L., & Kiss, J. Z. (2007). Polysialic acid-neural cell adhesion molecule in brain plasticity: From synapses to integration of new neurons. *Brain Research Reviews*, 56(1), 101–118.
<https://doi.org/10.1016/j.brainresrev.2007.05.014>
- Gennarini, G., Rougon, G., Deagostini-Bazin, H., Hirn, M., & Goidis, C. (1984). Studies on the transmembrane disposition of the neural cell adhesion molecule N-CAM. A monoclonal antibody recognizing a cytoplasmic domain and evidence for the presence of phosphoserine residues. *European Journal of Biochemistry*, 142(1), 57–64. <https://doi.org/10.1111/j.1432-1033.1984.tb08250.x>
- Gerardy-Schahn, R., Bethe, A., Brennecke, T., Mühlenhoff, M., Eckhardt, M., Ziesing, S., Lottspeich, F., & Frosch, M. (1995). Molecular cloning and functional expression of bacteriophage PK1E-encoded endoneuraminidase Endo NE. *Molecular Microbiology*, 16(3), 441–450. <https://doi.org/10.1111/j.1365-2958.1995.tb02409.x>
- Goldowitz, D., Barthels, D., Lorenzon, N., Jungblut, A., & Wille, W. (1990). Ncam gene expression during the development of cerebellum and dentate gyrus in the mouse. *Brain Research. Developmental Brain Research*, 52(1-2), 151–160.
[https://doi.org/10.1016/0165-3806\(90\)90230-v](https://doi.org/10.1016/0165-3806(90)90230-v)
- Goulden, B. D., Pacheco, J., Dull, A., Zewe, J. P., Deiters, A., & Hammond, G. R. V. (2019). A high-avidity biosensor reveals plasma membrane PI(3,4)P2 is predominantly a class I PI3K signaling product. *The Journal of Cell Biology*, 218(3), 1066–1079. <https://doi.org/10.1083/jcb.201809026>
- Green, M., Ishino, M., & Loewenstein, P. M. (1989). Mutational analysis of HIV-1 Tat minimal domain peptides: Identification of trans-dominant mutants that suppress HIV-LTR-driven gene expression. *Cell*, 58(1), 215–223.
[https://doi.org/10.1016/0092-8674\(89\)90417-0](https://doi.org/10.1016/0092-8674(89)90417-0)

- Greka, A., Navarro, B., Oancea, E., Duggan, A., & Clapham, D. E. (2003). Trpc5 is a regulator of hippocampal neurite length and growth cone morphology. *Nature Neuroscience*, 6(8), 837–845. <https://doi.org/10.1038/nn1092>
- Hammond, M. S. L., Sims, C., Parameshwaran, K., Suppiramaniam, V., Schachner, M., & Dityatev, A. (2006). Neural cell adhesion molecule-associated polysialic acid inhibits NR2B-containing N-methyl-D-aspartate receptors and prevents glutamate-induced cell death. *Journal of Biological Chemistry*, 281(46), 34859–34869. <https://doi.org/10.1074/jbc.M602568200>
- Hannan, M. A., Kabbani, N., Paspalas, C. D., & Levenson, R. (2008). Interaction with dopamine D2 receptor enhances expression of transient receptor potential channel 1 at the cell surface. *Biochimica Et Biophysica Acta*, 1778(4), 974–982. <https://doi.org/10.1016/j.bbamem.2008.01.011>
- Harteneck, C., Plant, T. D., & Schultz, G. (2000). From worm to man: Three subfamilies of TRP channels. *Trends in Neurosciences*, 23(4), 159–166. [https://doi.org/10.1016/s0166-2236\(99\)01532-5](https://doi.org/10.1016/s0166-2236(99)01532-5)
- He, H. T., Barbet, J., Chaix, J. C., & Goridis, C. (1986). Phosphatidylinositol is involved in the membrane attachment of NCAM-120, the smallest component of the neural cell adhesion molecule. *The EMBO Journal*, 5(10), 2489–2494. <https://doi.org/10.1002/j.1460-2075.1986.tb04526.x>
- Heiser, J. H., Schuwald, A. M., Sillani, G., Ye, L., Müller, W. E., & Leuner, K. (2013). Trpc6 channel-mediated neurite outgrowth in PC12 cells and hippocampal neurons involves activation of RAS/MEK/ERK, PI3K, and CAMKIV signaling. *Journal of Neurochemistry*, 127(3), 303–313. <https://doi.org/10.1111/jnc.12376>
- Heldt, S. A., Stanek, L., Chhatwal, J. P., & Ressler, K. J. (2007). Hippocampus-specific deletion of BDNF in adult mice impairs spatial memory and extinction of aversive memories. *Molecular Psychiatry*, 12(7), 656–670. <https://doi.org/10.1038/sj.mp.4001957>
- Hofmann, T., Schaefer, M., Schultz, G., & Gudermann, T. (2002). Subunit composition of mammalian transient receptor potential channels in living cells. *Proceedings of the National Academy of Sciences of the United States of America*, 99(11), 7461–7466. <https://doi.org/10.1073/pnas.102596199>
- Holbro, N., Grunditz, A., & Oertner, T. G. (2009). Differential distribution of endoplasmic reticulum controls metabotropic signaling and plasticity at hippocampal synapses. *Proceedings of the National Academy of Sciences of the*

- United States of America*, *106*(35), 15055–15060.
<https://doi.org/10.1073/pnas.0905110106>
- Jahan, K. S., Shi, J., Greenberg, H. Z. E., Khavandi, S., Baudel, M. M.-A., Barrese, V., Greenwood, I. A., & Albert, A. P. (2020). Marcks mediates vascular contractility through regulating interactions between voltage-gated Ca²⁺ channels and PIP2. *Vascular Pharmacology*, *132*, 106776. <https://doi.org/10.1016/j.vph.2020.106776>
- Janas, T., Nowotarski, K., & Janas, T. (2010). Polysialic acid can mediate membrane interactions by interacting with phospholipids. *Chemistry and Physics of Lipids*, *163*(3), 286–291. <https://doi.org/10.1016/j.chemphyslip.2009.12.003>
- Jessen, U., Novitskaya, V., Pedersen, N., Serup, P., Berezin, V., & Bock, E. (2001). The transcription factors CREB and c-Fos play key roles in NCAM-mediated neurogenesis in PC12-E2 cells. *Journal of Neurochemistry*, *79*(6), 1149–1160. <https://doi.org/10.1046/j.1471-4159.2001.00636.x>
- Johnson, C. P., Fujimoto, I., Rutishauser, U., & Leckband, D. E. (2005). Direct evidence that neural cell adhesion molecule (NCAM) polysialylation increases intermembrane repulsion and abrogates adhesion. *Journal of Biological Chemistry*, *280*(1), 137–145. <https://doi.org/10.1074/jbc.M410216200>
- Jucker, M., Mondadori, C., Mohajeri, H., Bartsch, U., & Schachner, M. (1995). Transient upregulation of NCAM mRNA in astrocytes in response to entorhinal cortex lesions and ischemia. *Molecular Brain Research*, *28*(1), 149–156. [https://doi.org/10.1016/0169-328X\(94\)00206-T](https://doi.org/10.1016/0169-328X(94)00206-T)
- Just, S., Chenard, B. L., Ceci, A., Strassmaier, T., Chong, J. A., Blair, N. T., Gallaschun, R. J., Del Camino, D., Cantin, S., D'Amours, M., Eickmeier, C., Fanger, C. M., Hecker, C., Hessler, D. P., Hengerer, B., Kroker, K. S., Malekiani, S., Mihalek, R., McLaughlin, J., Moran, M. M. (2018). Treatment with HC-070, a potent inhibitor of TRPC4 and TRPC5, leads to anxiolytic and antidepressant effects in mice. *PLOS ONE*, *13*(1), e0191225. <https://doi.org/10.1371/journal.pone.0191225>
- Keilhauer, G., Faissner, A., & Schachner, M. (1985). Differential inhibition of neurone-neurone, neurone-astrocyte and astrocyte-astrocyte adhesion by L1, L2 and NCAM antibodies. *Nature*, *316*(6030), 728–730. <https://doi.org/10.1038/316728a0>
- Kim, H., Kim, J., Jeon, J.-P., Myeong, J., Wie, J., Hong, C., Kim, H. J., Jeon, J.-H., & So, I. (2012). The roles of G proteins in the activation of TRPC4 and TRPC5

- transient receptor potential channels. *Channels*, 6(5), 333–343.
<https://doi.org/10.4161/chan.21198>
- Kiryushko, D., Korshunova, I., Berezin, V., & Bock, E. (2006). Neural cell adhesion molecule induces intracellular signaling via multiple mechanisms of Ca²⁺ homeostasis. *Molecular Biology of the Cell*, 17(5), 2278–2286.
<https://doi.org/10.1091/mbc.e05-10-0987>
- Kiselyov, V. V. (2010). Ncam and the FGF-receptor. *Advances in Experimental Medicine and Biology*, 663, 67–79. https://doi.org/10.1007/978-1-4419-1170-4_4
- Kleene, R., Cassens, C., Bähring, R., Theis, T., Xiao, M.-F., Dityatev, A., Schafer-Nielsen, C., Döring, F., Wischmeyer, E., & Schachner, M. (2010). Functional consequences of the interactions among the neural cell adhesion molecule NCAM, the receptor tyrosine kinase TrkB, and the inwardly rectifying K⁺ channel KIR3.3. *The Journal of Biological Chemistry*, 285(37), 28968–28979.
<https://doi.org/10.1074/jbc.M110.114876>
- Kleene, R., Mzoughi, M., Joshi, G., Kalus, I., Bormann, U., Schulze, C., Xiao, M.-F., Dityatev, A., & Schachner, M. (2010). Ncam-induced neurite outgrowth depends on binding of calmodulin to NCAM and on nuclear import of NCAM and fak fragments. *The Journal of Neuroscience : The Official Journal of the Society for Neuroscience*, 30(32), 10784–10798. <https://doi.org/10.1523/JNEUROSCI.0297-10.2010>
- Kleene, R., & Schachner, M. (2004). Glycans and neural cell interactions. *Nature Reviews. Neuroscience*, 5(3), 195–208. <https://doi.org/10.1038/nrn1349>
- Kochlamazashvili, G., Senkov, O., Grebenyuk, S., Robinson, C., Xiao, M.-F., Stummeyer, K., Gerardy-Schahn, R., Engel, A. K., Feig, L., Semyanov, A., Suppiramaniam, V., Schachner, M., & Dityatev, A. (2010). Neural cell adhesion molecule-associated polysialic acid regulates synaptic plasticity and learning by restraining the signaling through GluN2B-containing NMDA receptors. *Journal of Neuroscience*, 30(11), 4171–4183. <https://doi.org/10.1523/JNEUROSCI.5806-09.2010>
- Kolkova, K. (2010). Biosynthesis of NCAM. *Advances in Experimental Medicine and Biology*, 663, 213–225. https://doi.org/10.1007/978-1-4419-1170-4_14
- Kolkova, K., Novitskaya, V., Pedersen, N., Berezin, V., & Bock, E. (2000). Neural Cell Adhesion Molecule-Stimulated Neurite Outgrowth Depends on Activation of Protein Kinase C and the Ras–Mitogen-Activated Protein Kinase Pathway.

- Journal of Neuroscience*, 20(6), 2238–2246.
<https://doi.org/10.1523/JNEUROSCI.20-06-02238.2000>
- Kolkova, K., Stensman, H., Berezin, V., Bock, E., & Larsson, C. (2005). Distinct roles of PKC isoforms in NCAM-mediated neurite outgrowth. *Journal of Neurochemistry*, 92(4), 886–894. <https://doi.org/10.1111/j.1471-4159.2004.02919.x>
- Kruse, J., Mailhammer, R., Wernecke, H., Faissner, A., Sommer, I., Goridis, C., & Schachner, M. (1984). Neural cell adhesion molecules and myelin-associated glycoprotein share a common carbohydrate moiety recognized by monoclonal antibodies L2 and HNK-1. *Nature*, 311(5982), 153–155. <https://doi.org/10.1038/311153a0>
- Kumar, S., Chakraborty, S., Barbosa, C., Brustovetsky, T., Brustovetsky, N., & Obukhov, A. G. (2012). Mechanisms controlling neurite outgrowth in a pheochromocytoma cell line: The role of TRPC channels. *Journal of Cellular Physiology*, 227(4), 1408–1419. <https://doi.org/10.1002/jcp.22855>
- Kurosawa, N., Yoshida, Y., Kojima, N., & Tsuji, S. (1997). Polysialic acid synthase (ST8Sia II/STX) mRNA expression in the developing mouse central nervous system. *Journal of Neurochemistry*, 69(2), 494–503. <https://doi.org/10.1046/j.1471-4159.1997.69020494.x>
- Lepannetier, S., Gualdani, R., Tempesta, S., Schakman, O., Seghers, F., Kreis, A., Yerna, X., Slimi, A., Clippele, M. de, Tajeddine, N., Voets, T., Bon, R. S., Beech, D. J., Tissir, F., & Gailly, P. (2018). Activation of TRPC1 Channel by Metabotropic Glutamate Receptor mGluR5 Modulates Synaptic Plasticity and Spatial Working Memory. *Frontiers in Cellular Neuroscience*, 12, Article 318, 318. <https://doi.org/10.3389/fncel.2018.00318>
- Leshchyn'ska, I., Sytnyk, V., Morrow, J. S., & Schachner, M. (2003). Neural cell adhesion molecule (NCAM) association with PKC β 2 via β 1 spectrin is implicated in NCAM-mediated neurite outgrowth. *The Journal of Cell Biology*, 161(3), 625–639. <https://doi.org/10.1083/jcb.200303020>
- Li, H.-S., Xu, X.-Z. S., & Montell, C. (1999). Activation of a TRPC3-Dependent Cation Current through the Neurotrophin BDNF. *Neuron*, 24(1), 261–273. [https://doi.org/10.1016/s0896-6273\(00\)80838-7](https://doi.org/10.1016/s0896-6273(00)80838-7)
- Li, N., Teng, S.-W., Zhao, L., Li, J.-R., Xu, J.-L., Shuai, J.-C., & Chen, Z.-Y. (2021). Carboxypeptidase E Regulates Activity-Dependent TrkB Neuronal Surface

- Insertion and Hippocampal Memory. *Journal of Neuroscience*, 41(33), 6987–7002. <https://doi.org/10.1523/JNEUROSCI.0236-21.2021>
- Li, S., Leshchyns'ka, I., Chernyshova, Y., Schachner, M. & Sytnyk, V. (2013). The neural cell adhesion molecule (NCAM) associates with and signals through p21-activated kinase 1 (Pak1). *Journal of Neuroscience*, 33(2), 790–803. <https://doi.org/10.1523/JNEUROSCI.1238-12.2013>
- Liedtke, S., Geyer, H., Wuhrer, M., Geyer, R., Frank, G., Gerardy-Schahn, R., Zähringer, U., & Schachner, M. (2001). Characterization of N-glycans from mouse brain neural cell adhesion molecule. *Glycobiology*, 11(5), 373–384. <https://doi.org/10.1093/glycob/11.5.373>
- Liu, X., Bandyopadhyay, B. C., Singh, B. B., Groschner, K., & Ambudkar, I. S. (2005). Molecular analysis of a store-operated and 2-acetyl-sn-glycerol-sensitive non-selective cation channel. Heteromeric assembly of TRPC1-TRPC3. *Journal of Biological Chemistry*, 280(22), 21600–21606. <https://doi.org/10.1074/jbc.C400492200>
- Lock, J. T., & Parker, I. (2020). Ip3 mediated global Ca²⁺ signals arise through two temporally and spatially distinct modes of Ca²⁺ release. *ELife*, 9. <https://doi.org/10.7554/eLife.55008>
- Lopez-Fernandez, M. A., Montaron, M.-F., Varea, E., Rougon, G., Venero, C., Abrous, D. N., & Sandi, C. (2007). Upregulation of polysialylated neural cell adhesion molecule in the dorsal hippocampus after contextual fear conditioning is involved in long-term memory formation. *Journal of Neuroscience*, 27(17), 4552–4561. <https://doi.org/10.1523/JNEUROSCI.0396-07.2007>
- Malarkey, E. B., Ni, Y., & Parpura, V. (2008). Ca²⁺ entry through TRPC1 channels contributes to intracellular Ca²⁺ dynamics and consequent glutamate release from rat astrocytes. *Glia*, 56(8), 821–835. <https://doi.org/10.1002/glia.20656>
- Maness, P. F., & Schachner, M. (2007). Neural recognition molecules of the immunoglobulin superfamily: Signaling transducers of axon guidance and neuronal migration. *Nature Neuroscience*, 10(1), 19–26. <https://doi.org/10.1038/nn1827>
- Markram, K., Lopez Fernandez, M. A., Abrous, D. N., & Sandi, C. (2007). Amygdala upregulation of NCAM polysialylation induced by auditory fear conditioning is not required for memory formation, but plays a role in fear extinction.

- Neurobiology of Learning and Memory*, 87(4), 573–582.
<https://doi.org/10.1016/j.nlm.2006.11.007>
- Matsuda, T., & Cepko, C. L. (2004). Electroporation and RNA interference in the rodent retina in vivo and in vitro. *Proceedings of the National Academy of Sciences of the United States of America*, 101(1), 16–22.
<https://doi.org/10.1073/pnas.2235688100>
- McGurk, J. S., Shim, S., Kim, J. Y., Wen, Z., Song, H., & Ming, G.-L. (2011). Postsynaptic TRPC1 function contributes to BDNF-induced synaptic potentiation at the developing neuromuscular junction. *Journal of Neuroscience*, 31(41), 14754–14762. <https://doi.org/10.1523/JNEUROSCI.3599-11.2011>
- Minard, A., Bauer, C. C., Wright, D. J., Rubaiy, H. N., Muraki, K., Beech, D. J., & Bon, R. S. (2018). Remarkable Progress with Small-Molecule Modulation of TRPC1/4/5 Channels: Implications for Understanding the Channels in Health and Disease. *Cells*, 7(6), 52. <https://doi.org/10.3390/cells7060052>
- Mishra, B., Ohe, M. von der, Schulze, C., Bian, S., Makhina, T., Loers, G., Kleene, R., & Schachner, M. (2010). Functional role of the interaction between polysialic acid and extracellular histone H1. *Journal of Neuroscience*, 30(37), 12400–12413.
<https://doi.org/10.1523/JNEUROSCI.6407-09.2010>
- Miyano, K., Morioka, N., Sugimoto, T., Shiraishi, S., Uezono, Y., & Nakata, Y. (2010). Activation of the neurokinin-1 receptor in rat spinal astrocytes induces Ca²⁺ release from IP₃-sensitive Ca²⁺ stores and extracellular Ca²⁺ influx through TRPC3. *Neurochemistry International*, 57(8), 923–934.
<https://doi.org/10.1016/j.neuint.2010.09.012>
- Mühlenhoff, M., Eckhardt, M., & Gerardy-Schahn, R. (1998). Polysialic acid: three-dimensional structure, biosynthesis and function. *Current Opinion in Structural Biology*, 8(5), 558–564. [https://doi.org/10.1016/S0959-440X\(98\)80144-9](https://doi.org/10.1016/S0959-440X(98)80144-9)
- Mühlenhoff, M., Rollenhagen, M., Werneburg, S., Gerardy-Schahn, R., & Hildebrandt, H. (2013). Polysialic acid: Versatile modification of NCAM, SynCAM 1 and neuropilin-2. *Neurochemical Research*, 38(6), 1134–1143.
<https://doi.org/10.1007/s11064-013-0979-2>
- Muller, D., Djebbara-Hannas, Z., Jourdain, P., Vutskits, L., Durbec, P., Rougon, G., & Kiss, J. Z. (2000). Brain-derived neurotrophic factor restores long-term potentiation in polysialic acid-neural cell adhesion molecule-deficient

- hippocampus. *Proceedings of the National Academy of Sciences of the United States of America*, 97(8), 4315–4320. <https://doi.org/10.1073/pnas.070022697>
- Muller, D., Wang, C., Skibo, G., Toni, N., Cremer, H., Calaora, V., Rougon, G., & Kiss, J. (1996). Psa–ncam Is Required for Activity-Induced Synaptic Plasticity. *Neuron*, 17(3), 413–422. [https://doi.org/10.1016/s0896-6273\(00\)80174-9](https://doi.org/10.1016/s0896-6273(00)80174-9)
- Myeong, J., Ko, J., Kwak, M., Kim, J., Woo, J., Ha, K., Hong, C., Yang, D., Kim, H. J., Jeon, J.-H., & So, I. (2018). Dual action of the Gαq-PLCβ-PI(4,5)P2 pathway on TRPC1/4 and TRPC1/5 heterotetramers. *Scientific Reports*, 8(1), 12117. <https://doi.org/10.1038/s41598-018-30625-0>
- Nelson, R. W., Bates, P. A., & Rutishauser, U. (1995). Protein determinants for specific polysialylation of the neural cell adhesion molecule. *Journal of Biological Chemistry*, 270(29), 17171–17179. <https://doi.org/10.1074/jbc.270.29.17171>
- Neuner, S. M., Wilmott, L. A., Hope, K. A., Hoffmann, B., Chong, J. A., Abramowitz, J., Birnbaumer, L., O'Connell, K. M., Tryba, A. K., Greene, A. S., Savio Chan, C., & Kaczorowski, C. C. (2015). Trpc3 channels critically regulate hippocampal excitability and contextual fear memory. *Behavioural Brain Research*, 281, 69–77. <https://doi.org/10.1016/j.bbr.2014.12.018>
- Niethammer, P., Delling, M., Sytnyk, V., Dityatev, A., Fukami, K., & Schachner, M. (2002). Cosignaling of NCAM via lipid rafts and the FGF receptor is required for neurogenesis. *The Journal of Cell Biology*, 157(3), 521–532. <https://doi.org/10.1083/jcb.200109059>
- Ningoo, M., Plant, L. D., Greka, A., & Logothetis, D. E. (2021). Pip2 regulation of TRPC5 channel activation and desensitization. *The Journal of Biological Chemistry*, 296, 100726. <https://doi.org/10.1016/j.jbc.2021.100726>
- Novak, D. (2009). *Untersuchungen zur Interaktion zwischen dem neuronalen Zelladhäsionsmolekül NCAM und dem multiple PDZ-Domänen-enthaltenden Protein MUPPI im Nervensystem der Maus* [Doctoral dissertation]. Universität Hamburg.
- Ohe, M. von der, Wheeler, S. F., Wührer, M., Harvey, D. J., Liedtke, S., Mühlenhoff, M., Gerardy-Schahn, R., Geyer, H., Dwek, R. A., Geyer, R., Wing, D. R., & Schachner, M. (2002). Localization and characterization of polysialic acid-containing N-linked glycans from bovine NCAM. *Glycobiology*, 12(1), 47–63. <https://doi.org/10.1093/glycob/12.1.47>

- Oliveira, A. R., Reimer, A. E., & Brandão, M. L. (2006). Dopamine D2 receptor mechanisms in the expression of conditioned fear. *Pharmacology, Biochemistry, and Behavior*, *84*(1), 102–111. <https://doi.org/10.1016/j.pbb.2006.04.012>
- Oltmann-Norden, I., Galuska, S. P., Hildebrandt, H., Geyer, R., Gerardy-Schahn, R., Geyer, H., & Mühlhoff, M. (2008). Impact of the polysialyltransferases ST8SiaII and ST8SiaIV on polysialic acid synthesis during postnatal mouse brain development. *Journal of Biological Chemistry*, *283*(3), 1463–1471. <https://doi.org/10.1074/jbc.M708463200>
- Ono, S., Hane, M., Kitajima, K., & Sato, C. (2012). Novel regulation of fibroblast growth factor 2 (FGF2)-mediated cell growth by polysialic acid. *The Journal of Biological Chemistry*, *287*(6), 3710–3722. <https://doi.org/10.1074/jbc.M111.276618>
- Paratcha, G., Ledda, F., & Ibáñez, C. F. (2003). The Neural Cell Adhesion Molecule NCAM Is an Alternative Signaling Receptor for GDNF Family Ligands. *Cell*, *113*(7), 867–879. [https://doi.org/10.1016/s0092-8674\(03\)00435-5](https://doi.org/10.1016/s0092-8674(03)00435-5)
- Persohn, E., Pollerberg, G. E., & Schachner, M. (1989). Immunoelectron-microscopic localization of the 180 kD component of the neural cell adhesion molecule N-CAM in postsynaptic membranes. *The Journal of Comparative Neurology*, *288*(1), 92–100. <https://doi.org/10.1002/cne.902880108>
- Phelan, K. D., Mock, M. M., Kretz, O., Shwe, U. T., Kozhemyakin, M., Greenfield, L. J., Dietrich, A., Birnbaumer, L., Freichel, M., Flockerzi, V., & Zheng, F. (2012). Heteromeric canonical transient receptor potential 1 and 4 channels play a critical role in epileptiform burst firing and seizure-induced neurodegeneration. *Molecular Pharmacology*, *81*(3), 384–392. <https://doi.org/10.1124/mol.111.075341>
- Pillai-Nair, N., Panicker, A. K., Rodriguiz, R. M., Gilmore, K. L., Demyanenko, G. P., Huang, J. Z., Wetsel, W. C., & Maness, P. F. (2005). Neural cell adhesion molecule-secreting transgenic mice display abnormalities in GABAergic interneurons and alterations in behavior. *Journal of Neuroscience*, *25*(18), 4659–4671. <https://doi.org/10.1523/JNEUROSCI.0565-05.2005>
- Puram, S. V., Riccio, A., Koirala, S., Ikeuchi, Y., Kim, A. H., Corfas, G., & Bonni, A. (2011). A TRPC5-regulated calcium signaling pathway controls dendrite patterning in the mammalian brain. *Genes & Development*, *25*(24), 2659–2673. <https://doi.org/10.1101/gad.174060.111>

- Riccio, A., Li, Y., Moon, J., Kim, K.-S., Smith, K. S., Rudolph, U., Gapon, S., Yao, G. L., Tsvetkov, E., Rodig, S. J., Van't Veer, A., Meloni, E. G., Carlezon, W. A., Bolshakov, V. Y., & Clapham, D. E. (2009). Essential role for TRPC5 in amygdala function and fear-related behavior. *Cell*, *137*(4), 761–772. <https://doi.org/10.1016/j.cell.2009.03.039>
- Riccio, A., Li, Y., Tsvetkov, E., Gapon, S., Yao, G. L., Smith, K. S., Engin, E., Rudolph, U., Bolshakov, V. Y., & Clapham, D. E. (2014). Decreased anxiety-like behavior and $G\alpha_q/11$ -dependent responses in the amygdala of mice lacking TRPC4 channels. *Journal of Neuroscience*, *34*(10), 3653–3667. <https://doi.org/10.1523/JNEUROSCI.2274-13.2014>
- Riccio, A., Medhurst, A. D., Mattei, C., Kessel, R. E., Calver, A. R., Randall, A. D., Benham, C. D., & Pangalos, M. N. (2002). Mrna distribution analysis of human TRPC family in CNS and peripheral tissues. *Brain Research. Molecular Brain Research*, *109*(1-2), 95–104. [https://doi.org/10.1016/s0169-328x\(02\)00527-2](https://doi.org/10.1016/s0169-328x(02)00527-2)
- Rønn, L. C., Berezin, V., & Bock, E. (2000). The neural cell adhesion molecule in synaptic plasticity and ageing. *International Journal of Developmental Neuroscience*, *18*(2-3), 193–199. [https://doi.org/10.1016/S0736-5748\(99\)00088-X](https://doi.org/10.1016/S0736-5748(99)00088-X)
- Rønn, L. C., Dissing, S., Holm, A., Berezin, V., & Bock, E. (2002). Increased intracellular calcium is required for neurite outgrowth induced by a synthetic peptide ligand of NCAM. *FEBS Letters*, *518*(1-3), 60–66. [https://doi.org/10.1016/S0014-5793\(02\)02644-3](https://doi.org/10.1016/S0014-5793(02)02644-3)
- Rubaiy, H. N., Ludlow, M. J., Bon, R. S., & Beech, D. J. (2017). Pico145 - powerful new tool for TRPC1/4/5 channels. *Channels*, *11*(5), 362–364. <https://doi.org/10.1080/19336950.2017.1317485>
- Rubaiy, H. N., Ludlow, M. J., Henrot, M., Gaunt, H. J., Miteva, K., Cheung, S. Y., Tanahashi, Y., Hamzah, N., Musialowski, K. E., Blythe, N. M., Appleby, H. L., Bailey, M. A., McKeown, L., Taylor, R., Foster, R., Waldmann, H., Nussbaumer, P., Christmann, M., Bon, R. S., . . . Beech, D. J. (2017). Picomolar, selective, and subtype-specific small-molecule inhibition of TRPC1/4/5 channels. *Journal of Biological Chemistry*, *292*(20), 8158–8173. <https://doi.org/10.1074/jbc.M116.773556>

- Rutishauser, U. (2008). Polysialic acid in the plasticity of the developing and adult vertebrate nervous system. *Nature Reviews. Neuroscience*, *9*(1), 26–35. <https://doi.org/10.1038/nrn2285>
- Salido, G. M., Sage, S. O., & Rosado, J. A. (2009). Trpc channels and store-operated Ca(2+) entry. *Biochimica Et Biophysica Acta*, *1793*(2), 223–230. <https://doi.org/10.1016/j.bbamcr.2008.11.001>
- Sandi, C., Woodson, J. C., Haynes, V. F., Park, C. R., Touyarot, K., Lopez-Fernandez, M. A., Venero, C., & Diamond, D. M. (2005). Acute stress-induced impairment of spatial memory is associated with decreased expression of neural cell adhesion molecule in the hippocampus and prefrontal cortex. *Biological Psychiatry*, *57*(8), 856–864. <https://doi.org/10.1016/j.biopsych.2004.12.034>
- Sato, C., Hane, M., & Kitajima, K. (2016). Relationship between ST8SIA2, polysialic acid and its binding molecules, and psychiatric disorders. *Biochimica Et Biophysica Acta*, *1860*(8), 1739–1752. <https://doi.org/10.1016/j.bbagen.2016.04.015>
- Scarlett, C. (2003). Neuroanatomical development in the absence of PKC phosphorylation of the myristoylated alanine-rich C-kinase substrate (MARCKS) protein. *Developmental Brain Research*, *144*(1), 25–42. [https://doi.org/10.1016/S0165-3806\(03\)00155-X](https://doi.org/10.1016/S0165-3806(03)00155-X)
- Schachner, M. (1997). Neural recognition molecules and synaptic plasticity. *Current Opinion in Cell Biology*, *9*(5), 627–634. [https://doi.org/10.1016/s0955-0674\(97\)80115-9](https://doi.org/10.1016/s0955-0674(97)80115-9)
- Schindl, R., Frischauf, I., Kahr, H., Fritsch, R., Krenn, M., Derndl, A., Vales, E., Muik, M., Derler, I., Groschner, K., & Romanin, C. (2008). The first ankyrin-like repeat is the minimum indispensable key structure for functional assembly of homo- and heteromeric TRPC4/TRPC5 channels. *Cell Calcium*, *43*(3), 260–269. <https://doi.org/10.1016/j.ceca.2007.05.015>
- Schmidt, C. M., McKillop, I. H., Cahill, P. A., & Sitzmann, J. V. (1999). The role of cAMP-MAPK signalling in the regulation of human hepatocellular carcinoma growth in vitro. *European Journal of Gastroenterology & Hepatology*, *11*(12), 1393–1399. <https://doi.org/10.1097/00042737-199912000-00009>
- Seki, T., & Arai, Y. (1991). Expression of highly polysialylated NCAM in the neocortex and piriform cortex of the developing and the adult rat. *Anatomy and Embryology*, *184*(4), 395–401. <https://doi.org/10.1007/BF00957900>

- Selvaraj, S., Sun, Y., & Singh, B. B. (2010). Trpc channels and their implication in neurological diseases. *CNS & Neurological Disorders Drug Targets*, 9(1), 94–104. <https://doi.org/10.2174/187152710790966650>
- Selvaraj, S., Sun, Y., Watt, J. A., Wang, S., Lei, S., Birnbaumer, L., & Singh, B. B. (2012). Neurotoxin-induced ER stress in mouse dopaminergic neurons involves downregulation of TRPC1 and inhibition of AKT/mTOR signaling. *The Journal of Clinical Investigation*, 122(4), 1354–1367. <https://doi.org/10.1172/JCI61332>
- Senkov, O., Sun, M., Weinhold, B., Gerardy-Schahn, R., Schachner, M., & Dityatev, A. (2006). Polysialylated neural cell adhesion molecule is involved in induction of long-term potentiation and memory acquisition and consolidation in a fear-conditioning paradigm. *Journal of Neuroscience*, 26(42), 10888–10989. <https://doi.org/10.1523/JNEUROSCI.0878-06.2006>
- Shapiro, L., Love, J., & Colman, D. R. (2007). Adhesion molecules in the nervous system: Structural insights into function and diversity. *Annual Review of Neuroscience*, 30, 451–474. <https://doi.org/10.1146/annurev.neuro.29.051605.113034>
- Sheng, L., Leshchyns'ka, I., & Sytnyk, V. (2015). Neural cell adhesion molecule 2 promotes the formation of filopodia and neurite branching by inducing submembrane increases in Ca²⁺ levels. *Journal of Neuroscience*, 35(4), 1739–1752. <https://doi.org/10.1523/JNEUROSCI.1714-14.2015>
- Shi, J., Birnbaumer, L., Large, W. A., & Albert, A. P. (2014). Myristoylated alanine-rich C kinase substrate coordinates native TRPC1 channel activation by phosphatidylinositol 4,5-bisphosphate and protein kinase C in vascular smooth muscle. *FASEB Journal : Official Publication of the Federation of American Societies for Experimental Biology*, 28(1), 244–255. <https://doi.org/10.1096/fj.13-238022>
- Shiwaku, H., Katayama, S., Kondo, K., Nakano, Y., Tanaka, H., Yoshioka, Y., Fujita, K., Tamaki, H., Takebayashi, H., Terasaki, O., Nagase, Y., Nagase, T., Kubota, T., Ishikawa, K., Okazawa, H., & Takahashi, H. (2022). Autoantibodies against NCAM1 from patients with schizophrenia cause schizophrenia-related behavior and changes in synapses in mice. *Cell Reports. Medicine*, 3(4), 100597. <https://doi.org/10.1016/j.xcrm.2022.100597>
- Soboloff, J., Spassova, M., Hewavitharana, T., He, L. P., Luncsford, P., Xu, W., Venkatachalam, K., van Rossum, D., Patterson, R. L., & Gill, D. L. (2007). Trpc

- channels: Integrators of multiple cellular signals. *Handbook of Experimental Pharmacology*(179), 575–591. https://doi.org/10.1007/978-3-540-34891-7_34
- Song, K., Wei, M., Guo, W., Quan, L., Kang, Y., Wu, J.-X., & Chen, L. (2021). Structural basis for human TRPC5 channel inhibition by two distinct inhibitors. *ELife*, *10*. <https://doi.org/10.7554/eLife.63429>
- Sorkin, B. C., Hoffman, S., Edelman, G. M., & Cunningham, B. A. (1984). Sulfation and phosphorylation of the neural cell adhesion molecule, N-CAM. *Science (New York, N.Y.)*, *225*(4669), 1476–1478. <https://doi.org/10.1126/science.6474186>
- Storch, U., Forst, A.-L., Pardatscher, F., Erdogmus, S., Philipp, M., Gregoritzka, M., Mederos y Schnitzler, M., & Gudermann, T. (2017). Dynamic NHERF interaction with TRPC4/5 proteins is required for channel gating by diacylglycerol. *Proceedings of the National Academy of Sciences of the United States of America*, *114*(1), E37-E46. <https://doi.org/10.1073/pnas.1612263114>
- Storch, U., Forst, A.-L., Philipp, M., Gudermann, T., & Mederos y Schnitzler, M. (2012). Transient receptor potential channel 1 (TRPC1) reduces calcium permeability in heteromeric channel complexes. *The Journal of Biological Chemistry*, *287*(5), 3530–3540. <https://doi.org/10.1074/jbc.M111.283218>
- Stork, O., Welzl, H., Wolfer, D., Schuster, T., Mantei, N., Stork, S., Hoyer, D., Lipp, H., Obata, K., & Schachner, M. (2000). Recovery of emotional behaviour in neural cell adhesion molecule (NCAM) null mutant mice through transgenic expression of NCAM180. *The European Journal of Neuroscience*, *12*(9), 3291–3306. <https://doi.org/10.1046/j.1460-9568.2000.00197.x>
- Stork, O., Welzl, H., Wotjak, C. T., Hoyer, D., Delling, M., Cremer, H., & Schachner, M. (1999). Anxiety and increased 5-HT_{1A} receptor response in NCAM null mutant mice. *Journal of Neurobiology*, *40*(3), 343–355. [https://doi.org/10.1002/\(sici\)1097-4695\(19990905\)40:3<343::aid-neu6>3.0.co;2-s](https://doi.org/10.1002/(sici)1097-4695(19990905)40:3<343::aid-neu6>3.0.co;2-s)
- Strübing, C., Krapivinsky, G., Krapivinsky, L., & Clapham, D. E. (2001). Trpc1 and TRPC5 Form a Novel Cation Channel in Mammalian Brain. *Neuron*, *29*(3), 645–655. [https://doi.org/10.1016/s0896-6273\(01\)00240-9](https://doi.org/10.1016/s0896-6273(01)00240-9)
- Swierczynski, S. L., Siddhanti, S. R., Tuttle, J. S., & Blackshear, P. J. (1996). Nonmyristoylated MARCKS Complements Some but Not All of the Developmental Defects Associated with MARCKS Deficiency in Mice.

- Developmental Biology*, 179(1), 135–147.
<https://doi.org/10.1006/dbio.1996.0246>
- Tang, J., Lin, Y., Zhang, Z., Tikunova, S., Birnbaumer, L., & Zhu, M. X. (2001). Identification of common binding sites for calmodulin and inositol 1,4,5-trisphosphate receptors on the carboxyl termini of trp channels. *Journal of Biological Chemistry*, 276(24), 21303–21310.
<https://doi.org/10.1074/jbc.M102316200>
- Theis, T. (2011). *Functional roles of transient receptor potential canonical channels and myristoylated alanine-rich protein kinase C substrate as novel interaction partners of neuronal cell adhesion molecule NCAM and polysialic acid in Mus musculus* [Doctoral dissertation]. Department Biologie der Fakultät für Mathematik, Informatik un Naturwissenschaften, Universität Hamburg.
- Theis, T., Mishra, B., Ohe, M. von der, Loers, G., Prondzynski, M., Pless, O., Blackshear, P. J., Schachner, M., & Kleene, R. (2013). Functional role of the interaction between polysialic acid and myristoylated alanine-rich C kinase substrate at the plasma membrane. *The Journal of Biological Chemistry*, 288(9), 6726–6742. <https://doi.org/10.1074/jbc.M112.444034>
- Vangeel, L., & Voets, T. (2019). Transient Receptor Potential Channels and Calcium Signaling. *Cold Spring Harbor Perspectives in Biology*, 11(6).
<https://doi.org/10.1101/cshperspect.a035048>
- Vannier, B., Peyton, M., Boulay, G., Brown, D., Qin, N., Jiang, M., Zhu, X., & Birnbaumer, L. (1999). Mouse trp2, the homologue of the human trpc2 pseudogene, encodes mTrp2, a store depletion-activated capacitative Ca²⁺ entry channel. *Proceedings of the National Academy of Sciences of the United States of America*, 96(5), 2060–2064. <https://doi.org/10.1073/pnas.96.5.2060>
- Vawter, M. P. (2000). Dysregulation of the neural cell adhesion molecule and neuropsychiatric disorders. *European Journal of Pharmacology*, 405(1-3), 385–395. [https://doi.org/10.1016/S0014-2999\(00\)00568-9](https://doi.org/10.1016/S0014-2999(00)00568-9)
- Venkatachalam, K., Zheng, F., & Gill, D. L. (2003). Regulation of canonical transient receptor potential (TRPC) channel function by diacylglycerol and protein kinase C. *Journal of Biological Chemistry*, 278(31), 29031–29040.
<https://doi.org/10.1074/jbc.M302751200>

- Venkatachalam, K., Zheng, F., & Gill, D. L. (2004). Control of TRPC and store-operated channels by protein kinase C. *Novartis Foundation Symposium*, 258, 172-85; discussion 185-8, 263-6.
- Vita, V. M. de, Zapparoli, H. R., Reimer, A. E., Brandão, M. L., & Oliveira, A. R. (2021). Dopamine D2 receptors in the expression and extinction of contextual and cued conditioned fear in rats. *Experimental Brain Research*, 239(6), 1963–1974. <https://doi.org/10.1007/s00221-021-06116-6>
- Wang, G. X., & Poo, M.-M. (2005). Requirement of TRPC channels in netrin-1-induced chemotropic turning of nerve growth cones. *Nature*, 434(7035), 898–904. <https://doi.org/10.1038/nature03478>
- Wang, H., Cheng, X., Tian, J., Xiao, Y., Tian, T., Xu, F., Hong, X., & Zhu, M. X. (2020). Trpc channels: Structure, function, regulation and recent advances in small molecular probes. *Pharmacology & Therapeutics*, 209, 107497. <https://doi.org/10.1016/j.pharmthera.2020.107497>
- Wang, Y. (2017). *Transient Receptor Potential Canonical Channels and Brain Diseases* (Vol. 976). Springer Netherlands. <https://doi.org/10.1007/978-94-024-1088-4>
- Werneburg, S., Buettner, F. F. R., Mühlhoff, M., & Hildebrandt, H. (2015). Polysialic acid modification of the synaptic cell adhesion molecule SynCAM 1 in human embryonic stem cell-derived oligodendrocyte precursor cells. *Stem Cell Research*, 14(3), 339–346. <https://doi.org/10.1016/j.scr.2015.03.001>
- Westphal, N., Kleene, R., Lutz, D., Theis, T., & Schachner, M. (2016). Polysialic acid enters the cell nucleus attached to a fragment of the neural cell adhesion molecule NCAM to regulate the circadian rhythm in mouse brain. *Molecular and Cellular Neurosciences*, 74, 114–127. <https://doi.org/10.1016/j.mcn.2016.05.003>
- Westphal, N., Loers, G., Lutz, D., Theis, T., Kleene, R., & Schachner, M. (2017). Generation and intracellular trafficking of a polysialic acid-carrying fragment of the neural cell adhesion molecule NCAM to the cell nucleus. *Scientific Reports*, 7(1), 8622. <https://doi.org/10.1038/s41598-017-09468-8>
- Wright, D. J., Simmons, K. J., Johnson, R. M., Beech, D. J., Muench, S. P., & Bon, R. S. (2020). Human TRPC5 structures reveal interaction of a xanthine-based TRPC1/4/5 inhibitor with a conserved lipid binding site. *Communications Biology*, 3(1), 704. <https://doi.org/10.1038/s42003-020-01437-8>
- Wu, D., Huang, W., Richardson, P. M., Priestley, J. V., & Liu, M. (2008). Trpc4 in rat dorsal root ganglion neurons is increased after nerve injury and is necessary for

- neurite outgrowth. *Journal of Biological Chemistry*, 283(1), 416–426. <https://doi.org/10.1074/jbc.M703177200>
- Wu, X., Zagranichnaya, T. K., Gurda, G. T., Eves, E. M., & Villereal, M. L. (2004). A TRPC1/TRPC3-mediated increase in store-operated calcium entry is required for differentiation of H19-7 hippocampal neuronal cells. *Journal of Biological Chemistry*, 279(42), 43392–43402. <https://doi.org/10.1074/jbc.M408959200>
- Xiao, M.-F., Xu, J.-C., Tereshchenko, Y., Novak, D., Schachner, M., & Kleene, R. (2009). Neural cell adhesion molecule modulates dopaminergic signaling and behavior by regulating dopamine D2 receptor internalization. *Journal of Neuroscience*, 29(47), 14752–14763. <https://doi.org/10.1523/JNEUROSCI.4860-09.2009>
- Xie, J., Bi, Y., Zhang, H., Dong, S., Teng, L., Lee, R. J., & Yang, Z. (2020). Cell-Penetrating Peptides in Diagnosis and Treatment of Human Diseases: From Preclinical Research to Clinical Application. *Frontiers in Pharmacology*, 11, 697. <https://doi.org/10.3389/fphar.2020.00697>
- Yang, L.-P., Jiang, F.-J., Wu, G.-S., Deng, K., Wen, M., Zhou, X., Hong, X., Zhu, M. X., & Luo, H.-R. (2015). Acute Treatment with a Novel TRPC4/C5 Channel Inhibitor Produces Antidepressant and Anxiolytic-Like Effects in Mice. *PLOS ONE*, 10(8), e0136255. <https://doi.org/10.1371/journal.pone.0136255>
- Yao, H., Peng, F., Fan, Y., Zhu, X., Hu, G., & Buch, S. J. (2009). Trpc channel-mediated neuroprotection by PDGF involves Pyk2/ERK/CREB pathway. *Cell Death and Differentiation*, 16(12), 1681–1693. <https://doi.org/10.1038/cdd.2009.108>
- Zheng, J. (2013). Molecular mechanism of TRP channels. *Comprehensive Physiology*, 3(1), 221–242. <https://doi.org/10.1002/cphy.c120001>
- Zhu, Y., Lu, Y., Qu, C., Miller, M., Tian, J., Thakur, D. P., Zhu, J., Deng, Z., Hu, X., Wu, M., McManus, O. B., Li, M., Hong, X., Zhu, M. X., & Luo, H.-R. (2015). Identification and optimization of 2-aminobenzimidazole derivatives as novel inhibitors of TRPC4 and TRPC5 channels. *British Journal of Pharmacology*, 172(14), 3495–3509. <https://doi.org/10.1111/bph.13140>

8. Acknowledgements

I would like to thank Prof. Dr. Melitta Schachner for the opportunity of doing the Ph.D. in her group at the ZMNH. Also, I would like to thank the members of my thesis committee, Prof. Roland Bender and Dr. Sabine Hoffmeister-Ullerich, for their advice and ideas for my project.

I want to thank Dr. Ralf Kleene and Dr. Gabriele Loers for their help in organizing and discussing the experiments and for their advice and support in the project.

I also thank Ute Bork for her technical help and support, especially in the last year of my Ph.D.

I thank Prof. Kneussel's group for letting me use their equipment and for the technical help. In particular, I want to thank Yvonne Pechman for her support and help using the cell culture.

I want to thank my Ph.D. colleagues (in alphabetical order), Luciana, Ludovica, and Viviana, for the exchange of ideas, their support and cooperation, and the nice talks during the lunch and coffee breaks.

Finally, I would like to thank my parents, my sister, and my friends for their support. And I want to thank my girlfriend, who was always there helping and supporting me. “Moltes gràcies a tots i totes.”

9. Curriculum Vitae

Name: Laura Amores-Bonet

Date of birth: 27.11.1995

Education and experience

May 2019 – December 2022

PhD Student

Center for Molecular Neurobiology
Hamburg (ZMNH)

Prof. rer. Nat. Melitta Schachner

September 2017 – July 2018

MSc in neurosciences

Molecular biology and biochemistry
department, Autonomous University of
Barcelona

*“Defining the role of CRTC2 in nutrient
deprivation-induced autophagy in
astrocytes”*

Dr. Carles Saura and Dra. Roser Masgrau

September 2013 – June 2017

BSc in biomedical sciences

Autonomous University of Barcelona

A part of this work is published in:

Amores-Bonet, L., Kleene, R., Theis, T., & Schachner, M (2022). Interactions between the Polysialylated Neural Cell Adhesion Molecule and the Transient Receptor Potential Canonical Channels 1, 4, and 5 Induce Entry of Ca²⁺ into Neurons. *International Journal of Molecular Sciences*, 23(17).
<https://doi.org/10.3390/ijms231710027>

Languages

- Native in Catalan and Spanish.
- C1 level in English.

10. Appendix: Table of chemicals

Table A1. List of the chemicals, solutions, and reagents used for the experiments, including name, provider, and catalog number.

Chemicals, solutions, and reagents	Provider	Catalog number
1 kb Plus DNA Ladder	Thermo Fisher Scientific	SM1331
100 bp Plus DNA Ladder	Thermo Fisher Scientific	SM0321
Agarose	Carl Roth	3810.4
BrainPhys Neuronal medium	STEMCELL technologies	05792
BSA fatty acids-free	Sigma-Aldrich	A6003
B27 supplement	Thermo Fisher Scientific	17504044
Chondroitin sulfate sodium salt	Sigma-Aldrich	C4384
CloneAmp HiFi PCR TM premix	Clontech	639298
Colominic acid sodium	Sigma-Aldrich	C5762
cOmplete, EDTA-free Protease Inhibitor Cocktail	Roche	11873580001
DAPI	Thermo Fisher Scientific	D1306
DMEM	Thermo Fisher Scientific	61965026
DMEM/F12	Thermo Fisher Scientific	21331020
DMEM with L-glutamine	PAN Biotech	P04-04510
DNA Loading Dye (6x)	Thermo Fisher Scientific	R0611
Duolink® In Situ Detection Reagents Red	Sigma-Aldrich	DUO92008
Duolink® In Situ Probe Anti-Mouse MINUS / PLUS	Sigma-Aldrich	DUO92004 / DUO92001
Duolink® In Situ Probe Anti-Rabbit MINUS / PLUS	Sigma-Aldrich	DUO92005 / DUO92002
Dynabeads TM Protein A	Thermo Fisher Scientific	10001D
Dynabeads TM Protein G	Thermo Fisher Scientific	10003D

ECL Prime western blotting detection reagent	Amersham	RPN2232
ECL Select western blotting detection reagent	Amersham	RPN2235
Fluo-4 AM	Thermo Fisher Scientific	F14201
Glutathione-agarose beads	MERCK	G4510
GSK-417651A	BIOZOL	10-1434
HBSS	Sigma-Aldrich	H8264
HC-070	MedChemExpress	HY-112302
IPTG	Carl Roth	2316.3
L-Glutamine	Thermo Fisher Scientific	25030024
Lipofectamine™ 2000	Thermo Fisher Scientific	11668027
Lipofectamine™ LTX with Plus Reagent	Thermo Fisher Scientific	15338100
M084 hydrochloride	TOCRIS Bioscience	5807
Mini-PROTEAN TGX™ pre-cast gels	Bio-Rad Laboratories	4561086 or 4561096
MyTaq™ Red Mix	Meridian Bioscience	BIO-25043
Na-pyruvate	Thermo Fisher Scientific	11360039
Neurobasal medium	Thermo Fisher Scientific	21103049
Neurobasal A medium	Thermo Fisher Scientific	10888022
NeuroCult SMI Neuronal Supplement	STEMCELL technologies	05792
Ni-NTA agarose beads	QIAGEN	30210
NP-40	Calbiochem (MERCK)	492016
Non-essential amino acids (100x)	Thermo Fisher Scientific	11140035
Normal donkey serum	Dianova	017-000-121
Nuclease-free water	QIAGEN	1039498
PBS with Ca ²⁺ and Mg ²⁺	PAN Biotech	P04-35500
PBS without Ca ²⁺ and Mg ²⁺	PAN Biotech	P04-36500
Penicillin/Streptavidin	Sigma-Aldrich	P4333

Phire Animal Tissue Direct PCR kit	Thermo Fisher Scientific	F140WH
PhosSTOP EASYpack	Roche	4906845001
Pico145	MedChemExpress	HY-101507
PLL	Sigma-Aldrich	P1274
Pluronic® F-127	Sigma-Aldrich	P2443
PageRuler™ Plus Prestained Protein Ladder	Thermo Fisher Scientific	26619
Roti-Blue	Carl Roth	A152.1
Roti-Safe© GelStain	Carl Roth	3865.1
Shandon Immu-Mount™	Thermo Fisher Scientific	9990402
SKF 96365 hydrochloride	Cayman chemical	10009312
Stable peroxidase buffer (10X)	Thermo Fisher Scientific	34062
Thapsigargin	TOCRIS Bioscience	1138
Trypan blue solution 0.4%	Thermo Fisher Scientific	15250061
Trypsin + EDTA	PAN Biotech	P10-023100
Tween 20	Amresco (VWR)	M147

11. Eidesstattliche Erklärung

Ich versichere ausdrücklich, dass ich die Arbeit selbständig und ohne fremde Hilfe verfasst, andere als die von mir angegebenen Quellen und Hilfsmittel nicht benutzt und die aus den benutzten Werken wörtlich oder inhaltlich entnommenen Stellen einzeln nach Ausgabe (Auflage und Jahr des Erscheinens), Band und Seite des benutzten Werkes kenntlich gemacht habe.

Ferner versichere ich, dass ich die Dissertation bisher nicht einem Fachvertreter an einer anderen Hochschule zur Überprüfung vorgelegt oder mich anderweitig um Zulassung zur Promotion beworben habe.

Ich erkläre mich einverstanden, dass meine Dissertation vom Dekanat der Medizinischen Fakultät mit einer gängigen Software zur Erkennung von Plagiaten überprüft werden kann.



Unterschrift:

